UNIVERSIDADE ESTADUAL PAULISTA
"JÚLIO DE MESQUITA FILHO"
Campus de Botucatu

Morfologia, funcionamento e influência de fatores exógenos no sistema secretor de óleo em espécies vegetais com ênfase no papel do citoesqueleto no processo de secreção

LUIZ RICARDO DOS SANTOS TOZIN

Tese apresentada ao Instituto de Biociências, câmpus de Botucatu, UNESP, para obtenção do título de Doutor no Programa de Pós-Graduação em Ciências Biológicas (Botânica), Área de concentração: Morfologia e Diversidade Vegetal.

BOTUCATU-SP

2018

UNIVERSIDADE ESTADUAL PAULISTA
"JÚLIO DE MESQUITA FILHO"
Campus de Botucatu

UNIVERSIDADE ESTADUAL PAULISTA

"Julio de Mesquita Filho"

INSTITUTO DE BIOCIÊNCIAS DE BOTUCATU

Morfologia, funcionamento e influência de fatores exógenos no sistema secretor de óleo em espécies vegetais com ênfase no papel do citoesqueleto no processo de secreção

LUIZ RICARDO DOS SANTOS TOZIN

PROF[a] DR[a] TATIANE MARIA RODRIGUES

ORIENTADORA

Tese apresentada ao Instituto de Biociências, câmpus de Botucatu, UNESP, para obtenção do título de Doutor no Programa de Pós-Graduação em Ciências Biológicas (Botânica), Área de concentração: Morfologia e Diversidade Vegetal.

BOTUCATU-SP

2018

FICHA CATALOGRÁFICA ELABORADA PELA SEÇÃO TÉC. AQUIS. TRATAMENTO DA INFORM.
DIVISÃO TÉCNICA DE BIBLIOTECA E DOCUMENTAÇÃO - CÂMPUS DE BOTUCATU - UNESP
BIBLIOTECÁRIA RESPONSÁVEL: ROSEMEIRE APARECIDA VICENTE-CRB 8/5651

Tozin, Luiz Ricardo dos Santos.
Morfologia, funcionamento e influência de fatores exógenos no sistema secretor de óleo em espécies vegetais com ênfase no papel do citoesqueleto no processo de secreção / Luiz Ricardo dos Santos Tozin. - Botucatu, 2018

Tese (doutorado) - Universidade Estadual Paulista "Júlio de Mesquita Filho", Instituto de Biociências de Botucatu
Orientador: Tatiane Maria Rodrigues
Capes: 20300000

1. Actinas. 2. Lamiaceae. 3. Ultraestrutura (Biologia). 4. Citoesqueleto. 5. Herbivoria. 6. Microtúbulos.

Palavras-chave: Actina; Herbivoria; Lamiaceae; Microtúbulos; Ultraestrutura.

Dedicatória

Dedico essa conquista aos meus pais, Maria de Lourdes e José Luiz, e a minha vó Ana, que sempre acreditaram em mim, me apoiaram e estiveram ao meu lado.

Agradecimentos

À **Deus**, por mais essa conquista e por ter me dado suporte nos momentos difíceis.

À **Prof. Dra. Tatiane Maria Rodrigues**, pela dedicação em minha orientação, por confiar e acreditar em mim sempre me incentivando a crescer, por todos os ensinamentos, paciência, conselhos e amizade, pelo comprometimento à ciência e a todos os seus orientados e por ser o exemplo de profissional que um dia almejo me tornar.

À **Coordenação de Aperfeiçoamento de Pessoal de Nível Superior (CAPES)**, pela bolsa concedida no país e no exterior (PDSE processo: 88881.131495/2016-01).

Ao **Conselho Nacional de Desenvolvimento Científico e Tecnológico (CNPq)**, pelo apoio financeiro (Ed Universal 444205/2014-4).

Ao **Instituto de Biociências de Botucatu**, ao **Departamento de Botânica** e ao **Programa de Pós-graduação em Ciências Biológicas (Botânica)** pela infraestrutura.

Aos **docentes do Departamento de Botânica**¸ pela convivência, ensinamentos dentro e fora da sala de aula.

À todos **funcionários do Departamento de Botânica**, pela convivência, ensinamentos e auxílios.

À **equipe do Centro de Microscopia Eletrônica**, IBB, UNESP, pela assistência no processamento das amostras.

À **Prof. Dra. Marcia Ortiz Mayo Marques** e ao **Instituto Agronômico de Campinas (IAC)**, pela parceria e apoio.

Aos amigos do Laboratório de Pesquisa em Anatomia Vegetal I (LaPAV), **Diana, Fernanda, Hugo, Juan, Junior, Katiane, Maela, Maria Ivanilde, Muriel e Stefany**, pelo companheirismo, amizade e apoio.

Aos **amigos dos Laboratórios de Ecologia Vegetal, Fisiologia Vegetal e Anatomia Vegetal II**, pela convivência, amizade e por terem colaborado para tornar a caminhada mais leve.

À todos que me auxiliaram na condução dos experimentos em casa de vegetação, em especial ao **Dr. Filipe Bonfin** e a **Dra. Jordany Gomes**, pelo auxílio na obtenção das estacas; e ao **Felipe Girotto**, pelo imenso auxílio.

À **Angélica Rodrigues** e **Jennifer Búfalo,** pela convivência, amizade e apoio em todos os momentos ao longo desta etapa.

Ao **Dr. Jaideep Mathur**, por ter me recebido e me orientado durante o estágio sanduíche na University of Guelph.

Aos colegas de laboratório na University of Guelph, **Cole Anderson, Kathleen Delfosse, Kiah Barton, Laura Camero e Neeta Mathur**, por todos os ensinamentos e paciência.

Aos **amigos que fiz ao longo da minha estadia no Canadá**, que me forneceram suporte, em especial a **Fabieli Feitosa** e a **Geovanna Zaro**, que foram minha família e sempre estiveram ao meu lado.

Aos meus pais, **José Luiz** e **Maria de Lourdes**, e ao meu irmão, **Luiz Renato**, por serem minha base e meu espelho, e por todo apoio e amor imensurável em todos os momentos.

Aos **funcionários da Biblioteca Central da UNESP, Câmpus Botucatu**, pela edição da ficha catalográfica.

À todos que contribuíram de forma direta ou indireta para concretização deste trabalho. Muito obrigado!!!

SUMÁRIO

TOZIN, L. R. S. **Morfologia, funcionamento e influência de fatores exógenos no sistema secretor de óleo em espécies vegetais com ênfase no papel do citoesqueleto no processo de secreção.** 2018. 133p. TESE (DOUTORADO) – INSTITUTO DE BIOCIÊNCIAS, UNESP – UNIVERSIDADE ESTADUAL PAULISTA, BOTUCATU.

Resumo – A morfologia, histoquímica e ultraestrutura dos tricomas glandulares têm sido estudadas em muitas espécies vegetais. Entretanto, alguns aspectos têm sido pouco abordados, como o envolvimento do citoesqueleto na morfologia e funcionamento glandular. Estudo recente demonstrou a relação entre a predominância de filamentos de actina e microtúbulos em células secretoras e a composição da secreção em tricomas glandulares. Além disso, pesquisas têm comprovado o envolvimento dos elementos do citoesqueleto na origem e manutenção dos tricomas tectores em plantas, sem informações para os tricomas glandulares. Sabe-se que o funcionamento do citoesqueleto está relacionado com a disponibilidade do cálcio, sendo que baixas concentrações desse íon podem prejudicar processos modulados por microtúbulos e actina. Apesar da presença de tricomas glandulares representar um caráter constitutivo em diversas espécies vegetais, fatores exógenos podem influenciar o desenvolvimento e o funcionamento glandular. Estudos têm mostrado que o ataque de herbívoros induz a formação de tricomas glandulares, levando a produção de substâncias com potencial repelente ou inseticida. Os objetivos desse trabalho foram investigar o papel do citoesqueleto na morfogênese e funcionamento de tricomas glandulares e no transporte lipídico em células secretoras de óleo, além de investigar a influência da herbivoria no desenvolvimento e funcionamento de tricomas glandulares. Foram estudadas duas espécies de Lamiaceae (*Hyptis villosa* e *Ocimum gratissimum*) e a espécie modelo *Nicotiana benthamiana*. Experimentos com drogas inibidoras da polimerização do citoesqueleto e doses decrescentes de cálcio foram realizados com *O. gratissimum* e *H. villosa*. Plantas de *N. benthamiana* foram infiltradas com *Agrobacterium* modificado

para marcação de gotas de óleo, plastídios, retículo endoplasmático, actina e microtúbulos. Além disso, indivíduos de *O. gratissimum* foram submetidos ao ataque de formigas cortadeiras. Análises estruturais foram realizadas aos microscópios de luz (campo claro e confocal) e eletrônico (varredura e transmissão). Além disso, foram realizadas análises de composição química de voláteis e de trocas gasosas. Três morfotipos de tricomas glandulares foram identificados em *O. gratissimum*; microtúbulos foram intensamente marcados em células secretoras de lipídios, enquanto filamentos de actina foram fortemente marcados em células secretoras de compostos hidrofílicos. As drogas desestabilizantes do citoesqueleto e baixos níveis de Ca^{+2} não afetaram a morfologia externa dos tricomas; entretanto, acarretaram danos estruturais nas paredes e no protoplasto das células secretoras em *O. gratissimum* e *H. villosa*. A composição química dos voláteis não foi alterada pelos diferentes níveis de Ca^{+2}. Em *N. benthamiana* foi observado que as gotas de óleo se movimentam no citoplasma pelo retículo endoplasmático ancorado aos filamentos de actina, sugerindo um mecanismo de diferente do descrito em células animais. A herbivoria promoveu respostas diferenciais de cada morfotipo glandular em *O. gratissimum* sugerindo a ocorrência de uma compartimentalização de funções entre os tricomas; além disso, foram detectadas alterações na composição dos componentes voláteis produzidos. Esse trabalho envolveu diferentes abordagens, várias delas inéditas, para o estudo do sistema secretor de óleo em plantas. Diferentes aspectos sobre o sistema secretor de óleo em espécies vegetais foram elucidados, gerando novas perspectivas para estudos mais aprofundados.

Palavras-chave: actina, herbivoria, Lamiaceae, microtúbulos, *Nicotiana benthamiana*, óleo essencial, tricomas, ultraestrutura.

TOZIN, L. R. S. **Morphology, functioning and influence of exogenous factors in the oil secretory system in plant species with emphasis on the role of the cytoskeleton in the secretory process.** 2018. 133p. Ph.D. THESIS – INSTITUTE OF BIOSCIENCES, UNESP – UNIVERSIDADE ESTADUAL PAULISTA, BOTUCATU.

Abstract – The morphology, histochemistry and ultrastructure of glandular trichomes have been studied in many plant species. However, some aspects have been poorly approached, such as the involvement of the cytoskeleton on the gland morphology and functioning. Recent study demonstrated a relation between the predominance of actin filaments and microtubules in secretory cells and the secretion composition in glandular trichomes. In addition, researches have proven the involvement of the cytoskeletal elements in the origin and maintenance of non-glandular trichomes in plants, with no information for glandular trichomes. It is known that the cytoskeleton functioning is related with calcium availability and that low concentration of this ion can harm process modulated by actin filaments and microtubules. Despite the presence of glandular trichomes is a constitutive character in several plant species, exogenous factors can influence their development and functioning. Studies have showed that herbivore attacks induce the glandular trichomes formation, leading to the production of substances with repellent and insecticide potential. This work aimed to investigate the role of cytoskeleton in the glandular trichome morphogenesis and functioning, and in the lipid transport in oil secretory cells, in addition to investigate the influence of herbivory in the glandular trichomes formation and functioning. We studied two Lamiaceae species (*Hyptis villosa* and *Ocimum gratissimum*) and the model species *Nicotiana benthamiana*. Experiments with inhibitors of cytoskeletal element polymerization and decreasing calcium levels were performed with *H. villosa* and *O. gratissimum*. *N. benthamiana* plants were infiltrated with modified *Agrobacterium* for labeling lipid drops, plastids, endoplasmic reticulum, actin filaments and microtubules.

In addition, individuals of *O. gratissimum* were submitted to leaf-cutter ants attack. Structural analysis were performed using light (bright field and confocal) and electronic (scanning and transmission) microscopes. In addition, we performed analysis of the the chemical composition of the volatile components and of gas-exchanges. Three morphotypes of glandular trichomes were identified in *O. gratissimum*; microtubules were intensely labeled in secretory cells of lipophilic compounds, while actin filaments were strongly labeled in secretory cells of hydrophilic substances. The inhibitors of cytoskeletal elements polymerization and low levels of calcium did not affect the external morphology of the trichomes; however, lead to structural damages in the cell wall and protoplast of secretory cells of *O. gratissimum* and *H. villosa*. The chemical composition of volatile components was not affected by low levels of Ca^{+2}. In *N. benthamiana* we observed that lipid drops move in the cytoplasm by the endoplasmic reticulum anchored on the actin filaments; this suggests a different mechanism described for animal cells. The herbivory promoted differential answers in each glandular trichome morphotype in *O. gratissimum*; this suggests the occurrence of a compartmentalization of functions among the trichomes; in addition, we detected alterations in the chemical composition of the volatile components produced by attacked plants. This work involved different approaches, several of them innovative, for the study of the oil secretory system in plants. Different aspects about the oil secretory system in plants were elucidated, opening new avenues for further studies.

Keywords: actin, essential oil, herbivory, Lamiaceae, microtubules, *Nicotiana benthamiana*, trichomes, ultrastructure.

INTRODUÇÃO GERAL

Tricomas glandulares são apêndices epidérmicos uni ou multicelulares especializados na secreção de substâncias de natureza química diversa, que pode ser lipofílica, hidrofílica ou mista. Tais substâncias apresentam grande importância na interação da planta com o ambiente (Fahn 1979; Werker 2000; Evert 2006), podendo atuar na atração de polinizadores e agentes dispersores de frutos e sementes (Harbone 1993; Langenheim 2003; Castro & Machado 2006), além de conferir proteção contra ataques de herbívoros e patógenos, altas temperaturas e intensidade luminosa (Harbone 1993; Langenheim 2003; Valkama et al. 2003).

Os tricomas glandulares apresentam morfologia bastante variada, sendo comum a ocorrência de diferentes morfotipos glandulares em um mesmo órgão de uma mesma planta (Serrato-Valenti et al. 1997; Ascensão & Pais 1998; Tozin et al. 2015a; Silva et al. 2016). Nesse sentido, estudos recentes têm demonstrado que tricomas glandulares presentes num mesmo órgão podem produzir substâncias de natureza química diferente, propondo uma correlação entre o morfotipo glandular e a composição da secreção produzida (Tozin et al. 2015a; Silva et al. 2016).

Análises ultraestruturais mostram que os aspectos celulares dos tricomas glandulares estão associados com a composição da secreção produzida, sendo que a diversidade de organelas nas células secretoras varia de acordo com a natureza química da secreção (Werker 2000; Tozin et al. 2015a; Silva et al. 2016). Assim, em tricomas produtores de substâncias predominantemente lipofílicas, a característica ultraestrutural mais comum das células secretoras é a proliferação do retículo endoplasmático liso (Werker 2000; Silva et al. 2016), além da ocorrência de plastídios polimórficos desprovidos de tilacóides (Werker 2000; Evert 2006; Tozin et al. 2015a). Diferentemente, a principal característica das células secretoras de substâncias

hidrofílicas é a abundância de dictiossomos hiperativos na produção de vesículas (Fahn 1979; Evert 2006; Tozin et al. 2015a).

Apesar de reconhecida a origem protodérmica dos tricomas glandulares, estudos sobre o processo de formação dessas glândulas em nível celular são bastante escassos, principalmente no que se refere ao papel do citoesqueleto nos processos ontogenéticos. Trabalhos têm demonstrando o papel do citoesqueleto na formação e manutenção de tricomas tectores em *Arabidopsis* (Szymanski et al 1999; Kost et al. 1999; Mathur et al. 1999), mas não em tricomas glandulares. Os microtúbulos exercem papel fundamental na formação do pedúnculo e na iniciação de ramificações dos tricomas tectores, determinando sua morfologia básica, enquanto que os filamentos de actina atuam principalmente nas fases finais do desenvolvimento destes tricomas atuando no alongamento de suas ramificações e na manutenção de sua forma madura (Kost et al. 1999; Mathur et al. 1999). Estudos demonstram ainda que problemas na polimerização dos filamentos de actina podem impedir a formação de tricomas tectores em *Arabidopsis* (Szymanski et al. 1999). Quanto ao papel do citoesqueleto na origem e funcionamento de tricomas glandulares, estudos não foram encontrados.

No que se refere à atuação do citoesqueleto nos processos subcelulares da secreção em células vegetais, sabe-se que a manutenção de vacúolos e o movimento e ancoragem de vesículas e organelas no citoplasma são realizadas pelos filamentos de actina (Evert 2006 e literatura citada). Quanto aos microtúbulos, desde o século passado, estudos têm apontado seu envolvimento na movimentação intracelular das gotas de óleo em células animais (Welte et al. 1998; Targett-Adams et al. 2003; Zehmer et al. 2009). Mais recentemente, em trabalho envolvendo a marcação diferencial dos elementos do citoesqueleto por técnicas de imunofluorescência em tricomas glandulares de uma espécie de Lamiaceae, Tozin & Rodrigues (2017) mostraram intensa marcação

de microtúbulos em células secretoras de substâncias lipídicas, enquanto que filamentos de actina foram intensamente corados em células produtoras de secreção predominantemente hidrofílica, e ambos os elementos foram marcados em células secretoras se substâncias mista. Esses resultados são inéditos para células secretoras em plantas e reforçam a necessidade de estudos mais profundos para o melhor entendimento do envolvimento do citoesqueleto no processo secretor em células vegetais.

O funcionamento do citoesqueleto está intimamente relacionado com a disponibilidade de alguns minerais, principalmente o cálcio (Hepler 2005). A interação entre elementos do citoesqueleto e o cálcio tem sido demonstrada em estudos envolvendo células motoras (Yao et al. 2008; Chen et al. 2013), sendo conhecido seu papel como mediador na polimerização dos filamentos de actina (Hwang & Lee 2001; Chen et al. 2013). Assim, a deficiência de cálcio pode acarretar diversos problemas nos processos modulados pelo citoesqueleto (Hepler 2005), como se supõem ser o caso dos processos de desenvolvimento e funcionamento dos tricomas glandulares.

Além da disponibilidade de nutrientes importantes para o desenvolvimento vegetal, como o cálcio, outros fatores exógenos como intensidade luminosa, temperatura, injúrias mecânicas, dentre outros, podem influenciar a formação e funcionamento das estruturas secretoras nas plantas (Langenheim 2003; Rosner & Hanrup 2004; Moreira et al. 2008). Dentre estes fatores, o efeito da herbivoria no desenvolvimento e funcionamento do sistema secretor é um dos mais conhecidos (Dalin et al. 2008). Em diversas espécies de plantas, o ataque de herbívoros resulta na produção de maior densidade de tricomas glandulares (Baur et al. 1991; Dalin et al. 2008), o que tem sido associado a produção de substâncias com potencial repelente que levam a um incremento na proteção dos órgãos formados após ataque de herbívoros

(Dalin et al. 2008). Nesse sentido tem sido registrado que diversas espécies vegetais produzem substâncias induzidas especificamente pelo ataque de herbívoros – herbivore-induced plant volatiles (HIPVs) (Dicke et al. 2003; Unsicker et al. 2009; Tozin et al. 2015b).

Apesar da conhecida plasticidade dos tricomas glandulares no que se refere à densidade e funcionamento (Dalin et al. 2008; Tozin et al. 2015b, 2017), a presença dessas glândulas em órgãos aéreos vegetativos e/ou reprodutivos é um aspecto constitutivo comum a numerosas famílias de eudicotiledôneas, dentre elas Lamiaceae (Metcalfe & Chalk 1950). Espécies pertencentes à Lamiaceae possuem tricomas glandulares com morfologia diversificada como os principais sítios de secreção de metabólitos secundários que conferem a essas plantas propriedades aromática e medicinal (Fahn 1979; Ascensão et al. 1995).

Estudos sobre a morfologia de tricomas em espécies de Lamiaceae são abundantes, havendo informações sobre espécies pertencentes a diferentes gêneros (Werker et al. 1993; Ascensão et al. 1995, 1998; Serrato-Valenti et al. 1997; Ascensão & Pais 1998; Turner et al. 2000; Kaya et al. 2007; Milaneze-Gutierre et al. 2007; Huang et al. 2010; Rodrigues et al. 2013). De forma geral, apesar da abundância de estudos sobre a morfologia de tricomas em Lamiaceae, pesquisas envolvendo espécies nativas são escassas. Da mesma forma, trabalhos envolvendo os aspectos celulares da secreção em tricomas glandulares de Lamiaceae são restritos a poucas espécies (Ascensão et al. 1995; Ascensão & Pais 1998; Huang et al. 2010; Tozin & Rodrigues 2017).

Neste trabalho, estudamos as espécies *Hyptis villosa* Pohl ex Benth. e *Ocimum gratissimum* L. pertencentes a Lamiaceae. O gênero *Hyptis* é constituído por cerca de 400 espécies distribuídas do Sul dos Estados Unidos até a Argentina. No Brasil, possui cerca de 200 espécies, sendo pelo menos 146 endêmicas (Falcão & Menezes 2003;

Harley et al. 2013). Espécies deste gênero são amplamente utilizadas pela indústria farmacêutica e na medicina popular em diversos países devido as atividades antimicrobiana, antifúngica, anti-inflamatória e inseticida da secreção produzida por seus tricomas (Falcão & Menezes 2003). Além disso, estudos mostram que as substâncias extraídas de espécies de *Hyptis* apresentam potencial para a diminuição da carga viral do HIV (Falcão & Menezes 2003). No Cerrado paulista, *Hyptis villosa*, conhecida popularmente como hortelã-do-cerrado, é bastante comum (Durigan et al. 2004). Estudos demonstram que o óleo essencial produzido por esta espécie é rico em espatulenol, epi-α-cadinol e biciclogermacreno (Silva et al. 2013). Os tricomas glandulares de *H. villosa*, principais sítios produtores de tais substâncias bioativas, foram descritos por Tozin & Rodrigues (2017). Estes autores descreveram quatro morfotipos de tricomas glandulares, facilmente distinguíveis. O gênero *Ocimum* corresponde a um grupo de espécies com ampla importância econômica devido à produção de óleos essenciais largamente explorados por indústrias farmacêuticas e alimentícias. As espécies pertencentes a este gênero são amplamente distribuídas na África, América e Ásia (Orafidiya et al. 2004; Tchoumbougnang et al. 2006). *Ocimum gratissimum*, popularmente conhecida como alfavaca ou alfavaca-cravo, possui óleo essencial rico em eugenol (Silva et al. 1999; Fernandes et al. 2013) e 1-8 cineol (Silva et al. 1999). A espécie tem sido bastante utilizada como condimento e na medicina popular para o tratamento de diversas doenças (Albuquerque et al. 2007; Di Stasi et al. 2002) como reumatismo, paralisias e transtornos mentais (Effraim et al. 2001). Além disso, diversos trabalhos têm demonstrado as propriedades bactericida (Matasyoh et al. 2007) e fungicida (Faria et al. 2006) de seus extratos. Entretanto, estudos sobre as características morfológicas das glândulas produtoras dos compostos bioativos nessa espécie não foram encontrados.

Além das duas espécies de Lamiaceae mencionadas acima, nesse trabalho empregamos a espécie modelo *Nicotiana benthamiana* Domin (Solanaceae) para estudos com abordagens moleculares. *Nicotiana benthamiana*, conhecida popularmente como tabaco, tem sido amplamente utilizada na literatura para estudos em associação com *Agrobacterium*, a fim de se promover a marcação de estruturas específicas com proteínas fluorescentes – GFP, RFP, YFP (Wahlroos et al. 2003; Sohn et al. 2014; Petre et al. 2017). A espécie produz grande quantidade de óleo, e, portanto, mostrou-se um importante modelo para o estudo do sistema secretor.

Os objetivos desse trabalho foram investigar o papel do citoesqueleto na morfogênese e funcionamento de tricomas glandulares e no transporte lipídico em células secretoras de óleo, além de investigar a influência da herbivoria no desenvolvimento e funcionamento de tricomas glandulares. Para isso, a) descrevemos a morfologia, histoquímica e aspectos subcelulares dos tricomas glandulares de *O. gratissimum*, com ênfase na distribuição dos elementos do citoesqueleto; b) investigamos o efeito do cálcio e de drogas desestabilizantes do citoesqueleto nos aspectos morfogenéticos, subcelulares e funcionais dos tricomas glandulares de *H. villosa* e *O. gratissimum*; c) investigamos a dinâmica do transporte intracelular de gotas de óleo utilizando a espécie modelo *Nicotiana benthamiana* (tabaco); e d) avaliamos a influência da herbivoria por formigas cortadeiras na densidade glandular e na composição química dos voláteis em *O. gratissimum*.

REFERÊNCIAS BIBLIOGRÁFICAS

Albuquerque, U.P.; Medeiros, P.M.; Almeida, A.L.S.; Monteiro, J.M.; Lins Neto, M.F.; Melo, J.G.; Santos, J.P. (2007). Medicinal plants of the caatinga (semi-arid) vegetation of NE Brazil: a quantitative approach. J Ethnopharmacol v. 114, 325–354.

Ascensão, L.; Marques, N.E.; Pais, M.S. (1995). Glandular Trichomes on Vegetative and Reproductive Organs of *Leonotis leonurus* (Lamiaceae). Ann Bot. v.75, 619-626.

Ascensão, L.; Figueiredo, A.C.; Barroso, J.G.; Pedro, L.G.; Schripsema, J.; Deans, S.G.; Scheffer, J.J.C. (1998). *Plectranthus madagascariensis*: morphology of the glandular trichomes, essential oil composition, and its biological activity. Int J Plant Sci. v.159, 31-38.

Ascensão, L.; Pais, M.S. (1998) The leaf capitate trichomes of *Leonotis leonurus*: histochemistry, ultrastructure and secretion. Ann Bot. v. 81, 263-271.

Baur, R.; Binder, S.; Benz, G. (1991). Non glandular leaf trichomes as short-term inducible defence of the grey alder, *Alnus incana* (L.), against the chrysomelid beetle, *Agelastica alni* L. Oecologia v. 87, 219–226.

Castro, M.M.; Machado, S.R. (2006). Células e tecidos secretores. In: Anatomia vegetal. Apezzatto-da-Glória, B. & Carmello-Guerreiro, S. M. (2006). (Eds). Viçosa, UFV.

Chen, D.; Acharya, B. R.; Liu, W.; Zhang, W. (2013). Interaction between calcium and actin in guard cell and pollen signaling networks. Plants. v. 2(4), 615-634.

Dalin, P.; Agren, J.; Björkman, C.; Huttumen, P.; Kärkkäinen, K. (2008). Leaf Trichome Formation and Plant Resistance to Herbivory. In: Schaller A. (ed). Induced Plant Resistance to Herbivory. Springer Science+Business Media.

Dicke, M.; Agrawal, A.A.; Bruin, J. (2003). Plants talk, but are they deaf? Trends in Plant Science v. 8, 403–405.

Di Stasi, L.C.; Oliveira, G.P.; Carvalhaes, M.A.; Queiroz Jr, M.; Tien, O.S.; Kakinami, S.H.; Reis, M.S. (2002). Medicinal plants popularly used in the Brazilian Tropical Atlantic Forest. Fitoterapia 73, 69–91.

Durigan, G.; Baitello, J.B.; Franco, G.A.D.C.; Siqueira, M.F. (2004). Plantas do Cerrado Paulista: Imagens de uma paisagem ameaçada. Páginas & Letras Editora e Gráfica, São Paulo.

Effraim, K.D.; Jacks, T.W.; Sodipo, O.A. (2001). Histopathological studies on the toxicity of *Ocimum gratissimum* leave extract on some organs of rabbit. African. Journal Biomedical Research 6: 21-25.

Evert, R.F. (2006). Esau's Plant Anatomy. 3a. ed. Wiley-Interscience, New Jersey.

Fahn, A. (1979). Secretory tissues in plants. Academic Press, London.

Falcão, D.Q.; Menezes, F.S. (2003). Revisão etnofarmacológica, farmacológica e química do gênero *Hyptis*. Rev Bras Farm. v. 84(3), 69-74.

Faria, T.J.; Ferreira, R.S.; Yassumoto, L.; Souza, J.R.P.; Ishikawa, N.K.; Barbosa, A.M. (2006). Antifungal activity of essential oil isolated from *Ocimum gratissimum* L. (eugenol chemotype) against phytopathogenic fungi. Braz Arch Biol Technol v. 49: 867-871.

Fernandes, V.F.; Almeida, L.B.; Feijó, E.V.R.S.; Silva, D.C.; Oliveira, R.A.; Mielke, M.S.; Costa, L.C.B. (2013). Light intensity on growth, leaf micromorphology and essential oil production of *Ocimum gratissimum*. Rev Bra Farmac 23(3): 419-424.

Harbone, J.B. (1993). Plant toxins and their effects on animals. In: Introduction to Ecological Biochemistry. Academic Press, London, 71-103p.

Harley, R.; França, F.; Santos, E.P.; Santos, J.S.; Pastore, J.F. (2013). Lamiaceae. In: Lista de Espécies da Flora do Brasil. http://floradobrasil.jbrj.gov.br/jabot/floradobrasil/FB8183 (18 Outubro 2013).

Hepler, P.K. (2005). Calcium: a central regulator of plant growth and development. Plant Cell, v.17, 2142-2155.

Huang, S.S.; Liao, J.P.; Kirchoff, B.K. (2010). Calcium distribuition and function in the glandular trichomes of *Lavandula pinnata* L. J Tor Bot Soc. v.137, 1-15.

Hwang, J.; Lee, Y. (2001). Abscisic acid-induced actin reorganization in guard cells of dayflower is mediated by cytosolic calcium levels and by protein kinase and protein phosphatase activities. Plant Physiol. v. 125(4), 2120-2128.

Kaya, A.; Demirci, B.; Baser, K.H.C. (2007). Micromorphology of glandular trichomes of *Nepeta congesta* Fisch. & Mey. var. *congesta* (Lamiaceae) and chemical analysis of the essential oils. S Afr J Bot. v. 73, 29-34.

Kost, B.; Mathur, J.; Chua, N. (1999). Cytoskeleton in plant development. Current Opinion in Plant Biol. v.2, 462-470.

Langnheim, J.H. (2003). Plant resins: chemistry, evolution, ecology and ethnobotany. Portland, Cambridge: Timber Press.

Matasyoh, L.G.; Matasyoh, J.C.; Wachira, F.N.; Kinyua, M.G.; Muigai, A.G.W.; Mukiama, T.K. (2007). Chemical composition and antimicrobial activity of the essential oil of *Ocimum gratissimum* L. growing in Eastern Kenya. Afr J Biotechnol v. 6, 760-765.

Mathur, J.; Speilhofer, P.; Kost, B.; Chua, N. (1999). The actin cytoskeleton is required to elaborate and maintain spatial patterning during trichome cell morphogenesis in *Arabidopsis thaliana*. Development. v. 126, 5559-5568.

Metcalfe, C.R.; Chalk, L. (1950). Anatomy of the dicotyledons II. Claredon, Oxford. 1500p.

Milaneze-Gutierre, M.A.; Famelli, M.C.; Capel, L.S.; Romagnolo, M.B. (2007). Caracterização morfológica dos tricomas foliares e caulinares de duas espécies de Lamiaceae conhecidas popularmente como “falso-boldo”. Acta Sci Biol Sci. v.29, 125-130.

Moreira, X.; Sampedro, L.; Zas, R.; Solla, A. (2008). Alterations of the resin canal system of *Pinus pinaster* seedlings after fertilization of healthy and of a *Hylobius abieties* attacked stand. Trees. v. 22, 771-777.

Orafidiya, L.O.; Agbani, E.O.; Iwalewa, E.O.; Adelusola, K.A.; Oyedapo, O.O. (2004). Studies on the acute and sub-chronic toxicity of the essential oil of *Ocimum gratissimum* L. leaf. Phytomedicine v. 11, 71–76.

Petre, B.; Win, J.; Menke, F.L.H.; Kamoun, S. (2017). Protein-protein interaction assays with effector-GFP fusions in *Nicotiana benthamiana*. Methods in Molecular Biology v.1659, 85-98.

Rodrigues, L.; Póvoa, O.; Teixeira, G.; Figueiredo, A.C.; Moldão, M.; Monteiro, A. (2013). Trichomes micromorphology and essential oil variation at different developmental stages of cultivated and wild growing *Mentha pulegium* L. populations from Portugal. Indus Crops Produc. v.43, 692-700.

Rosner, S.; Hannrup, B. (2004). Resin canal traits relevant for constitutive resistance of Normay spruce against bark beetles: environmental and genetic variability. For Ecol Manage. v. 200, 77-87.

Serrato-Valenti, G.; Bisio, A.; Cornara, L.; Ciarallo, G. (1997) Structural and histochemical investigation of the glandular trichomes of *Salvia aurea* L. leaves, and chemical analysis of the essential oil. Ann Bot. v.79, 329-336.

Silva, R.F.; Rezende, C.M.; Santana, H.C.D.; Vieira, R.F.; Bizzo, H.R. (2013). Scents from Brazilian Cerrado: chemical composition of the essential oil from the leaves of *Hyptis villosa* Pohl ex Benth (Lamiaceae). J Essent Oil Res. v. 25(5), 415-418.

Silva, M.G.V; Craveira, A.A.; Matos, F.J.A.; Machado, M.I.L.; Alencar, J.W. (1999). Chemical variation during daytime of constituents of the essential oil of *Ocimum gratissimum* leaves. Fitoterapia v. 70, 21-34.

Silva, S.C.M.; Tozin, L.R.S.; Rodrigues, T.M. (2016). Morphological and histochemical characterization of secretory sites of bioactive compounds in *Lantana camara* L. (Verbenaceae) leaves. Botany v. 94, 321-336.

Sohn, S.H.; Frost, J.; Kim, Y.H.; Choi, S.K.; Lee, Y.; Seo, M.S.; Lim, S.H.; Choi, Y.; Lomonossoff, G. (2014). Cell-autonomous-like silencing of GFP-partitioned transgenic *Nicotiana benthamiana*. J Exp Bot v.65, 4271-4283.

Szymanski, D.B.; Marks, D.; Wick, S.M. (1999). Organized f-actin is essential for normal trichome morphogenesis in *Arabidopsis*. Plant Cell v.11, 2331-2347.

Targett-Adams, P.; Chambers, D.; Gledhill, S.; Hope, R.G.; Coy, J.F.; Girod, A.; McLauchlan, L. (2003). Live cell analysis and targeting of the lipid droplet-binding adipocyte differentiation-related protein. J. Biol. Chem v.278(18), 15998–1600.

Tchoumbougnang, F.; Amvam Zollo, P.H.; Aviessi, F.; Alitonou, G.A.; Sohounhloue, D.K.; Ouamba, J.M.; Tsomambet, A.; Andissa, N.O.; Dagne, E.; Agnaniet, H.; Bessière, J.M.; Menut, C. (2006). Variability in the chemical compositions of the essential oils of five *Ocimum* species from Tropical African area. J Essent Oil Res v. 18, 194–199.

Tozin, L.R.S.; Marques, M.O.M.; Rodrigues, T.M. (2017). Herbivory by leaf-cutter ants changes the glandular trichomes density and the volatile components in an aromatic plant model. AoB Plants v.9(6), plx057.

Tozin, L.R.S; Carvalho, S.F.; Machado, S.R.; Rodrigues, T.M. (2015a). Glandular trichome diversity on leaves of *Lippia origanoides* Kunth and *Lippia stachyoides* Cham. (Verbenaceae): morphology, histochemistry and ultrastructure. Botany v. 93, 297-306.

Tozin, L.R.S.; Marques, M.O.M.; Rodrigues, T.M. (2015b). Glandular trichome density and essential oil composition in leaves and inflorescences of *Lippia origanoides* Kunth (Verbenaceae) in the Brazilian Cerrado. An Acad Bras Cienc v. 87(2), 943-953.

Tozin, L.R.S.; Rodrigues, T.M. (2017). Morphology and histochemistry of glandular trichomes in *Hyptis villosa* Pohl ex Benth. (Lamiaceae) and differential labeling of cytoskeletal elements. Act Bot Bras v.31(3), 330-343.

Turner, G.W.; Gershenzon, J.; Croteau, R.B. (2000). Distribution of peltate glandular trichomes on developing leaves of peppermint. Plant Physiol. v.124, 655-663.

Unsicker, S.B.; Kunert, G.; Gershenzon, J. (2009). Protective perfumes: the role of vegetative volatiles in plant defense against herbivores. Curr Opin Plant Biol v. 12, 479–485.

Valkama, E.; Salminen, J.P.; Koricheva, J.; Pihlaja, K. (2003). Comparative analysis of leaves trichome structure and composition of epicuticular flavonoids in Finnish Birch species. Ann Bot. v. 91(6), 643-655.

Welte, M.A.; Gross, S.P.; Postner, M.; Block, S.M.; Wieschaus, E.F. (1998). Developmental regulation of vesicle transport in *Drosophila* embryos: forces and kinetics. Cell v.92, 547–557.

Werker, E.; Putievsky, E.; Ravid, U.; Dudai, N.; Katzir, I. (1993). Glandular hair and essential oil in developing leaves of *Ocimum basilicum* L. (Lamiaceae). Ann Bot. v.71, 43-50.

Werker, E. (2000). Trichome Diversity and Development. Adv Bot Res. v.31.

Zehmer, J.K.; Huang, Y.; Peng, G.; Pu, J.; Anderson, R.G.W.; Liu P. (2009). A role for lipid droplets in inter-membrane lipid traffic. Protemics. v9, 914-921.

Yao, H.; Xu, Q.; Yuan, M. (2008). Actin dynamics mediates the changes of calcium level during the pulvinus movement of *Mimosa pudica*. Plant Signal Behav, v. 3(11), 954-960.

Conforme estabelecido pelo Programa de Pós-Graduação em Ciências Biológicas (Botânica) do IBB, UNESP, os resultados obtidos durante a execução deste Projeto de Doutorado foram reunidos em quatro artigos científicos para publicação.

Artigo 1: Distribution, morphology and histochemistry of glandular trichomes in *Ocimum gratissimum* L. (Lamiaceae) emphasizing the cytoskeletal elements involvement in the secretory process

Artigo 2: Influence of cytoskeletal polymerization inhibiting drugs and low levels of Ca^{+2} on glandular trichomes of two Lamiaceae species

Artigo 3: Dynamic of intracellular lipid drop transport involves actin filaments and endoplasmic reticulum in Tobacco cells

Artigo 4: Herbivory by leaf-cutter ants changes the glandular trichomes density and the volatile components in an aromatic plant model
(*Publicado:* AoB Plants, vol. 9(6), plx057, 2017 – A2 Qualis Biodiversidade CAPES)

CAPÍTULO 1

Distribution, morphology and hisochemistry of glandular trichomes in *Ocimum gratissimum* L. (Lamiaceae) emphasizing the involvement of cytoskeletal elements in the secretory process

Luiz Ricardo dos Santos Tozin* & Tatiane Maria Rodrigues

São Paulo State University (UNESP), Institute of Biosciences of Botucatu (IBB), Department of Botany, Botucatu, SP, Brazil.

*Author for correspondence (ricardo.tozin@gmail.com)

ABSTRACT

The morphology, histochemistry and ultrastructure of the glandular trichomes have been exhaustively studied in several plants and their subcellular features are closely related with the composition of secretion produced. Studies have purposed the fundamental role of the cytoskeleton elements in the intracellular processes of secretion culminating with the storage of the exudate in cellular compartments or its release to outside. However, this topic has been poorly studied in secretory cells of plants. *Ocimum gratissimum* (Lamiaceae) is an aromatic species widely utilized as condiment and in the popular medicine. Here, we analyzed the distribution, morphology, histochemistry and ultrastructure of the glandular trichomes of *O. gratissimum*, emphasizing the distribution of the cytoskeletal elements. Glandular trichomes were observed in stem, leaf, bract, sepal and adaxial surface of petal. Three morphotypes of glandular trichomes were identified secreting different categories of chemical compounds. Plastids devoid of grana and smooth endoplasmic reticulum were abundant in cells secreting lipophilic

substances whereas hyperactive dictyosomes characterized the cytoplasm of the cells producing mostly hydrophilic compounds. Microtubules were intensively immunolabeling in cells secreting mostly lipophilic substances; and actin filaments were strongly marked in cells secreting hydrophilic compounds. The convergent techniques in microscopy used enabled us to establish a correlation among the glandular morphotypes, their subcellular aspects, the prevalence of the cytoskeletal elements and the secretion composition.

Keywords: actin filaments, glandular hairs, microtubule, secretion, ultrastructure.

INTRODUCTION

Glandular trichomes are external secretory structures with diverse morphology and that can be present in vegetative and/or reproductive organs of several plant groups (Ascensão et al. 1995; Werker 2000). Different morphotypes of glandular trichomes may occur side by side in the same organ and produce secretion with distinct chemical composition (Ascensão et al. 1995; Silva et al. 2016; Tozin & Rodrigues 2017).

Several work have demonstrated that the subcellular features of the glandular trichomes are closely related with the type of secretion produced (Ascensão & Pais 1998; Werker 2000; Argyropoulou et al. 2010; Tozin et al. 2015). Hydrophilic substances are produced by cells rich in dictyosomes, whereas lipophilic compounds are produced mainly by smooth endoplasmic reticulum and plastids (Werker 2000; Evert 2006; Tozin & Rodrigues 2017).

The intracellular processes of secretion culminate with the storage of the exudate in cellular compartments or with the release of the exudate to the extracellular medium, involve the movement of organelles and secretion bodies inside the cytosol (Fahn 1979; Evert 2006), in wich the cytoskeletal elements are fundamental. In this sense, Tozin &

Rodrigues (2017) postulated that in plant gland cells the microtubules can be involved in the oil drops movement, such as demonstrated for animal cells (Zehmer et al. 2009 and references therein); and that the actin filaments are responsible for the movement of secretory vesicle in plant cells active in production of hydrophilic compounds, as known for animal cells (Valderrama et al. 2001; Stamnes 2002). However, studies on this issue involving secretory cells in plants are restricted to *Hyptis villosa* (Lamiaceae) (Tozin & Rodrigues 2017) and deserve more attention, mainly because new studies are showing that the mechanism for lipid drops displacement could be different in plants and animal cells (Tozin et al. *In Prep*.).

Lamiaceae species are known by the presence of glandular trichomes secreting substances with economic and ecologic values (Ascensão et al. 1999; Serrato-Valentini et al. 1997; Rodrigues et al. 2013; Tozin & Rodrigues 2017). The genus *Ocimum*, collectively called basil, belongs to an economically important group of plants due the production of essential oil widely exploited by the pharmaceutical and food industries. The *Ocimum* species are largely distributed in Africa, America and Asia (Orafidiya et al. 2004; Tchoumbougnang et al. 2006). *Ocimum gratissimum* L., one of the most important species of the genus, is popularly named as "alfavaca-cravo" or tree basil. It is widely used as a condiment and in the popular medicine for several diseases (Di Stasi et al. 2002; Albuquerque et al. 2007). In addition, work have demonstrated their antibacterial (Matasyoh et al. 2007) and antifungal (Faria et al. 2006) properties. Despite the economic importance of *O. gratissimum*, studies about the morphological features of the glands producing their bioactive compounds were not found.

In this paper we analyzed the distribution, morphology, histochemistry and ultrastructure of the glandular trichomes in reproductive and vegetative aerial organs of *O. gratissimum*, emphasizing the involvement of the cytoskeleton elements in the

secretory process. Correlations among the subcellular features of the secretory cells, predominance of actin filaments or microtubules and the secretion composition were established.

MATERIAL AND METHODS

Plant material

Ocimum gratissimum individuals growing in the medicinal garden from Lageado Experimental Farm, Botucatu city, São Paulo state, Brazil, were sampled. Samples of stem (15 mm below the shoot apex), expanded and non-senescent leaves and inflorescence parts (bracts, sepal, petal, stamen and pistil) were collected from adult plants (n = 5).

Vouchers were deposited in the Irina Delanova Gemtchújnicov Herbarium (BOTU), of the Department of Botany, Institute of Biosciences of Botucatu, IBB, UNESP, Botucatu, São Paulo, Brazil, under registration number 32798.

Distribution and morphological analysis

Samples of stem, leaves, bracts and flowers were observed with Leica M205C stereomicroscope for analyze the distribution of the glandular trichomes.

For histological studies, freshly hand-cut sections (10 μm thick) were stained with Safrablau (Bukatsch 1972); and semi-permanent slides were mounted with glycerin jelly. In addition, samples were fixed in FAA 50 (Johansen 1940), dehydrated in an ethanol series, and embedded in Leica® historesin. Cross sections (7 μm thick) obtained in a rotary microtome were stained with 0.05% toluidine blue O, pH 3.7 (O'Brien et al. 1964), and then mounted in Entellan® on permanent slides. The relevant results were documented using a Leica DMR photomicroscope with digital camera.

Histochemistry

To detect the main classes of chemical compounds present in the glands, freshly hand-cut sections of leaves were treated with the following reagents: Lugol for starch grains and alkaloids (Johansen 1940), Sudan IV and Sudan Black for total lipids (Pearse 1980), Nadi reagent for terpenoids (David and Carde 1964), ferric trichloride for phenolic compounds (Johansen 1940), periodic acid-Schiff (PAS) for water-insoluble polysaccharides (Amaral et al. 2001), Wagner reagent for alkaloids (Furr and Mahlberg 1981), and bromophenol blue for total proteins (Mazia et al. 1953).

Scanning electron microscopy (SEM)

For analysis of glandular micromorphology, samples excised from the middle portion of the leaf blade were fixed in 2.5% glutaraldehyde with 0.1 M phosphate buffer, pH 7.3, overnight at 4 °C, post-fixed in 1% osmium tetroxide, dehydrated in a graduated acetone series, critical-point dried, mounted on aluminum stubs and the gold-coated (Robards 1978). The material was examined with a FEI Quanta™ scanning electron microscope at 12.5 kV.

Transmission electron microscopy (TEM)

To analyses of the subcellular features of the glands, samples excised from the middle portion of the leaf blade were fixed in 2.5% glutaraldehyde in 0.1 M phosphate buffer, pH 7.3 for 24 h; post-fixed with 1% osmium tetroxide aqueous solution in the same buffer for 1 h; dehydrated in an acetone series; and then embedded in Araldite® resin. Ultra-thin sections were placed in formavar film-coated grids and stained with

uranyl acetate and lead citrate (Reynolds 1963). The samples were examined using a FEI Tecnai™ Spirit transmission electron microscope at 80 kV.

Immunolabeling of cytoskeletal elements for confocal microscopy

For immunolabeling of actin filaments and microtubules, cross sections obtained from the middle portion of fresh leaf blades were fixed with formaldehyde 4%, incubated in triton X-100 0.2% and in anti-β-tubulin-FITC (1:100 in PBS with BSA 1%) (Sigma–Aldrich®, St. Louis, MO, USA) at room temperature. After, the samples were incubated in phalloidin-rhodamine (500 µg/1 ml in methanol) (Sigma–Aldrich®, St. Louis, MO, USA) at room temperature. The slides were mounted in DAPI (Fluoroshield with DAPI, Sigma–Aldrich®, St. Louis, MO, USA), and examined in a Leica TCS SP5 confocal microscope under 488-nm, 543-nm, and 405-nm laser lines (Tozin & Rodrigues 2017).

RESULTS

Distribution of glandular trichomes in vegetative and reproductive organs

Glandular and non-glandular trichomes covered vegetative and reproductive organs of *O. gratissimum*. Glandular trichomes were observed in the stem (Fig. 1A) and in both surfaces of leaf blades (Fig. 1B), bracts (Fig. 1C) and sepals (Fig. 1D), in addition to the adaxial surface of petals (Fig. 1E). Close to the ovary numerous non-glandular trichomes covered the adaxial surface of petal (Fig. 1F).

Three morphotypes of glandular trichomes (here named I, II and III) were identified and their differential distribution in vegetative and reproductive organs is provided in Table 1.

Morphology of glandular trichomes

The morphotype I is composed of a large globose head with four cells in one layer (Fig. 2A-D), and a body constituted by a lenticular narrow stalk cell and one basal cell (Fig. 2A, E). This morphotype is sunken in deep depressions on the leaf blade (Fig. 2A, B) and is protuberant in the midrib (Fig. 2C). The head cells are covered by smooth cuticle that ruptures following the head circumference (Fig. 2D). In the active secretory stage, secretion accumulates in the large subcuticular space (Fig. 2A, E). The walls of head cells are moderately thin (Fig. 2F-G) and fibrillar content is observed in the periplasmic space (Fig. 2G); plasmodemata connect the head cells among themselves and to the stalk (Fig. 2F, H). The nucleus of head cells are voluminous (Fig. 2F); the cytoplasm is dense and abundant with numerous plastids devoid of grana and with dense aspect; the vacuoles are small; oil droplets are observed free in the cytoplasm (Fig. 2F, G). The stalk cell exhibits abundant and dense cytoplasm with plastids devoid of grana, vesicles, small vacuoles with fibrillar content (Fig. 2H), smooth endoplasmic reticulum and mitochondria. Abundant material with fibrillar aspect fills the wide periplasmic space (Fig. 2H).

The morphotype II is composed of a globose unicellular head (Fig. 3A-D) and body with unicellular stalk and one slightly elongated basal cells (Fig. 3A-C). This morphotype is protuberant in the midrib (Fig. 3B) and sunken in deep depressions along the leaf blade (Fig. 3A, C). The cuticle of head cells is distended originating a large subcuticular space (Fig. 3 A, E) that is filled with secretion with homogenous and fibrillar aspect (Fig. 3E). No signals of rupture were detected in the cuticle, but trichomes with shrunken and shriveled aspect (Fig. 3D) were commonly found. In the active secretory stage, the head cells present thin walls with loose aspect (Fig. 3E); the cytoplasm is abundant and dense with proliferate rough endoplasmic reticulum,

hyperactive dictyosomes, mitochondria with dilated cristae, plastids, vesicles, polysomes and oil drops (Fig. 3E-G); the plastids are devoid of grana and contain osmiophilic globules and starch grains (Fig. 3F); some plastids exhibit prolamellar body (Fig. 3G). The vacuoles are small and filled with fibrillar content (Fig. 3E-G) or oil bodies (Fig. 3G). The stalk cell presents walls with numerous plasmodemata connecting it to the head cell (Fig. 3H); the nucleus is large with irregular contour and the cytoplasm is abundant with numerous polysomes, rough endoplasmic reticulum, mitochondria, oil drops and plastids; the plastids are devoid of grana and contain electron dense inclusions (Fig. 3H).

The morphotype III is composed of a round two-celled head (Fig. 4A-B) and a body with a unicellular stalk and a basal cell (Fig. 4A). The head cells are covered by cuticle that ruptures by a transversal line (Fig. 4C-D) to release the secretion with flocculate aspect accumulated in the subcuticular space (Fig. 4E-Inset). In the active secretory stage, the head cells present moderately thick walls with cellulose microfibrils loosely arranged; these walls are characterized by labyrinthine projections toward the cytoplasm (Fig. 4E-G). In head cells, the cytoplasm is dense and abundant, characterized by hyperactive dictyosomes, extensive rough endoplasmic reticulum, polysomes, mitochondria and vesicles (Fig. 4E-G); the plastids are devoid of grana and contain osmiophilic inclusions of different sizes (Fig. 4F). Small vacuoles with membranous inclusions are observed (Fig. 4G). The stalk cell presents thick anticlinal walls and thin periclinal walls (Fig. 4H); the cytoplasm is abundant with numerous mitochondria, plastids devoid of grana and containing osmiophilic inclusions and smooth endoplasmic reticulum; large oil bodies are observed free in the cytoplasm and several small vacuoles with fibrillar material occur in the stalk cell (Fig. 4H).

Histochemistry of the glandular trichomes

Different categories of chemical constituents were histochemically identified in the glandular trichomes (Table 2) (Figure 5A-M). Lipophilic compounds were identified mainly in the head cells of the morphotype I, and in the stalk cells of the all morphotypes. Hidrophilic compounds were predominantly detected in the head cells of the morphotype II and III (Table 2).

Immunolabeling of the cytoskeletal elements on Confocal Microscopy

The distribution of the cytoskeletal elements was different along the parts constituents of the glandular trichomes and among the glandular morphotypes (Fig. 6A-I). In the morphotype I (Fig. 6A-C) actin filaments were moderately marked in the stalk cell (Fig. 6A); and microtubules were moderately labeled in the head cells (Fig. 6B) and strongly marked in stalk cell (Fig. 6B). The morphotypes II (Fig. 6D, F) and III (Fig. 6G, I) showed moderate marking for actin filaments in the head and stalk cells; microtubules were more intensely marked in their stalk cells (Fig. 6E, H).

DISCUSSION

In this paper we identified three different morphotypes of glandular trichomes with differential distribution in vegetative and reproductive organs of *O. gratissimum*. The use of conventional and confocal light microscopy associated to scanning and transmission electron microscopy enabled us to establish a correlation among the glandular morphotypes, the subcellular features of the gland cells, the abundance of the different cytoskeletal elements and the secretion composition.

The presence of three morphotypes of glandular trichomes as demonstrated in the present study appears to be an important characteristic to the *Ocimum* genus. Naidoo

et al. (2013) have demonstrated the same morphotypes for *O. obovatum*, and Werker et al. (1993) for *O. basilicum*. Since they are the main sites of production of essential oils (Werker et al. 1993; Naidoo et al. 2013), these glandular trichomes can be associated to the economic value of the *Ocimum* species. In fact, terpenes were here histochemically detected in all glandular morphotypes of *O. gratissimum*, mainly in the the morphotype I. However, in addition to lipophilic compounds, our histochemical tests showed hydrophilic compounds in these glands, characterizing the mixed nature of the secretion in *O. gratissimum*.

The substances secreted by glandular trichomes have an important role in ecological interaction, allowing the plant survival in many different environments (Harbone 1993; Langenheim 2003). Essential oils can provide protection against herbivores and pathogens (Dicke et al. 2003; Unsicker et al. 2009; Tozin et al. 2017), whereas polysaccharides can act in maintaining the tissues hydrated, and lubricating meristems and young organs (Ascensão et al. 1999; Tozin et al. 2015). Phenolic compounds can protect the cells against adverse effects of the UV-B radiation from excessive sunlight intensity (Liakoura et al. 1997; Silva et al. 2016).

The distinctive glandular morphotypes presented differential distribution among the *O. gratissimum* organs. This fact can be related with the differential function of each glandular morphotype (Werker 2000), associated to the differences on the main classes of compounds in each glandular morphotype. According to our histochemical tests, the morphotype I appears to be the mainly site of essential oil production. In fact, the presence of plastids devoid of grana and smooth endoplasmic reticulum, as observed in the cytoplasm of the head and stalk cells of this glandular morphotype is indicative of lipidic compound production (Fahn 1979; Evert 2006; Tozin & Rodrigues 2017). The presence of lipids in the stalk cell suggests their participation in the secretory process,

probably providing precursors for the secretion synthesis (Argyropoulou et al. 2010; Tozin et al. 2015). The abundance of plasmodemata connecting the head cells and the stalk cell supports the hypothesis that the secretion precursors can be transported via symplast from the stalk to the head cells (Tozin et al. 2015).

The morphotypes II and III produce mixed secretion, since hydrophilic and lipophilic compounds were histochemically detected in their cells. The head cells of morphotypes II and III reacted strongly for the presence of neutral polysaccharides. Lipids were absent in these cells. In fact, hyperactive dictyosomes were the predominant organelle in the head cells of both morphotypes and have been associated with hydrophilic secretion production (Ascensão et al. 1999; Evert 2006). The presence of plastids devoid of grana in the stalk cell of morphotypes II and III is a remarkable feature; and it has been responsible for the lipophilic secretion production in this cell (Fahn 1979; Evert 2006; Tozin & Rodrigues 2017). So, in these morphotypes the head is the main site of hydrophilic compound production, and the stalk are involved in synthesis of lipophilic substances.

The presence of plastids with starch grains as observed in the morphotype II is not a common feature for head cells of glandular trichomes. This finding suggests that the energy necessary for the production of secretion in these glands comes from the degradation of carbohydrates present in the plastids (Nepi et al. 1996; Paiva & Machado 2008).

The presence of cell wall with labyrinthine projections in glands, as observed here in the morphotype III, deserves some attention and has been reported for a few plant species (Bourett et al. 1994; Gama et al. 2016; Tozin & Rodrigues 2017). The outgrowths of the cell walls increase the surface of the cell boundaries favoring the exchanges between symplast and apoplast during the secretory process (Gunning & Pate

1969). This aspect has been associated with more efficiency in the process of release of secretion (Gunning & Pate 1969; Evert 2006; Tozin & Rodrigues 2017).

In the morphotype I, the essential oils are released from the head cell via ecrine (Evert 2006). The lipidic compounds cross the cell wall due to the mechanical pressure applied by the protoplasm (Paiva 2016) and accumulate in the subcuticular space. In the morphotypes II and III, the great amount of vesicles produced by the dictyosomes suggests granuclocrine process (Evert 2006; Tozin et al. 2015) for secretion release to the subcuticular space. In this process, the vesicles merge with the plasma membrane and release the secretion in the apoplastic space (Evert 2006).

In all the glandular morphotypes, the exudate is released from the protoplast and accumulates in the subcuticular spaces. The release of secretion from the head cells seems to follow different ways among the glandular morphotypes. The secretion moves out from the glandular head via cuticle ruptures, in the morphotype I and III. The rupture of the cuticle on the head cells seems to be a common feature to glandular trichomes in other Lamiaceae species (Ascensão et al. 1995; Serrato-Valentini et al. 1997; Tozin & Rodrigues 2017). In the morphotype II no cuticle ruptures was observed, suggesting that the secretion accumulated in the subcuticular is able to cross the cuticle to achieve the external environment (Silva et al. 2016); the presence of glandular trichomes with shrunken and shriveled aspect in the post-secretory stage is another evidence of this process.

Concerning the immunolabeling of the cytoskeletal elements, actin filaments were strongly marked in cells secreting mainly hydrophilic compounds such as the head cells of morphotypes II and III. On the other hand, the marking for microtubules was intensely positive in head cells of morphotype I, and in the stalk cells of morphotype II and III. In such cells, our histochemical tests showed intense oil production. More

intense reaction for actin filaments in cells producing mainly hydrophilic compounds and stronger labeling of microtubules in cells secreting lipophilic substances was also reported by Tozin & Rodrigues (2017) in a pioneer work on the cytoskeleton on secretory cells in plants. These findings corroborate the involvement of the actin filaments in the movement of vesicles secreting hydrophilic compounds (Valderrama et al. 2001; Stamnes 2002; Tozin & Rodrigues 2017). So, we suggest that the vesicles produced by the dictyosomes in the head cells of morphotypes II and III are transported until the plasmalemma by action of actin filaments. If actin filaments are involved in intracellular transport of oil bodies in these cells needs further investigation. Concerning the microtubules function, this work suggest their involvement in the oil drop transport and anchorage (Gross et al. 2000; Zehmer et al. 2009 and references therein; Tozin & Rodrigues 2017); however, new studies are proposing that the oil drops produced by the endoplasmic reticulum are displaced on it by the actin filaments, with no association with the microtubules (Tozin et al. *In prep*); on the other hand, the plastids are clearly the main site of oil drops produced in the glandular trichomes described here. This aspect deserves more attention and should be checked. Experimental studies involving the use of drugs inhibitory of polymerization cytoskeleton elements are being performed and can expand the knowledge on actin filaments and microtubules for the functioning of glandular trichomes.

Acknowledgments

We thank CNPq (444205/2014-4) for the financial support and staff of the Centro de Microscopia Eletrônica, IBB, UNESP, for helping in the sample preparation.

REFERENCES

Albuquerque UP, Medeiros PM, Almeida ALS, Monteiro JM, Lins Neto MF, Melo JG, Santos JP. 2007. Medicinal plants of the caatinga (semi-arid) vegetation of NE Brazil: a quantitative approach. Journal of Ethnopharmacology 114: 325–354.

Amaral LIV, Pereira MFDA, Cortelazzo AL. 2001. Formação das substâncias de reserva durante o desenvolvimento de sementes de Urucum (*Bixa orellana* L. - Bixaceae). Acta Bot. Bras. 15: 125–132.

Argyropoulou C, Akoumianakiloannidou A, Christodoulakis SN, Fasseas C. 2010. Leaf anatomy and histochemistry of *Lippia citriodora* (Verbenaceae). Australian Journal of Botany 58: 398-409.

Ascensão L, Marques N, Pais MS. 1995. Glandular Trichomes on Vegetative and Reproductive Organs of *Leonotis leonurus* (Lamiaceae). Annals of Botany 75: 619-626.

Ascensão L, Mota L, Castro MM. 1999. Glandular Trichomes on the Leaves and Flowers of *Plectranthus ornatus*: Morphology, Distribution and Histochemistry. Annals of Botany 84: 437-447.

Ascensão L, Pais MS. 1998. The Leaf Capitate Trichomes of *Leonotis leonurus*: Histochemistry, Ultrastructure and Secretion. Annals of Botany 81: 263-271.

Bourett TM, Howard RJ, O´Keefe DP, Hallahan DL. 2014. Gland development on leaf surfaces of *Nepeta racemosa*. International Journal of Plant Science 155(6): 623-632.

Bukatsch F. 1972. Bermerkungen zur Doppelfärbung Astrablau–Safranin. Mikrokosmos, 61: 255.

David R, Carde JP. 1964. Coloration differentielle des inclusions lipidique et terpeniques des pseudophylles du *Pin maritime* au moyen du reactif Nadi. Comptes Rendus de l' Academie dês Sciences Paris. Biologies 258: 1338–1340.

Dicke M, van Poecke RMP, de Boer JG. 2003. Inducible indirect defence of plants: from mechanisms to ecological functions. Basic Appl Ecol 4: 27–42.

Di Stasi LC, Oliveira GP, Carvalhaes MA, Queiroz Jr, M, Tien OS, Kakinami SH, Reis MS. 2002. Medicinal plants popularly used in the Brazilian Tropical Atlantic Forest. Fitoterapia 73: 69–91.

Evert RF. 2006. Esau's Plant Anatomy. 3a. ed. Wiley-Interscience, New Jersey.

Fahn A. 1979. Secretory tissues in plants. Academic Press, London.

Faria TJ, Ferreira RS, Yassumoto L, Souza JRP, Ishikawa NK, Barbosa AM 2006. Antifungal activity of essential oil isolated from *Ocimum gratissimum* L. (eugenol chemotype) against phytopathogenic fungi. Braz Arch Biol Technol 49: 867-871.

Furr M, Mahlberg PG. 1981. Histochemical analyses of laticifers and glandular trichomes in Cannabis sativa. J. Nat. Prod. 44: 153–159.

Gama TSS, Aguiar-Dias AC, Demarco D. 2016. Transfer cells in trichomatous nectary in *Adenocalymma magnificum* (Bignoniaceae). Anais da Academia Brasileira de Ciências 88(1 suppl.): 527:537.

Gross SP, Welte MA, Block SM, Wieschaus EF. 2000. Dynein-mediated cargo transport in vivo. A switch controls travel distance. J. Cell. Biol. 148: 945–956.

Gunning BES, Pate JS. 1969. “Transfer cells”: plant cells with wall ingrowths, specialized in relation to short distance transport of solutes – their occurrence, structure, and development. Protoplasma 68: 107-133.

Harbone JB. 1993. Ecological biochemistry. 4th ed. Academic Press, London, UK.

Johansen DA. 1940. Plant michrotechnique. McGraw-Hill, New York.

Langenheim JH. 2003. Plant resins: chemistry, evolution, ecology and ethnobotany. Portland, Cambridge: Timber Press.

Liakoura V, Stepfanou M, Manetas Y, Cholevas C, Karabourniotis G. 1997. Trichome density and its UV-B protective potential are affected by shading and leaf position on the canopy. Environmental and Experimental Botany 38: 223-229

Matasyoh LG, Matasyoh JC, Wachira FN, Kinyua MG, Muigai AGW, Mukiama TK 2007. Chemical composition and antimicrobial activity of the essential oil of *Ocimum gratissimum* L. growing in Eastern Kenya. Afr J Biotechnol 6: 760-765.

Mazia D, Brewer PA, Alfert M. 1953. The cytochemical staining and measurement of protein with mercuric bromphenol blue. The Biological Bulletin 104: 57-67.

Naidoo Y, Kasim N, Heneidak S, Nicholas A, Naidoo G. 2013. Foliar secretory trichomes of *Ocimum obovatum* (Lamiaceae): micromorphological structure and histochemistry. Plant, Systematics and Evolution 299: 873-885.

Nepi, M., Ciampolini, F., Pacini, E. 1996. Development and ultrastructure of *Cucurbita pepo* nectaries of male flowers. Ann. Bot. 78: 95–104.

O'Brien TP, Feder N, Mccully ME. 1964. Polychromatic staining of plant cell walls by toluidine blue. Protoplasma 59: 368-373.

Orafidiya LO, Agbani EO, Iwalewa EO, Adelusola KA, Oyedapo OO. 2004. Studies on the acute and sub-chronic toxicity of the essential oil of *Ocimum gratissimum* L. leaf. Phytomedicine 11: 71–76.

Paiva EAS. 2016. How do secretory products cross the plant cell wall to be released? A new hypothesis involving cyclic mechanical actions of the protoplast. Annals of Botany 117: 533-540.

Paiva EAS, Machado SR. 2008. The floral nectary of *Hymenaea stigonocarpa* (Fabaceae, Caesalpinioideae): Structural aspects during floral development. Annals of Botany 101: 125– 133.

Pearse AGE. 1980. Histochemistry theoretical and applied: preparative and optical technology. 4.ed. Edinburgh: Churchill Livingston, 439p.

Reynolds ES. 1963. The use of lead citrate at high pH as an electron-opaque stain in electron microscopy. J. Cell Biol. 17: 208–212.

Robards AW. 1978. An introduction to techiniques for scanning electron microscopy of plant cells. in: Electron Microscopy and Cytochemistry of Plant Cells. J. L. Hall. (eds.). New York, Elsevier.

Rodrigues L, Póvoa O, Teixeira G, Figueiredo AC, Moldão M, Monteiro A. 2013. Trichomes micromorphology and essential oil variation at different developmental stages of cultivated and wild growing *Mentha pulegium* L. populations from Portugal. Industrial Crops and Products 43: 692-700.

Serrato-Velentini G, Bisio A, Cornara L, Ciarallo G. 1997. Structural and Histochemical Investigation of the Glandular Trichomes of *Salvia aurea* L. Leaves, and Chemical Analysis of the Essential Oil. Annals of Botany 79: 329-36.

Silva SCM, Tozin LRS, Rodrigues TM. 2016. Morphological and histochemical characterization of secretory sites of bioactive compounds in *Lantana camara* L. (Verbenaceae) leaves. Botany 94: 321-336.

Stamnes M. 2002. Regulating the actin cytoskeleton during vesicular transport. Current Opinion in Cell Biology 14: 428-433.

Tchoumbougnang F, Amvam Zollo PH, Aviessi F, Alitonou GA, Sohounhloue DK, Ouamba JM, Tsomambet A, Andissa NO, Dagne E, Agnaniet H, Bessière JM, Menut C. 2006. Variability in the chemical compositions of the essential oils of five *Ocimum* species from Tropical African area. Journal of Essential Oil Research 18: 194–199.

Tozin LRS, Marques MOM, Rodrigues TM. 2017. Herbivory by leaf-cutter ants changes the glandular trichomes density and the volatile components in an aromatic plant model. AoB Plants 9(6): plx057.

Tozin LRS, Rodrigues TM. 2017. Morphology and histochemistry of glandular trichomes in *Hyptis villosa* Pohl ex Benth. (Lamiaceae) and differential labeling of cytoskeletal elements. Acta Botanica Brasilica 31(3): 330-343.

Tozin LRS, Carvalho SF, Machado SR, Rodrigues TM. 2015. Glandular trichome diversity on leaves of *Lippia origanoides* Kunth and *Lippia stachyoides* Cham. (Verbenaceae): morphology, histochemistry and ultrastructure. Botany 93: 297-306.

Unsicker SB, Kunert G, Gershenzon J. 2009. Protective perfumes: The role of vegetative volatiles in plant defense against herbivores. Current Opinion in Plant Biology 12: 479–485

Valderrama F, Duran JM, Babia T, Barth H, Renau-Piqueras J, Egea G. 2001. Actin microfilaments facilitate the retrograde transport from the Golgi complex to the endoplasmic reticulum in mammalian cells. Traffic 2: 717-726.

Werker E. 2000. Trichome Diversity and Development. Advances in Botanical Research 31.

Werker E, Putievsky E, Ravid U, Dudai N, Katzir I. 1993. Glandular hairs and essential oil in developing leaves of *Ocimum basilicum* L. (Lamiaceae). Annals of Botany 71: 43–50.

Zehmer JK, Huang Y, Peng G, Pu J, Anderson RGW, Liu P. 2009. A role for lipid droplets in inter-membrane lipid traffic. Proteomics 9(4): 914-921.

TABLES

Table 1. Distribution of three morphotypes of glandular trichomes in the vegetative and reproductive organs of O*cimum gratissimum* (Lamiaceae).

Organs/region	Glandular morphotypes		
	I	II	III
Stem	+	+	+
Leaf blade (abaxial surface)	+	+	+
Leaf blade (adaxial surface)	+	+	+
Bract (abaxial surface)	+	+	+
Bract (adaxial surface)	-	+	+
Sepal (abaxial surface)	+	+	+
Sepal (adaxial surface)	-	+	+
Petal (abaxial surface)	-	-	-
Petal (adaxial surface)	-	+	-
Filament	-	-	-
Style	-	-	-
Ovary	-	-	-

Note: +, presence; -, absence.

Table 2. Histochemical tests to three morphotypes of glandular trichomes in leaves of *Ocimum gratissimum* (Lamiaceae).

Metabolic group	Reagent	I		II		III	
		HC	SC	HC	SC	HC	SC
Total lipids	Sudan IV	++	++	-	+	-	++
Total lipids	Sudan Black	++	++	-	+	-	++
Terpenes	Nadi reagent	++	+	-	+	-	++
Phenolic compounds	Ferric trichloride	-	-	++	+	-	-
Alkaloids	Wagner reagent	-	-	-	-	-	-
Proteins	Bromophenol blue	-	++	++	-	+	-
Neutral polysaccharides	PAS	-	-	++	+	++	-

Note: SC, stalk cell; HC, head cell; +, ++ abundance relative; -, absence; PAS, periodic acid-Schiff's.

LEGENDS OF FIGURES

Figure 1. Distribution of glandular trichomes in vegetative and reproductive organs of *Ocimum gratissimum*. (A) Cross sections of stem under light microscopy. Gt: glandular trichome. (B) Cross section of leaf blade under light microscopy showing the glandular trichomes (Gt). Ngt: non-glandular trichomes. (C) Cross section of bract under light microscopy showing the glandular trichomes (Gt) in both surfaces. (D) Cross sections of sepal under light microscopy. Gt: glandular trichome. (E) Cross sections of petal under light microscopy showing the only glandular trichome (Gt) morphotype present in this organ. (F) Cross sections of petal in its basal part under light microscopy showing numerous non-glandular trichomes (Ngt). Bars: 100 μm.

Figure 2. Morphotype I of glandular trichome in *Ocimum gratissimum*. (A) Light micrograph showing trichome with head cells (Hc) with subcuticular space (Ss), stalk cell (Sc) and basal cell (Bc). (B-D) Scanning electron micrographs. (B-C) The glandular trichome in the leaf blade (B) and midrib (C). (D) Detail showing the cuticle (ct) ruptures exposing the head cells (Hc). (E-H) Transmission electron micrographs. (E) General aspect of the trichome with electron dense head cells (Hc) and subcuticular space (Ss). Sc: stalk cell. Bc: basal cell. (F-G) Head cells (Hc) showing dense cytoplasm with plastids (Pl) devoid of grana, small vacuoles (Va), and oil droplets (Ol) free in the cytoplasm. Note the voluminous nucleus (Nu). Cw: cell wall; Sc: stalk cell. (H) Stalk cell with dense cytoplasm with plastids (Pl) devoid of grana and vesicles (Ve). The arrow indicates plasmodemata connecting it to the head cells. Note the periplasmic space (Ps) filled with fibrillar material. Cw: cell wall. Bars: A-D = 25 μm; E = 10 μm; H = 0.5 μm; F-G = 1 μm.

Figure 3. Morphotype II of glandular trichome in *Ocimum gratissimum*. (A) Light micrograph showing trichome with head cell (Hc), stalk cell (Sc) and basal cell (Bc). (B-D) Scanning electron micrographs. (B-C) Glandular trichome in the midrib (B) and leaf blade (C). (D) Glandular trichome with shrunken and shriveled aspect in the post-secretory stage. (E-H) Transmission electron micrographs. (E) Head cell showing wide subcuticular space (Ss), and dense cytoplasm with rough endoplasmic reticulum (Rer), dictyosomes (Di) and vacuoles (Va). Cw: cell wall. (F) Detail of head cell showing hyperactive dictyosomes (Di), rough endoplasmic reticulum (Rer), mitochondria (Mi), plastids (Pl) with starch grain (St) and small vacuoles (Va). (G) Head cell with nucleus (Nu), cytoplasm dense with rough endoplasmic reticulum (Rer), dictyosomes (Di), vesicles (Ve), plastids (Pl) with prolamellar body (Pb), small vacuoles (Va) and oil droplets (Ol). (H) Stalk cell showing numerous periclinal wall with plasmodemata (arrow) connecting to the head cell (Hc), voluminous nucleous (Nu), and cytoplasm with rough endoplasmic reticulum (Rer), abundant polysomes and plastids (Pl) devoid of grana containing osmiophilic inclusions. Bars: A-D = 10 μm; E = 1 μm; F-H = 0.5 μm.

Figure 4. Morphotype III of glandular trichome in *Ocimum gratissimum*. (A) Light micrograph showing glandular trichome with head cells (Hc), stalk cell (Sc) and basal cell (Bc). (B-D) Scanning electron micrographs. (B) Overview of the glandular trichome with two head cells. (C) Detail showing the cuticle ruptures (arrowheads). (D) Detail showing the head cells (Hc) exposed after cuticle (Ct) ruptures. (E-H) Transmission electron micrographs. (E) Head cell with thick cuticle (Ct), cell wall (Cw) with labyrinthine projections (*), and dense cytoplasm with extensive rough

endoplasmic reticulum (Rer) and plastids (Pl). The inset shows the subcuticular space filled by flocculated secretion. (F) Detail of the head cell showing rough endoplasmic reticulum, plastids (Pl) with large osmiophilic inclusions, mitochondria (Mi) and vacuoles (Va). *: labyrinthine projections in cell walls. (G) Head cell with labyrinthine projections (*) in the wall (Cw), hyperactive dictyosomes (Di), vesicles (Ve) and small vacuoles (Va). (H) Stalk cell showing thick anticlinal cell wall (Cw), and cytoplasm with numerous small vacuoles (Va) with fibrillary content, plastids (Pl) devoid of grana, and large oil (Ol) drop. Bars: A-D = 10 μm; E, F, H = 1 μm; G = 0.5 μm.

Figure 5. Histochemical tests of glandular trichomes in *Ocimum gratissimum* leaf blade. (A-D) Morphotype I. (E-I) Morphotype II. (J-M) Morphotype III. (A, J) Sudan IV. (B, E) Sudan black. (C, F, K) Nadi reagent. (D, H, L) Bromophenol blue. (G) Ferric Trichloride. (I, M) PAS. Bars: 20 μm.

Figure 6. Immunolabeling of cytoskeletal elements in the glandular trichomes in *Ocimum gratissimum* (Lamiaceae) leaf blade under confocal microscopy. (A-C) Morphotype I. (D-F) Morphotype II. (G-I) Morphotype III. (A, D, G) F-actin labeling by phalloidin-rhodamine. (B, E, H) Microtubule labeling by anti-β-tubulin-FITC. (C, F, I) F-actin and microtubule labeling by anti-β-tubulin-FITC and phalloidin-rhodamine. Bars: 10 μm.

FIGURES

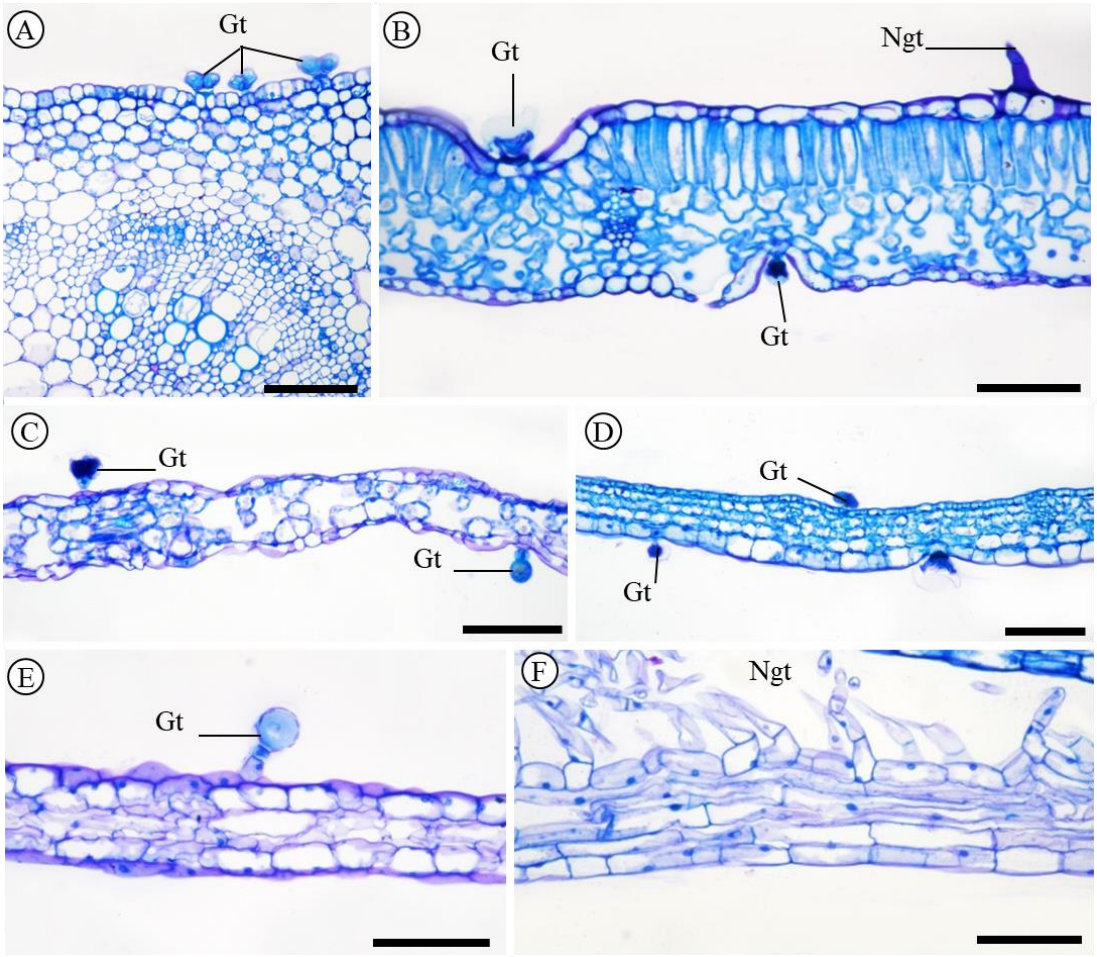

Figure 1

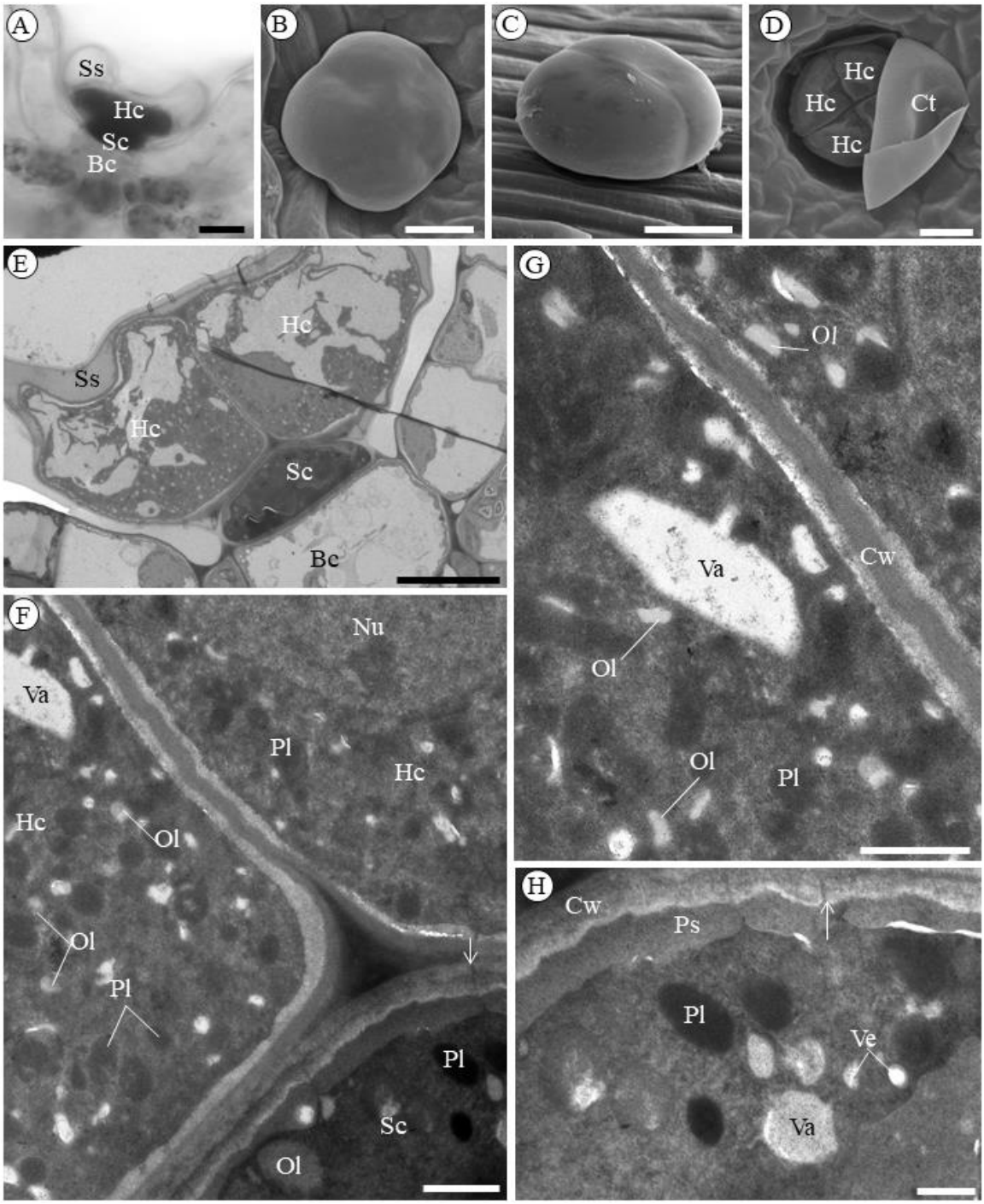
A
Ss
Hc
Sc
Bc
B
C
D
Hc
Hc
Ct
Hc
E
Hc
Ss
Hc
Sc
Bc
G
Ol
Va
Cw
Ol
Ol
Pl
F
Nu
Va
Pl
Hc
Hc
Ol
Ol
Pl
Pl
Sc
Ol
H
Cw
Ps
Pl
Ve
Va

Figure 2

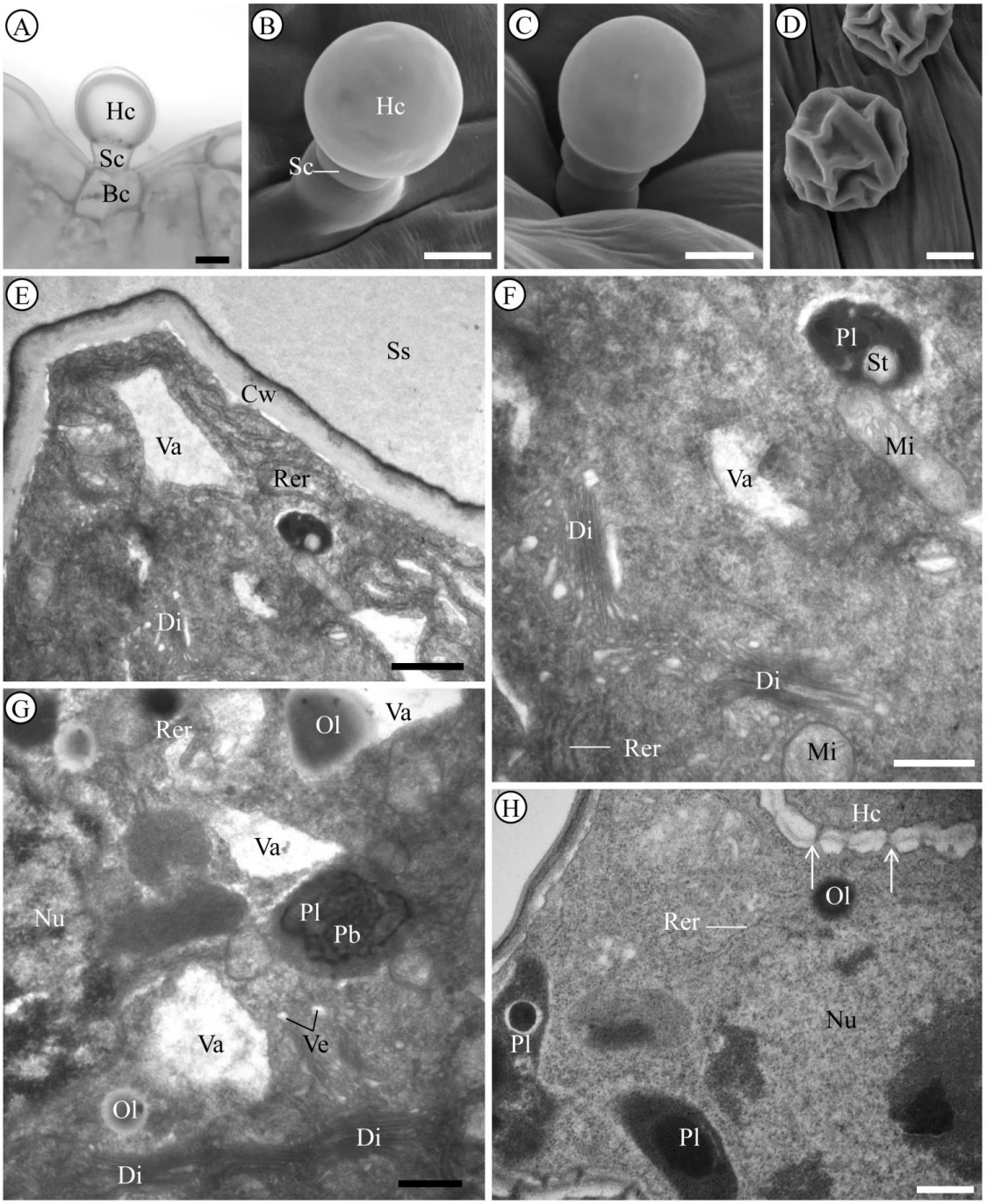
A
Hc
Sc
Bc
B
Hc
Sc
C
D
E
Ss
Cw
Va
Rer
Di
F
Pl
St
Mi
Va
Di
Di
Rer
Mi
G
Rer
Ol
Va
Va
Nu
Pl
Pb
Va
Ve
Ol
Di
Di
H
Hc
Ol
Rer
Nu
Pl
Pl

Figure 3

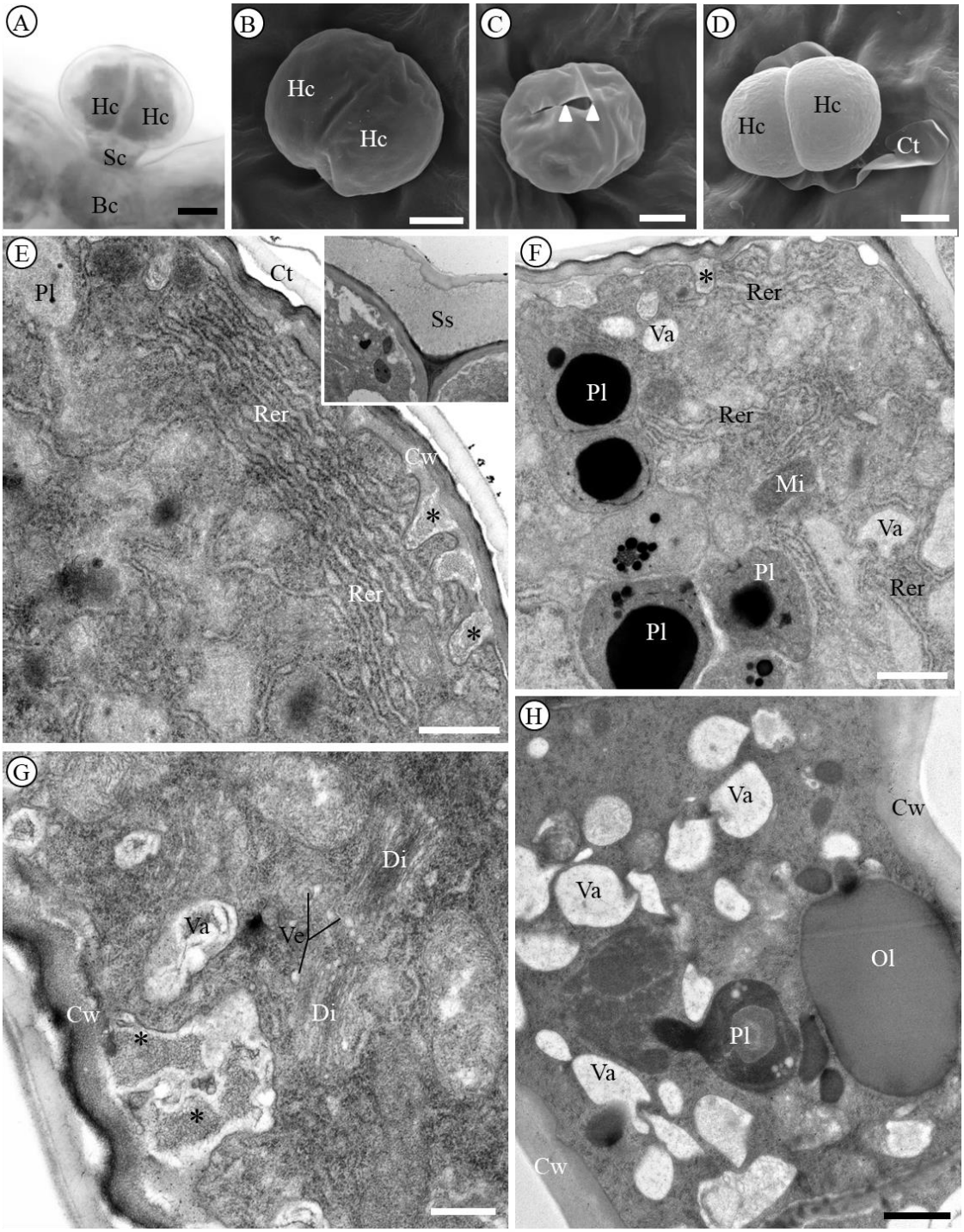
A
Hc
Hc
Sc
Bc
B
Hc
Hc
C
D
Hc
Hc
Ct
E
Pl
Ct
Ss
Rer
Cw
Rer
F
Va
Rer
Pl
Rer
Mi
Va
Pl
Rer
Pl
G
Di
Va
Ve
Cw
Di
H
Va
Cw
Va
Ol
Pl
Va
Cw

Figure 4

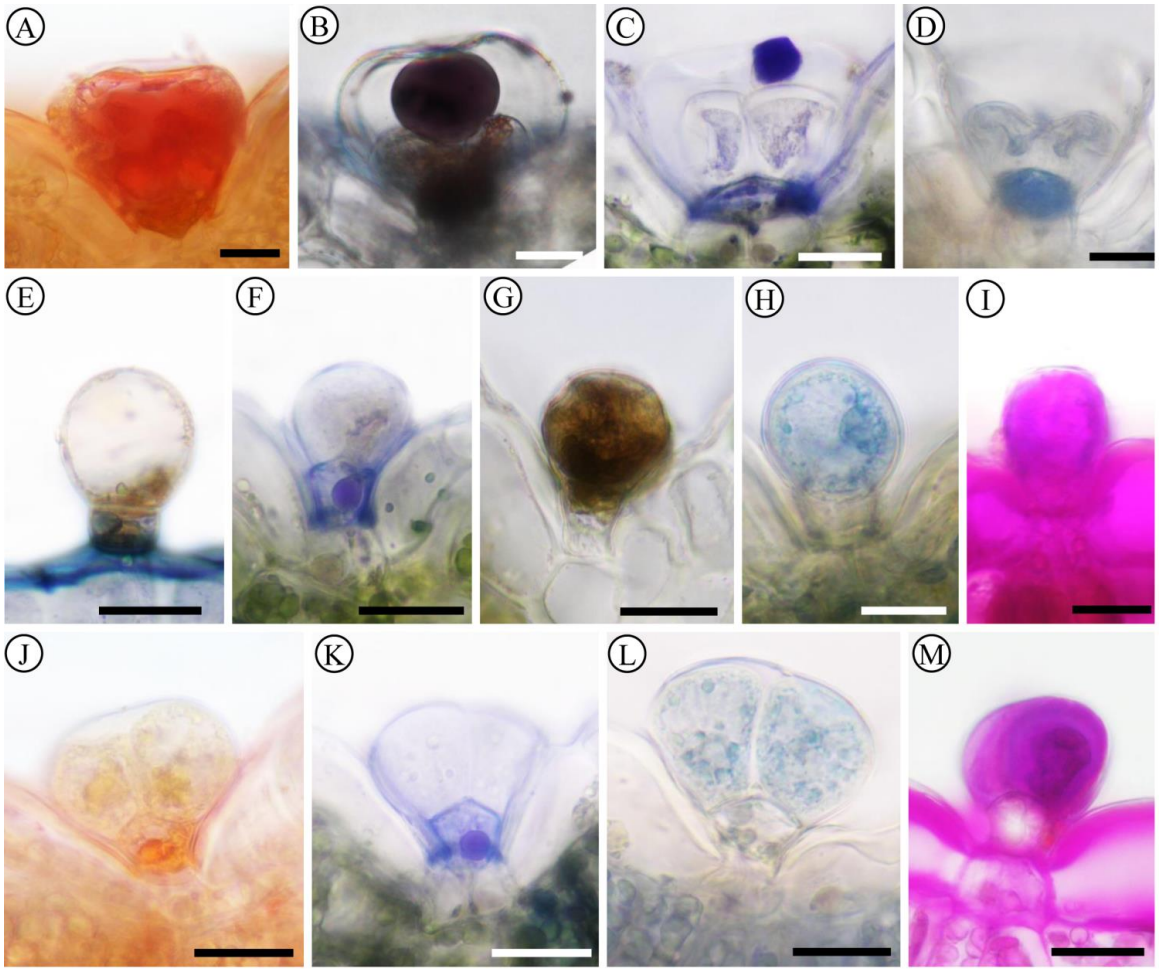

Figure 5

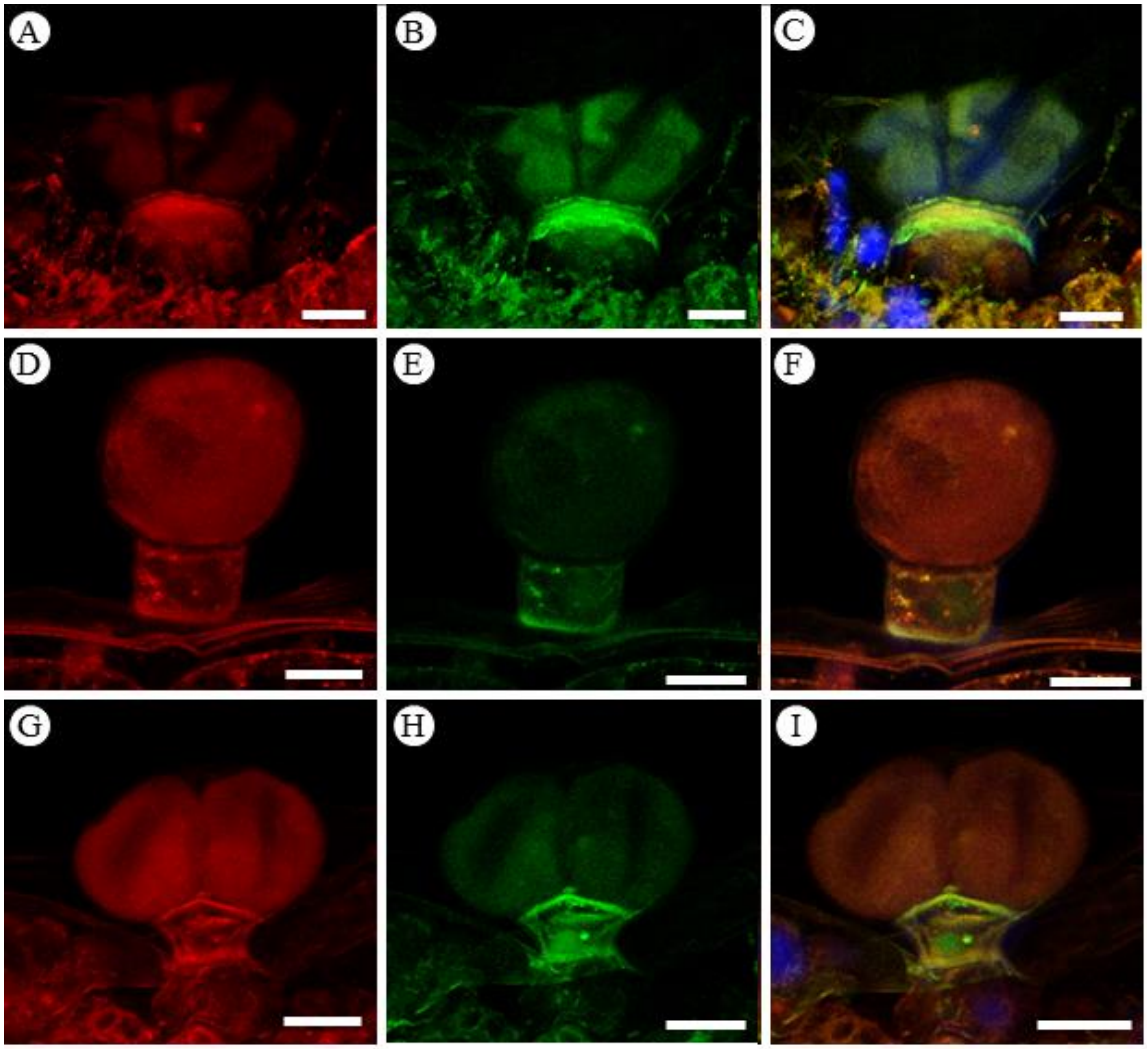

Figure 6

Capítulo 2

Influence of cytoskeletal polymerization inhibiting drugs and levels of Ca^{+2} on glandular trichomes of two Lamiaceae species

Luiz Ricardo dos Santos Tozin[1]*, Marcia Ortiz Mayo Marques[2], Tatiane Maria Rodrigues[1]

[1]São Paulo State University (UNESP), Institute of Biosciences of Botucatu (IBB), Department of Botany, Botucatu, SP, Brazil.

[2]Agronomic Institute of Campinas (IAC), Laboratory of Natural Products, Campinas, SP, Brazil.

*Corresponding author (ricardo.tozin@gmail.com)

ABSTRACT

The cellular features of glandular trichomes have been extensively studied in plants belong to different families, but the role of the cytoskeleton in the gland morphology and functioning has been neglected. We investigated the morphological and subcellular alterations in glandular trichomes of two Lamiaceae species resultant from problems in the cytoskeleton polymerization caused by destabilizing drugs and low levels of Ca^{+2}, a known modulator of cytoskeleton activity. Plants of *Hyptis villosa* and *Ocimum gratissimum* were submitted to Oryzalin and Cytochalasin D and 240 mgL^{-1}, 160 mgL^{-1}, 80 mgL^{-1}, 40 mgL^{-1} and 0 $mgL^{-1}$of Ca^{+2}. The samples were analyzed using confocal and scanning and transmission electron microscopy. Gas-exchange indixes and the volatile components composition were analyzed in *O. gratissimum* plants under Ca^{+2} treatments.

Both, cytoskeleton destabilizing drugs and the low levels of Ca^{+2}, lead to morphological alterations in wall structure of glandular head cells in both species, in addition to degradation of the cytoplasm and its organelles. The immunolabeling of cytoskeletal elements produced differential marking for each treatment. The gas exchange indexes decreased in plants submitted to low levels of Ca^{+2}; and the essential oil composition was not affected. Our results show that both, cytoskeleton destabilizing drugs and low levels of Ca^{+2}, cause similar structural alterations in glandular trichomes, leading to problems mainly concerning on the secretion release. New studies involving molecular approaches must be conducted to elucidate the role of the cytoskeletal elements during the morphogenesis and functioning of glandular trichomes.

Keywords: actin filaments, glandular hairs, *Hyptis*, microtubules, *Ocimum*.

1. INTRODUTION

The origin, morphology and subcellular features involved in the secretory process of glandular trichomes have been issues exhaustively studied for several plant species (Ascensão & Pais 1998; Papini et al. 2010; Argyropoulou et al. 2010; Appezzato-da-Glória et al. 2012; Naidoo et al. 2012; Amrehn et al. 2014; Tozin et al. 2015; Silva et al. 2016; Tozin & Rodrigues 2017 and references therein). However, some important aspects such as the role of the cytoskeletal elements in the gland morphology and functioning have been neglected.

Recent studies have demonstrated the relation between the predominance of the actin filaments and microtubules in the secretory cells and the composition of secretion in glandular trichomes of *Hyptis villosa* (Tozin & Rodrigues 2017) and *Ocimum gratissimum* (Tozin & Rodrigues, *in prep*), suggesting the involvement of these elements in the intracellular processes of production, transport and release of the

exsudate. In addition, researches have showed the involvement of cytoskeleton elements in the origin and maintenance of non-glandular hairs in model species (Szymanski et al 1999; Kost et al. 1999; Mathur et al. 1999), but not in glandular trichomes. In this sense, it has been assumed that microtubules play an important role in the stalk formation and branching initiation in non-glandular hairs, while actin filaments are key elements in the elongation of the branches and maintenance of the shape of mature non-glandular hairs (Kost et al. 1999; Mathur et al. 1999). In *Arabidopsis*, it has been proved that the non-polimerization of actin filaments avoids the formation of non-glandular hairs (Szymanski et al. 1999). So, it is presumed that problems concerning the cytoskeleton polymerization can also cause structural and functional anomalies in glandular hairs, but supporting studies are lacking.

The proper functioning of cytoskeleton in plant cells is closely associated to the availability of some minerals, mainly the calcium (Ca^{+2}) (Hepler 2005). The essentiality of Ca^{+2} in the cytoskeleton polymerization has been demonstrated in the movement of pulvinus (Yao et al. 2008), stomata cells and in pollen tube growth (Chen et al. 2013). Concerning the to secretory systems in plants, Huang et al. (2010) showed that reduced amount of secretion is produced in *Lavandula pinnata* plants under low Ca^{+2} concentrations; this could be resultant from the reduction in the photosynthetic performance caused by low levels of Ca^{+2} (Chaves et al. 2003; Zhang et al. 2010; Kudoyrova et al. 2013).

In this paper, we investigated morphological and subcellular alterations in glandular trichomes of two Lamiaceae species resultant from problems in the cytoskeleton polymerization caused by destabilizing drugs and low levels of Ca^{+2}. Indexes of gas-exchanges under different Ca^{+2} levels are presented searching for relation with the essential oil production. For this, we employed *Ocimum gratissimum* and *Hyptis villosa*,

two Lamiaceae species which glandular trichomes have morphology and ultrastructure known (Tozin & Rodrigues 2017; Tozin & Rodrigues *in prep*.). Due the easy recognition of their glandular morphotypes, these species appears to be good models to studies under experimental conditions.

2. MATERIAL AND METHODS

2.1. Plant material

For cuttings, stem fragments of *Ocimum gratissimum* and *Hyptis villosa* approximately 10 cm long were placed in trays containing commercial substrate (Bioplant®, Nova Ponte, Minas Gerais, Brazil) and maintained under humid conditions until rooting. After 35 days, plants were transferred to 6.0 L pots filled with complete Hoagland and Arnon's (1950) n^{o}. 2 nutrient solution at 75% ionic concentration (*O. gratissimum*) and at 50% ionic concentration (*H. villosa*), based on previous tests. The pots were kept in a greenhouse under mean maximum and minimum air temperatures of 26.5°C and 21.5°C, respectively, and a mean relative humidity of 75% until harvesting. The solutions were prepared using deionized water and were constantly aerated and renewed every two weeks to minimize nutrient depletion or pH changes.

Vouchers were deposited in the Irina Delanova Gemtchújnicov Herbarium (BOTU), of the Department of Botany, Institute of Biosciences of Botucatu, IBB, UNESP, Botucatu, São Paulo, Brazil, under registration numbers 32798 and 32799.

2.2. Treatments with cytoskeleton destabilizing drugs

At 60 days after transplanting to the hydroponic system, plants of *H. villosa* (n = 5) and *O. gratissimum* (n = 5) were subjected to cytoskeleton destabilizing drugs treatments. The treatments consisted of total control (H_2O); DMSO 0.1% (Control);

Oryzalin (10 and 50 µM) in DMSO 0.1% - destabilizing drug of microtubules; and Cytochalasin D (10 and 30 µM) in DMSO 0.1% - destabilizing drug of actin filaments. The concentration of each treatment was determined based on the technique of Mathur et al. (1999) and preliminary tests. The apex of each plant was sprayed with the treatment every 24 h. After 10 days, newly formed leaf primordia were collected to be processed for analysis in confocal and scanning and transmission electron microscopes.

2.3. Treatment with Ca^{+2} levels and experimental design

At 60 days after transplanting to the hydroponic system, plants of *O. gratissimum* and *H. villosa* were subjected to Ca^{+2} treatments. The treatments for *O. gratissimum* consisted of a control (240 mgL^{-1} of Ca^{+2}) and four levels of Ca^{+2} 160 mgL^{-1}, 80 mgL^{-1}, 40 mgL^{-1} and 0 mgL^{-1}. For *H. villosa*, the plants were submitted to the 160 mgL^{-1} (control), 80 mgL^{-1} and 40 mgL^{-1} and 0 mgL^{-1}. The control for each species was established based on previous tests. The pots were arranged in a randomized design in a greenhouse with four pots (n = 4) exposed to each treatment.

At 18 days after the application of the treatments, a new expanded leaf pair of each plant, from both species, was collected to be analyzed in confocal and scanning and transmission electron microscope. Simultaneously, *O. gratissimum* plants were used to measure the rates of leaf gas-exchange. Finally, samples of leaves and inflorescences of *O. gratissimum* were collected to analysis of volatile components composition.

2.4. Scanning electron microscopy (SEM)

For analysis of glandular micromorphology and density, leaves samples were fixed in 2.5% glutaraldehyde with 0.1 M phosphate buffer, pH 7.3, overnight at 4 °C, dehydrated in a graduated acetone series, critical-point dried, mounted on aluminum

stubs, gold-coated (Robards 1978). The material was examined with a FEI Quanta™ scanning electron microscope.

The glandular density in leaves was calculated in 1 mm^2 using the Scandium software with an image-capture system coupled to the scanning electron microscope. The data were submitted to ANOVA followed by Tukey test, at a 5% probability level.

2.5. Transmission electron microscopy (TEM)

To analyses of the subcellular features of the glands, leaves fragments were fixed in 2.5% Karnovsky in 0.1 M phosphate buffer, pH 7.3 for 24 h; post-fixed with 1% osmium tetroxide aqueous solution in the same buffer for 1 h; dehydrated in an acetone series; and embedded in Araldite® resin. Ultra-thin sections were stained with uranyl acetate and lead citrate (Reynolds 1963). The samples were examined using a FEI Tecnai™ Spirit transmission electron microscope.

2.6. Immunolabeling of cytoskeletal elements for confocal microscopy

For immunolabeling of actin filaments and microtubules, cross sections of fresh leaves were fixed in 4% paraformaldehyde in PBS for 1h; washed in PBS (3 x 20 min); incubated in 0.2% triton x-100 for 15 min; washed in PBS (3 x 5 min); incubated in phalloidin-rhodamine (1:900 in PBS) for 25 min; washed in PBS (3 x 5 min); incubated in anti-β-tubulin-FITC (1:100 in PBS with 1% BSA); washed in PBS (3 x 5 min); and mounted in DAPI. The material was analyzed with confocal microscope Leica TCS SP5, and the relevant results were documented.

2.7. Measurements of leaf gas-exchange rates

For measure the gas-exchange, we analyzed plants after 18 days of exposure to Ca^{+2} experiment. Four plants (n = 4) of each treatment were measured for: the net photosynthetic rate (Pn, in μmol m^{-2} s^{-1}), stomatal conductance (g_s in mol m^{-2} s^{-1}), intracellular carbon concentration (Ci μmolCO_2 mol^{-1}air), transpiration rate (Tr in mmol m^{-2} s^{-1}), water use efficiency (WUE mol CO_2 (mmol H2O)$^{-1}$), and carboxylation efficiency (Pn/Ci mmol m^{-2} s^{-1} Pa^{-1}) in the second fully expanded leaves using an *Infra-Red Gas Analyzer* (Li-6400, LI-COR, Inc., Lincoln, NE), between 09:00 am and 10:00 am. The CO_2 concentration reference used during evaluations was the level present in the environment, ranging from 390 to 410 μmol CO_2 mol^{-1} and temperature of 29 °C, humidity of 41% and light level PPFD of 1500 μmol m^{-2} s^{-1}. The data were submitted to ANOVA followed by Tukey test, at a 5% probability level.

2.8. Essential oil composition

To analyze the composition of the volatile compounds, leaves and inflorescences exposed to the treatment for 18 days were collected. Plants (n = 3) of each treatment were analyzed. Samples with 0.45 g were placed in vial with 15 mL of deionized water. The vials were submitted a hydrodistillation-like method. They were placed in water at 95 °C for 1 h; posteriorly, it was utilized the solid-phase microextraction (SPME) technique. The volatile phase was exposed to CAR/PDMS fiber (Carboxen/Polydimethylsiloxane, film thickness 75 μm, Supelco, Bellefonte, PA, EUA) for 15 and 30 min; and it was designated as capture great time 15 min.

The fiber was injected in the gas chromatograph, and the qualitative and quantitative (area normalization method) analysis of the essential oil was performed on a gas chromatograph coupled to a mass spectrometer (CG-MS, Shimadzu, QP- 5000), with an OV-5 fused silica capillary column (30 m x 0.25 mm x 0.25 μm, Ohio Valley Specialty

Chemical, Inc.), operating at an MS ionization voltage of 70 eV, with helium as the carrier gas (1.0 mL/min.). The following chromatography conditions were used: injector at 240 °C, detector at 230 °C, split 1/20, and the temperature program: 50 °C, 2 min; 50 °C - 180 °C, 3 °C/min; 180 °C – 230 °C, 10 °C/min. The compounds were identified by comparison of the acquired mass spectra with those stored in the GC/MS database of the system (NIST 62 lib.) and retention indices (Adams 2007). The retention indices (RI) were obtained from the injection of a mixture of n-alcanes (Sigma-Aldrich, C9-C24), employing the same temperature program conditions described above for GC/MS, applying the equation of Van den Dool and Kratz (1963). For each sample the fiber was conditioned in GC-FID (Shimadzu, GC-2010/AOC-20i) with the temperature program: 50 °C - 240 °C, 7 °C/min.

3. RESULTS

3.1. Effects of cytoskeleton destabilizing drugs in the glandular trichomes

3.1.1. Morphology and ultrastructure

The general aspects of *O. gratissimum* and *H. villosa* leaf surfaces remained constant in all treatments (Fig. 1A-C and 2A-C), i.e., glandular and non-glandular trichomes were formed independently of the treatments.

In *O. gratissimum*, three morphotypes of glandular trichomes were analyzed and we focused on the features of their head cells. The morphotype I has a wide four-celled head; under control treatment, the head cells exhibited slightly thin walls with regular aspect, in addition to dense and abundant cytoplasm with numerous plastids devoid of grana and vesicles (Fig. 1D). Under Oryzalin treatment, the cell walls seemed thicker presented irregular contour (Fig. 1E); consequently, the plasmalemma also showed

more irregular contour (Fig. 1E); the cytoplasm presented irregular appearance with denser and homogenous areas (Fig. 1E) and clearer areas filled with flocculate aspect (Fig. 1F); fewer plastids and vesicles were observed (Fig. 1F, G) in comparison to control; the organelles were poorly defined (Fig. 1E-F); and oil drops remained present free in the cytoplasm (Fig. 1E, F). Under Cytochalasin D, the cell walls showed pronounced foldings and cytoplasm showed a fibrillar aspect; plastids and mitochondria were observed (Fig. 1G). The morphotype II has a unicellular head. Under the control treatment showed head cells with thin walls with regular contour (Fig. 1H); the cytoplasm was dense with hyperactive dictyosomes, rough endoplasmic reticulum, mitochondria with dilated cristae and plastids devoid of grana containing osmiophilic inclusions; the vacuoles were scarce and small (Fig. 1H). Under Oryzalin treatment, the vacuome became more developed (Fig. 1I); few dictyosomes, vesicles and profiles of rough endoplasmic reticulum were observed (Fig. 1I-J). The plastids became more electron-dense (Fig. 1I); and multivesicular body were observed (Fig. 1J-Inset). Ribosomes were more abundant (Fig. 1J). Under treatment with Cytochalasin D, the cell walls acquired irregular contour (Fig. 1K) and electron-lucent impregnations (Fig. 1L); the cytoplasm presented flocculate aspect and the ribosomes were abundant (Fig. 1 K, L); the vacuome were more developed in compare to control (Fig. 1 K, L); organelles presented lower definition of membranes (Fig. 1K-L). The morphotype III has a bicellular head. Under the control treatment presented head cells with walls forming labyrinthine projections (Fig. 1M); subcuticular space with homogeneous secretion (Fig. 1); and abundant cytoplasm of head cells showed dictyosomes, extensive rough endoplasmic reticulum, and small plastids devoid of thylakoids and with osmiophilic inclusions (Fig. 1M). Under Oryzalin treatment, these cell walls showed less developed labyrinthine projections (Fig. 1N); the cytoplasm presented voluminous plastids filled

with osmiophilic inclusions, mitochondria, dictyosomes and rough endoplasmic reticulum (Fig. 1N-O).Secretion were accumulated in the subcuticular space (Fig. 1N). Under Cytochalasin D treatment, the head cell walls did not show labyrinthine projections, but exhibited irregular aspect with foldings (Fig. 1P); the cytoplasm was denser (Fig. 1P) and showed extensive rough endoplasmic reticulum (Fig. 1P). Dictyosomes and plastids were less evident (Fig. 1P).

Three morphotypes of glandular trichomes of *H. villosa* were analyzed. The morphotype I has a four-celled head with conspicuous subcuticular space. Under the control treatment, the head cells present dense and abundant cytoplasm with numerous plastids with tubular inclusions (Fig. 2D-Inset). A wide subcuticular space filled with secretion was commonly observed (Fig. 2D). Under Oryzalin treatment, the cytoplasm of head cells was very denser with low definition of organelles; the subcuticular space was absent (Fig. 2E-F). Until now, this glandular morphotype under Cytochalasin D treatment was not found for analysis in MET. The morphotype II has a bicellular head and a wide subcuticular space. Under the control treatment showed walls forming labyrinthine ingrowths in head cells (Fig. 2G); the abundant cytoplasm of these cells contained hyperactive dictyosomes, smooth and rough endoplasmic reticulum and small plastids devoid of grana (Fig. 2G and Inset). Under Oryzalin treatment, the cell walls did not present labyrinthine projects and the subcuticular space is less developed (Fig. 2H); the cytoplasm showed proliferative rough endoplasmic reticulum, numerous plastids with osmiophilic inclusions, abundant dictyosomes and vesicles (Fig. 2H-I). Some organelles showed degradation signals (Fig. 2I). The Cytochalasin D also promoted the inhibition of the labyrinthine projects formation; the cytoplasm was flocculated with plastids with tubular system poorly developed, abundant ribosomes, multivesicular bodies and large vacuoles (Fig. 2J-K). Rough endoplasmic reticulum was

observed as whorls that surrounded portions of the cytoplasm (Fig. 2J). The morphotype III has a unicelular rounded head and a large unicelular pedestal. Under the control treatment exhibited head cells with thin walls, large nucleus and voluminous vacuoles (Fig. 2L); the cytoplasm was dense with electron-dense plastids, mitochondria and rough endoplasmic reticulum (Fig. 2L). Under Oryzalin treatment, the nucleus was reduced with irregular contour; the vacuome became more developed with membranous and flocculate inclusions (Fig. 2M); the plastids appeared in process of lysis, with degenerate areas (Fig. 2N). The Cytochalasin D induced the proliferation of rough endoplasmic reticulum; the plastids showed more intense lysis signals (Fig. 2O). No alteration in the cell wall was observed in this glandular morphotype.

3.1.2. Immunolabeling of cytoskeletal elements in confocal microscopy

In the glandular trichomes of *O. gratissimum*, the microtubule labeling was strongly affected by the Oryzalin; in this species, the actin filaments remained reactive to the immunolabeling after the treatments (Fig. 3). On the other hand, the immunolabeling of the microtubules and actin filaments were not affected by the Oryzalin and the Cytochalasin D, respectively, in the glandular trichomes of *H. villosa* (Fig. 4).

3.2. Effects of Ca^{+2} decrease in the glandular trichomes

3.2.1 Morphology and density of the glandular trichomes

In *O. gratissimum*, different levels of Ca^{+2} did not affect the density of each morphotype of glandular trichomes in both leaf blade surfaces (Tab. 1). However, the general features of the leaf surface and the morphology of the glandular trichomes were affected by the low levels of Ca^{+2} (Fig. 5A-E). Plants subjected to total absence of Ca^{+2} showed leaves with epidermal cells with irregular and wrinkled shape and collapsed

areas (Fig. 5E). All morphotypes of glandular trichomes showed withered aspect and ruptured cuticle (Fig. 5E). Points of detachment of glandular trichomes were commonly observed (Fig. 5E). Under the treatment with 40 mgL^{-1} of Ca^{+2} the leaves showed ordinary epidermal cells with slightly irregular format; but the morphological aspects of the glandular trichomes were preserved (Fig. 5D). On the other hand, the trichome morphology of plants subjected to 80 mgL^{-1} (Fig. 5C) and 160 mgL^{-1} (Fig. 5B) of Ca^{+2} did not differ from control (240 mgL^{-1}) (Fig 5A).

In *H. villosa*, the density of glandular hairs in the adaxial leaf blade surface was affected by the Ca^{+2} levels; each morphotype answered in a different way to the Ca^{+2} levels (Table 2). The amount of glandular trichomes in the abaxial leaf surface was very high, becoming difficult their precise measurement; so, we opted for not including data on glandular density on the abaxial leaf surface here. Plants submitted to 0 mgL^{-1} did not form new leaves, so morphological and morphometric analyzes were not performed in this treatment. Under treatment with 80 and 40 mgL^{-1} of Ca^{+2} the leaves showed ordinary epidermal cells with slightly irregular format (Fig. 5G, H), in comparison with control treatment (Fig. 5F); however, the glandular trichome morphology was not affected (Fig. 5F-H).

3.2.2. Ultrastructure

In *O. gratissmum*, the ultrastructural features of all the morphotypes of glandular trichomes were strongly affected when the Ca^{+2} level decreased (Fig 6A-F and Fig. 7A-I). The morphotype I, under control, exhibited slightly thin cell walls with regular aspect, and dense and abundant cytoplasm with numerous plastids devoid of grana and small vacuoles (Fig. 6A); under 160 mgL^{-1} of Ca^{+2}, the head cell acquired walls with irregular contour with folding (Fig. 6B), and cytoplasm similar to the control (Fig. 6A,

B); under 80 mgL^{-1} of Ca^{+2} the cytoplasm and its organelles showed signals of degradation, with poor visualization of membranes and clear and dark regions, and the vacuome became developed (Fig. 6C); under 40 mgL^{-1} of Ca^{+2} the walls showed loose aspect, and the cytoplasm became completely degraded with poor visualization of membranes (Fig. 6D). The morphotype II, under control, has head cells with thin walls with regular contour (Fig. 6E), and dense cytoplasm with hyperactive dictyosomes, rough endoplasmic reticulum, mitochondria and plastids devoid of grana containing osmiophilic inclusions; under 40 mgL^{-1} of Ca^{+2} electron-dense bodies were observed in the periplasmic space and immersed in the cell wall matrix, and electron-dense ramifications were observed in the cuticle (Fig 6F); the cytoplasm showed strong signals of degradation (Fig. 6F). The morphotype III, under control, presented head cells with walls forming labyrinthine projections, and abundant cytoplasm with dictyosomes, extensive rough endoplasmic reticulum, and small plastids devoid of grana and with osmiophilic inclusions (Fig. 7A-B); under 160 and 80 mgL^{-1} of Ca^{+2} (Fig. 7C-E) the cellular features were similar to the control (Fig. 7A-B); under 40 mgL^{-1} of Ca^{+2} the labyrinthine projections were not formed, and the internal layer of the cell wall became homogeneous and irregular; the cytoplasm presented mitochondria with dilated cristae (Fig. 7F-G); under 0 mgL^{-1} of Ca^{+2} the cell walls presented the internal layer with loose aspect, intercalated with fibrillar material, and the cytoplasm presented homogeneous aspect, with hyperactive dictyosomes and mitochondria (Fig. 7H-I).

In *H. villosa*, the ultrastructural changes promoted with the decrease in Ca^{+2} level (Fig. 8A-I) were similar to those described for *O. gratissimum*. The morphotype I, under control, has dense and abundant cytoplasm with numerous plastids with tubular inclusions (Fig. 8A); under 40 mgL^{-1} of Ca^{+2} plastids became electron-denser with oil drops inclusions (Fig. 8B-C); the nucleus acquired an irregular outline (Fig. 8B); the

cell walls became irregularly thicked and the cellulose microfibrills were loosely arranged (Fig. 8C). The morphotype II, under control, showed walls forming labyrinthine projections and abundant cytoplasm contained hyperactive dictyosomes, smooth and rough endoplasmic reticulum, small plastids devoid of grana and vacuole (Fig. 8D); under 80 mgL^{-1} of Ca^{+2}, the labyrinthine projections of the cell walls became more abundant and deeper (Fig. 8E); these walls and projections showed a loose appearance (Fig. 8E); the cytoplasm became electron denser and some organelles showed degradation of their matrix originating new vacuoles; myelin-like figures were observed in these cells (Fig. 8E); under 40 mgL^{-1} of Ca^{+2}, the labyrinthine projections of the cell wall maintained abundance similar to the control, but their appearance were loose (Fig. 8F), and vesicles were observed in the cytoplasm (Fig. 8F). The morphotype III, under control, exhibited thin cell walls, large nucleus, and dense cytoplasm with electron-dense plastids, mitochondria and rough endoplasmic reticulum and vacuoles (Fig. 9A); this morphotype was not strongly affected by 80 mgL^{-1} of Ca^{+2} (Fig. 9B); and under 40 mgL^{-1} of Ca^{+2} the organelles exhibited degraded membranes (Fig. 9C).

3.2.3. Immunolabeling of cytoskeletal elements on confocal microscopy

In *O. gratissimum*, the actin filaments and the microtubules immunolabeling were strongly affected by the treatments deficient in Ca^{+2} levels in the morphotype I (Fig. 10A-E), II (Fig. 10F-J) and III (Fig. 10K-O). The immunolabeling of both cytoskeletal elements were positively related with Ca^{+2} level. Reduction in the Ca^{+2} availability promoted weak immunolabeling of the actin filaments and microtubules in all glandular morphotypes.

When subjected to 80 mgL^{-1} of $Ca^{+}2$, glandular trichomes of *H. villosa* showed immunolabeling similar to the control (Fig. 11A-R); and plants subjected to 40 mgL^{-1} of Ca^{+2} showed weaker immunolabeling of both cytoskeletal elements in all morphotypes.

3.2.4. Measurements of leaf gas-exchange rates of *O. gratissimum*

Plants subjected to 40 and 0 mgL^{-1} of Ca^{+2} exhibited lower Pn and Pn/Ci compared with the control (Fig. 12). Individuals exposed to 40 and 0 mgL^{-1} of Ca^{+2} showed 49% and 70% reduction, respectively in the photosynthetic rate in relation to the control group (Fig. 12). The g_s and Tr were decreased from the 160 mgL^{-1} of Ca^{+2}, and were constant among the other treatments. The *Ci* and WUE were not affected by the Ca^{+2} levels (Fig. 12).

3.2.5. Essential oil composition of *O. gratissimum*

Thirty-four different compounds were identified in the essential oil of leaves of *O. gratissimum*, corresponding to approximately 96% of the total components of the oil. The major compounds identified were 1,8-cineole (25.79%), β-selinene (17.39%), eugenol (16.61%), (E)-caryophyllene (11.13%), (Z)-β-ocimene (6.38%) and α-selinene (4.55%) (Tab. 3). In the essential oils from inflorescences twenty-seven substances were identified and the major constituents were 1,8-cineole (25.41%), (E)-caryophyllene (13.21%), eugenol (11.61%), β-selinene (9.05%) and (Z)-β-ocimene (7.40%) (Tab. 4). The treatments with low levels of Ca^{+2} affected mainly the minority compounds in both leaves and inflorescences (Tab.3; Tab. 4). In the inflorescence, the β-selinene increased to 12.75% in the absence of Ca^{+2} (Tab. 4).

4. DISCUSSION

Our results report for the first time morphological, subcellular and functional alterations in glandular trichomes caused by drugs inhibiting cytoskeletal polymerization and low levels of Ca^{+2}, using two Lamiaceae species as model. This work is pioneer since the information available in literature on the role of cytoskeletal elements in origin and maintenance of trichomes concern only on the non-glandular hairs (Szymanski et al 1999; Kost et al. 1999; Mathur et al. 1999).

Our data showed that in both, *H. villosa* and *O. grassimum*, the glandular trichomes developed with normal external morphology when treated with cytoskeletal inhibitory drugs; however, their ultrastructural aspects were strongly affected by Cytochalasin D, Oryzalin and low levels of Ca^{+2}, mainly concerning their cell wall structure. In a subcellular level, it is known that the cytoskeletal elements are indispensable in the cell wall synthesis, being microtubules responsible by the control of alignment of cellulose microfibrils during the cell wall formation and govern the cell wall expansion (Evert 2006). In addition, maintenance of vacuoles and movement and anchorage of vesicles and organelles (Evert 2006 and literature therein), including intracellular movement and interaction of lipid bodies with endoplasmic reticulum, peroxisomes and mitochondria (Zehmer et al. 2009) are feasible by cytoskeletal elements. Actin filaments are involved mainly in the movement of vesicles and organelles (Evert 2006; Tozin & Rodrigues 2017); and the microtubules are related to the oil transport (Zehmer 2009; Tozin & Rodrigues 2017). In fact, in a general way, our data show that the treatments with Cytocalasin D and Oryzalin, inhibitory drugs of polymerization of actin filaments and microtubules, respectively, affect mainly the ultrastructure of the cell walls of the glandular trichomes and produce alterations in cytoplasmic features of secretory cells.

Since these drugs caused non-formation of subcuticular spaces accumulators of secretion (Werker 2000; Silva et al. 2016) and of labyrinthine walls facilitators of

secretion release (Gunning & Pate 1969; Tozin & Rodrigues 2017) in trichomes typically carrying these features, we can suggest that the process of exudate elimination from the cytoplasm may have been harmed. However, we expect that even with eventual alterations, the production of secretion continue to occur in the gland cells and suggests that the produced secretion remain accumulated inside the cell and may obliterate the cytoplasm producing images of dark electron dense contrast. This accumulated secretion inside the cytoplasm could stimulate a degrading process resembling an autolysis system (Sirikantaramas et al. 2008). This explain the visualization of clear areas alternating with dark areas in the cytoplasm, large vacuoles, organelles with lyse signals, presence of mutlivesicular bodies and abundance of rough endoplasmic reticulum and polysomes in the gland cells of plants under treatments with drugs inhibiting cytoskeletal polymerization.

The massive presence of polysomes and rough endoplasmic reticulum in drugs treated glandular trichomes of *H. villosa* are probably indicative of production of lytic enzymes (Matile 1975; Evert 2006). In addition, the presence of multivesicular bodies identified in the glandular trichomes treated with drugs can be involved with the cytoplasmic lyses (Tse et al. 2004). The multivesicular bodies are considered prevacuolar compartments that coalesce on the endocytic pathway to lytic vacuole formation (Tse et al. 2004; Evert 2006). The lytic vacuoles rupture is associated to the dissolution of the nucleus and cytoplasm autolysis and is responsible for the recycling of cellular compartment, such plastids and mitochondria (Evert 2006). In this sense, the presence of myelin-like figures in some treatments can also be associated to authophagic process and degeneration of organels (van Doorn & Papini 2016). The presence of the rough endoplasmic reticulum forming concentric whorls as observed in glandular morphotype II of *H. villosa* is considered a subcellular signal of stress

(Rodrigues et al. 2014) and are common in cells with distorted metabolic activity (Ishikawa 1996). These whorls can give rise to vesicles with a double membrane involved in the process of cell death (Huang and Klionsky 2002; Cacas 2010).

Although evident ultrastructural changes have occurred in glandular trichomes of plants treated with Cytocalasin D and Oryzalin, the imunolabeling of both cytoskeletal elements remained possible under confocal microscopy. This fact can occur because the antibodies can connect with cytoskeletal proteins even if they are not polymerized and functional (Lengsfeld et al. 1974; Dancker et al. 1975). Or yet, the treatments with drugs inhibiting cytoskeletal polymerization could have affected the actin and microtubules polymerization but not totally avoided it. In fact, the glandular trichomes were formed and presented apparently normal external morphology under all the treatments here employed. However, the presence of Ca^{+2} in ideal levels is crucial for the polymerization of cytoskeletal elements (Hepler 2005) and it was here demonstrated by the gradated lower reaction in imunolabeling of actin and microtubules under confocal microscopy according accomplishing the decrease of Ca^{+2} levels in both species.

The Ca^{+2} availability seems to be related to the maintenance of morphological and ultrastructural aspects of the glandular trichomes and physiological parameters of both plants studied here. The treatments with variable levels of Ca^{+2} also seem to have promoted intense morphological alterations in the analyzed material. These changes include irregularities in the leaf blade surface, presence of withered trichomes with cells walls with loose or completely disorganized feature in the trichomes and lyse signals in the cytoplasm of the gland cells, reaching the abscission of trichomes under the total absence of Ca^{+2}. In the same way, as previously discussed regarding the cytoskeleton polymerization inhibitory drugs, the low levels of Ca^{+2} promoted ultrastructural

alterations in the gland cells, mainly concerning the wall structure and cytoplasm lysis. The formation of loose cell walls with abnormal aspect and the occurrence of cytoplasm degradation were common to all morphotypes of glandular trichomes submitted to Ca^{+2} deficits. The Ca^{+2} is a crucial regulator of growth and development in plants and their role in the synthesis and maintenance of cell walls is well established (Hepler 2005; Taiz & Zeiger 2004) being known that low Ca^{+2} concentration promotes ruptures in the cell walls (Hepler 2005).

Huang et al. (2010) demonstrated that glandular trichomes treated with calcium chelator and calcium channel blocker presented similar damages described above; and that the amount of secretion production is drastically reduced. In this work, we observed that the reduction in the levels of Ca^{+2} do not affect the essential oil composition. In the both analyzed organs the essential oil composition remains constant even under the total absence of this mineral. Nevertheless, we performed the essential oil analyzes using the all leaves. If the oil yield is affected, we are unable to affirm because we did not get enough plant material to yield analysis. However, our data showed that the stomatal conductance and the assimilation decreased according to the Ca^{+2} decreasing. When these physiological parameters are reduced, it is supposed that the carbon fixation also decreases (Chaves et al. 2003; Zhang et al. 2010; Kudoyrova et al. 2013), which would result in a reduction in the yield of essential oils.

In conclusion, our results show that changes in cytoskeletal polymerization caused by destabilizing drugs or low levels of Ca^{+2} can affect the subcellular features of glandular trichomes in *H. villosa* and *O. gratissimum*. Low levels of Ca^{+2} (40 and 0 mgL^{-1}) reduce the photosynthetic rates, but the essential oils composition is maintained. Further studies involving molecular approach must be conducted to elucidate the role of

the cytoskeletal elements during the glandular trichomes morphogenesis and functioning.

Acknowledgements

We thank the CNPq (444205/2014-4) for the financial support; the staff of the Centro de Microscopia Eletrônica (CME), IBB, UNESP, for helping in the sample preparation; and Dr. Amanda Cristina Esteves Amaro for the IRGA analyzes.

REFERENCES

Adams RP. 2007. Identification of essential oil components by gas chromatography/mass spectroscopy, Allured Publ. Corp, Carol Stream, 804 p.

Amrehn E, Heller A, Spring O. 2014. Capitate glandular trichomes of *Helianthus annuus* Asteraceae): ultrastructure and cytological development. Protoplasma 251(1): 161-167

Appezzato-da-Glória B, Costa FB, Silva VC, Gobbo-Neto L, Rehder VLG, Hayashi AH. 2012. Glandular trichomes on aerial and underground organs in *Chrysolaena* species (Vernonieae – Asteraceae): Structure, ultrastructure and chemical composition. Flora 207: 878-997.

Argyropoulou C, Akoumianakiloannidou A, Christodoulakis SN, Fasseas C. 2010. Leaf anatomy and histochemistry of *Lippia citriodora* (Verbenaceae). Australian Journal of Botany 58: 398-409.

Ascensão L, Pais MS. 1998 The leaf capitate trichomes of *Leonotis leonurus*: histochemistry, ultrastructure and secretion. Ann Bot. 81: 263-271.

Cacas J-L. 2010. Devil inside: does plant programmed cell death involve the endomembrane system? Plant Cell Environ 33: 1453–1473.

Chen D, Acharya BR, Liu W, Zhang W. 2013. Interaction between calcium and actin in guard cell and pollen signaling networks. Plants 2(4): 615-634.

Chaves MM, Maroco JP, Pereira JP. 2003. Understanding plant responses to drought – from genes to the whole plant. Functional Plant Biology 30: 239–264.

Dancker P, Low I, Hasselbach W, Wieland TH. 1975. Interaction of actin with phalloidin: polymerization and stabilization of F-actin. Biochimica et Biophysica Acta 400: 407-414.

Evert RF. 2006. Esau's Plant Anatomy. 3a. ed. Wiley-Interscience, New Jersey.

Gunning BES, Pate JS. 1969. “Transfer cells”: plant cells with wall ingrowths, specialized in relation to short distance transport of solutes – their occurrence, structure, and development. Protoplasma 68: 107-133.

Hepler PK. 2005. Calcium: a central regulator of plant growth and development. Plant Cell 17: 2142-2155.

Hoagland DR, Arnon DI. 1950. The water:culture method for growing plants withoutsoil. Berkeley: California Agricultural Experiment Station. 32p.

Huang SS, Liao JP, Kirchoff BK. 2010. Calcium distribuition and function in the glandular trichomes of *Lavandula pinnata* L.. Journal of Torrey Botanical Society 137: 1-15.

Huang WP, Klionsky DJ. 2002. Autophagy in yeast: a review of the molecular machinery. Cell Struct Funct 27: 409–420.

Ishikawa HA. 1996. Ultrastructural features of chilling injury: injured cells and the early events during chilling of suspension-cultured mung bean cells. American Journal of Botany 83: 825–835.

Kost B, Mathur J, Chua N. 1999.Cytoskeleton in plant development.Current Opinion in Plant Biology 2: 462-470.

Kudoyarova GR, Kholodova VP, Veselov DS. 2013. Current State of the Problem of Water Relations in Plants under Water Deficit. Russian Journal of Plant Physiology 60(2): 165–175.

Lengsfeld AM, Low I, Wieland T, Dancker P, Hasselbach W. 1974. Interaction of Phalloidin with Actin. Proc. Nat. Acad. Sci. 71(7): 2803-2807.

Mathur J, Speilhofer P, Kost B, Chua N. 1999. The actin cytoskeleton is required to elaborate and maintain spatial patterning during trichome cell morphogenesis in *Arabidopsis thaliana*. Development 126: 5559-5568.

Matile, P. 1975. The lytic compartment of plant cells (Cell Biol. Monogr., Vol 1) Springer-Verlag, Berlin and New York.

Naidoo Y, Heneidak S, Gairola S, Nicholas A, Naidoo G. 2012. The leaf secretory scales of *Combretum molle* (Combretaceae): morphology, ultrastructure and histochemistry. Plant Syst Evol 298: 25-32.

Papini A, Tani G, Di Falco P, Brighigna L. The ultrastructure of the development of *Tillandsia* (Bromeliaceae) trichome. Flora 205: 94-100.

Reynolds ES. 1963. The use of lead citrate at high pH as an electron-opaque stain in electron microscopy. Journal of Cell Biology 17: 208-212.

Robards AW. 1978. An introduction to techiniques for scanning electron microscopy of plant cells. In: Electron Microscopy and Cytochemistry of Plant Cells. J. L. Hall. (eds.). New York, Elsevier.

Rodrigues TM, Buarque PFSM, Coneglian AG, Reis DC. 2014. Light and temperature induce variations in the density and ultrastructure of the secretory spaces in the diesel-tree (*Copaifera langsdorffii* Desf.—Leguminosae). Trees 28: 613-623.

Silva SCM, Tozin LRS, Rodrigues TM. 2016. Morphological and histochemical characterization of secretory sites of bioactive compounds in Lantana camara L. (Verbenaceae) leaves. Botany 94: 321-336.

Sirikantaramas S, Yamazaki M, Saito K. 2008. Mechanism of resistance to self-produced toxic secondary metabolites in plants. Phytochemistry Reviews 7: 467-477.

Szymanski DB, Marks D, Wick SM. 1999. Organized f-actin is essential for normal trichome morphogenesis in *Arabidopsis*. Plant Cell 11: 2331-2347.

Taiz L, Zeiger E. 2004. Fisiologia vegetal. Porto Alegre: Artmed.

Tse YC, Mo B, Hillmer S, Zhao M, Lo SW, Robinson DG, Jiang L. 2004. Identifi cation of multivesicular bodies as prevacuolar compartments in *Nicotiana tabacum* BY-2 cells. Plant Cell 16: 672–693.

Tozin LRS, Rodrigues TM. 2017. Morphology and histochemistry of glandular trichomes in *Hyptis villosa* Pohl ex Benth. (Lamiaceae) and differential labeling of cytoskeletal elements. Acta Botanica Brasilica 31(3): 330-343.

Tozin LRS, Carvalho SF, Machado SR, Rodrigues TM. 2015. Glandular trichome diversity on leaves of *Lippia origanoides* Kunth and *Lippia stachyoides* Cham. (Verbenaceae): morphology, histochemistry and ultrastructure. Botany 93: 297-306.

Van Den Dool H, Kratz DJ. 1963. A generalization of the retention index system including liner temperature programmed gas-liquid partition chromatography. Journal of Chromatography 11: 463-467.

van Doorn WG, Papini A. 2016. Plastid degeneration in *Tillandsia albida* (Bromeliaceae) and *Lobivia rauschii* (Cactaceae) provides evidence about the origin and destiny of multilamellar bodies in plants. Phytomorphology 66: 103-112

Werker E. 2000. Trichome diversity and development. Advances in Botanical Research 31: 1-35.

Zehmer JK, Huang Y, Peng G, Pu J, Anderson RGW, Liu P. 2009. A role for lipid droplets in inter-membrane lipid traffic. Proteomics 9(4): 914-921.

Zhang YH, Chen LJ, He JL, Qian LS, Wu LQ, Wang RF. 2010. Characteristics of chlorophyll fluorescence and antioxidative system in super-hybrid rice and its parental cultivars under chilling stress. Biologia Plantarum 54(1): 164-168.

Yao H, Xu Q, Yuan M. 2008. Actin dynamics mediates the changes of calcium level during the pulvinus movement of *Mimosa pudica*. Plant Signal Behavior 3(11): 954-960.

TABLES

Table 1. Density of each morphotype of glandular trichomes in 1 mm² in both leaf surface of *Ocimum gratissiumum* L. submitted to different Ca^{+2} levels.

Treatments (mgL^{-1})	Abaxial leaf surface			Adaxial leaf surface		
	Glandular morphotypes			Glandular morphotypes		
	I	II	III	I	II	III
240 (Control)	38 a	9 a	49 a	15 a	5 a	33 a
160	29 a	8 a	29 a	16 a	8 a	20 a
80	25 a	7 a	30 a	15 a	2 a	16 a
40	26 a	10 a	30 a	31 a	8 a	34 a
0	21 a	25 a	29 a	14 a	10 a	20 a
P value	0.542	0.06	0.351	0.367	0.227	0.409
F value	0.802	3.055	1.201	1.159	1.594	1.081
DF	4,19	4,19	4,19	4,19	4,19	4,19

Means followed by same letter do not indicate statistical differences (Tukey test $p < 0.05$).

Table 2. Density of each morphotype of glandular trichomes in 1 mm² in the adaxial leaf surface of *Hyptis villosa* Pohl ex Benth. submitted to different Ca^{+2} levels.

Treatments (mgL^{-1})	Glandular morphotypes		
	I	II	III
160 (Control)	19.5 a	19.5 b	76.5 a
80	9 b	63 a	80 a
40	14 ab	33 b	34 b
P value	0.020	< 0.001	< 0.001
F value	6.245	16.726	26.996
DF	2,11	2,11	2,11

Means followed by same letter do not indicate statistical differences (Tukey test $p < 0.05$).

Table 3. Chemical composition of the volatile components (%) from leaves of *Ocimun gratissimum* L. submitted to different Ca^{+2} levels.

Compound	Treatments (mgL^{-1})					p	F	RI	RI*
	240	160	80	40	0				
α-pinene	0,52	0.53	0.63	0.73	0.64	0.133	2.273	933	939
Sabinense	0.62	0.71	0.78	0.80	0.65	0.574	0.761	974	975
β-pinene	2.23	2.24	2.41	2.51	2.44	0.829	0.364	976	979
3-octanone	0.00	0.06	0.00	0.14	0.00	0.584	0.751	987	983
Myrcene	1.11	1.21	1.26	1.89	2.19	0.074	2.973	993	990
α-terpinene	0.06	0.09	0.04	0.03	0.16	0.859	0.250	1009	1017
ρ-cymene	0.14	0.00	0.04	0.44	0.59	0.079	2.894	1025	1024
1,8-cineole	25.79	29.00	21.22	20.01	24.51	0.143	2.143	1034	1031
(Z)-β-ocimene	6.38	6.86	7.17	6.34	9.26	0.760	0.465	1041	1037
(E)-β-ocimene	0.22	0.22	0.31	0.18	0.00	0.110	2.489	1051	1050
γ-terpinene	0.29	0.24	0.20	0.37	0.62	0.080	2.875	1060	1059
n-octanol *	0.00 b	0.06 b	0.00 b	0.00 b	0.38 a	<0.001	34.988	1073	1068
Terpinolene	0.00	0.04	0.04	0.03	0.00	0.732	0.523	1089	1088
2-nonanol	0.00	0.00	0.00	0.00	0.41 a	0.010	11.235	1104	1098
α-terpinol *	0.36 a	0.42 a	0.27 ab	0.13 b	0.13 b	0.030	4.539	1192	1188
Eugenol	16.61	17.62	18.85	11.28	12.82	0.288	1.448	1361	1359
α-copaene	1.29	1.00	1.30	1.87	1.33	0.103	2.571	1381	1376
β-bourboneno *	0.03 b	0.09 b	0.08 b	0.42 a	0.00	0.002	10.130	1389	1388
β-cubebene	0.09	0.15	0.27	0.29	0.00	0.423	1.047	1395	1388
β-elemene	0.41	0.53	0.66	0.62	0.28	0.219	1.734	1396	1390
(E)-caryophyllene	11.13	8.45	11.13	11.10	8.43	0.551	0.802	1425	1419
β-copaene	0.03	0.00	0.03	0.09	0.00	0.37	1.228	1434	1432
α-trans-bergamotene	0.78	0.64	0.78	1.04	1.05	0.140	2.359	1441	1434
α-guaiene	0.05	0.05	0.13	0.12	0.00	0.213	1.761	1443	1439
α-humulene	1.54	1.40	1.63	1.67	1.33	0.713	0.535	1458	1454
allo-aromadendrene	0.76	0.57	0.59	0.60	0.81	0.707	0.545	1465	1460
α-neocallitropsene	0.12	0.14	0.12	0.09	0.12	0.994	0.051	1482	1476
germacrene D	1.86	2.55	3.88	3.10	1.05	0.230	1.682	1486	1485
β-selinene	17.39	15.13	16.34	20.50	17.45	0.051	1.779	1493	1485
α-selinene	4.55	4.10	4.76	5.23	4.69	0.234	1.663	1501	1498
γ-cadinene	0.00	0.00	0.04	0.04	0.00	0.519	0.932	1516	1513
7-epi-α-selinene	1.05	0.98	1.11	1.31	1.14	0.076	2.940	1522	1522
δ-cadinene	0.38	0.36	0.45	0.36	0.29	0.893	0.267	1528	1523
caryophyllene oxide	0.81	1.00	0.65	1.39	1.66	0.462	0.978	1586	1583
Total itentified	**96.60**	**96.46**	**97.15**	**94.71**	**94.42**				

RI= Retention index calculated; RI*= Retention index (Adams 2007); * = indicate substances with statistical differences, and means followed by different letters indicate the differences (Tukey test $p < 0.05$).

Table 4. Chemical composition of the volatile components (%) from inflorescences of *Ocimum gratissimun* L. submitted to different Ca^{+2} levels.

Compoud	Treatments (mgL^{-1})			p	F	RI	RI*
	240	80	0				
α-pinene	2.11	1.33	1.10	0.202	2.117	933	939
sabinene	2.15	1.62	1.24	0.238	1.838	974	975
β-pinene	6.40	4.88	4.20	0.227	1.915	976	979
myrcene	3.42	2.77	2.25	0.205	2.088	993	990
α-terpinene	0.18	0.13	0.06	0.594	0.569	1009	1017
1,8-cineole	25.41	25.69	26.04	0.986	0.014	1034	1031
(Z)-β-ocimene	7.40	8.68	5.01	0.087	3.781	1041	1037
(E)-β-ocimene	0.29	0.41	0.26	0.184	2.275	1051	1050
γ-terpinene	0.42	0.37	0.41	0.80	0.230	1060	1059
terpinolene	0.07	0.00	0.00	0.368	1.236	1089	1088
2-nonanol	0.09	0.06	0.00	0.444	1.000	1104	1098
α-terpinol	0.47	0.39	0.38	0.555	0.650	1192	1188
eugenol	11.61	10.66	10.88	0.946	0.056	1361	1359
α-copaene	1.84	1.70	1.61	0.159	0.856	1381	1376
β-bourboneno	0.00	0.00	0.08	0.368	1.365	1389	1388
β-cubebene	0.44	0.46	0.33	0.672	0.425	1395	1388
β-elemene	0.65	0.78	0.80	0.547	0.669	1396	1390
(E)-caryophyllene	13.21	13.79	13.81	0.925	0.079	1425	1419
α-trans-bergamotene	1.71	1.67	1.83	0.909	0.097	1441	1434
α-humulene	1.67	1.89	2.09	0.254	1.738	1458	1454
allo-aromadendrene	0.82	0.88	0.92	0.820	0.206	1465	1460
germacrene D	3.73	4.75	3.99	0.599	0.599	1486	1485
β-selinene *	9.05 b	9.77 ab	12.75 a	0.036	6.076	1493	1485
α-selinene	3.15	3.53	4.20	0.177	2.343	1501	1498
7-epi-α-selinene	0.73	0.81	1.05	0.120	3.076	1522	1522
δ-cadinene	0.32	0.38	0.49	0.157	2.561	1528	1523
caryophyllene oxide *	0.39 b	0.41 b	1.94 a	0.002	22.100	1586	1583
Total identified	**97.74**	**97.81**	**97.72**				

RI= Retention index calculated; RI*= Retention index (Adams 2007); * = indicate substances with statistical differences, and means followed by different letters indicate the differences (Tukey test $p < 0.05$).

LEGENDS OF FIGURES

Figure 1. Ultrastructural aspects of glandular trichomes of *Ocimum gratissimum* submitted to cytoskeletal inhibitory drugs under Scanning (**A-C**) and Transmission (**D-Q**) Electron Microscopy. **A-G** Morphotype I. **H-L** Morphotype II. **M-P** Morphotype III. **A, D, H, M** Control. **B, E-F, I-J, N-O** Oryzalin treatment. **C, G, K-L, P** Cytochalasin D treatment. **D** Detail of head cell showing cell wall (Cw) with regular aspects and dense cytoplasm with numerous plastids (Pl), vesicles (Ve) and vacuoles (Va). **E** Detail of head cell with irregular cell wall (Cw) and plasmalemma. Ol: oil droplet. **F** Detail of dense cytoplasm with few plastids (Pl), numerous vesicles (Ve) and oil drop (Ol). Va: vacuole. **G** Head cell showing cell wall (Cw) with pronounced infoldings, and cytoplasm with plastids (Pl) and mitochondria (Mi). **H** Head cell with walls (Cw) with regular contour, and dense cytoplasm of head cell with hyperactive dyctiosomes (Di), rough endoplasmic reticulum (Rer), mitochondria (Mi) and plastids (Pl) with osmiophilic inclusions. Va: vacuole. **I** Detail of head cell with plastids (Pl) with irregular contour and large vacuole (Va). Cw: cell wall. **J** Cytoplasm of head cell with vacuole (Va), mitochondria (Mi) and dictyosomes (Di). Inset shows multivesicular body. **K** Head cell with electron lucent cytoplasm with small vacuoles (Va) and organelles with lower definition. Cw: cell wall. **L** Detail of head cell showing lipophilic impregnation (arrow) in the cell wall. Pl: plastids; Va: vacuole. **M** Head cell with walls (Cw) forming labyrinthine projections (*), subcuticular space (Ss) with homogeneous secretion, and abundant cytoplasm with dictyosomes (Di), extensive rough endoplasmic reticulum (Rer), and small plastids (Pl) devoid of thylakoids and with osmiophilic inclusions. Mi: mitochondria; Ps: periplasmatic space. **N** Head cells with walls (Cw) with labyrinthine projections (*) less developed, and cytoplasm with voluminous

plastids (Pl) with osmiophilic inclusions, mitochondria (Mi) and rough endoplasmic reticulum (Rer). Ss: subcuticular space; Va: vacuole. **O** Detail of cytoplasm showing plastids (Pl), mitochondria (Mi) and rough endoplasmic reticulum (Rer). Cw: cell wall. **P** Head cell with walls (Cw) with irregular aspect with infoldings, and dense cytoplasm with mitochondria (Mi) and plastids (Pl). Scale bars: A-C = 50 μm; D, I, K, N, P = 1 μm; E-G, H, J, L, M, O = 0.5 μm.

Figure 2. Ultrastructural aspects of glandular trichomes of *Hyptis villosa* submitted to cytoskeletal inhibitory drugs under Scanning (**A-C**) and Transmission (**D-Q**) Electron Microscopy. **D-F** Morphotype I. **G-K** Morphotype II. **L-O** Morphotype III. **A, D, G, L** Control. **B, E-F, H-I, M-N** Oryzalin treatment. **C, J-K, O** Cytochalasin D treatment. **D** General view of morphotype I. Inset shows plastids with tubular inclusions. **E** Head cells (Hc) with electron dense cytoplasm. **F** Detail of head cell showing plastids (Pl) and dilated smooth endoplasmic reticulum (Ser). Cw: cell wall. **G** Head cell with cell wall (Cw) showing labyrinthine ingrowths (*) and cytoplasm with plastids (Pl), smooth endoplasmic reticulum (Ser) and vacuole (Va). Inset shows hyperactive dictyosome. **H** Head cell with dense cytoplasm with numerous plastids (Pl), vacuoles (Va) and nucleus with regular contour. Cw: cell wall. **I** Detail of head cell with plastids (Pl) with regular aspects, mitochondria and degradated organelles (Og). Cw: cell wall. **J** Detail of head cell showing the flocculated cytoplasm and rough endoplasmic reticulum (Rer) with whorls. **K** Detail showing plastids (Pl) dictyosomes (Di) and multivesicular body (arrowhead). Cw: cell wall. **L** Head cell with dense cytoplasm with plastids (Pl), mitochondria (Mi) and vacuole (Va). Cw: cell wall; Nu: nucleus. **M** Head cell with vacuome (Va) developed, plastids (Pl) and multivesicular body (Arrow head). Nu: nucleous. **N** Detail showing plastids (Pl) in process of lysis and vacuome developed. **O**

Detail of head cell with rough endoplasmic reticulum (Rer) proliferated and plastids (Pl) with undefined membranes. Va: vacuole. Scale bars: A-C = 50 μm; D, J = 5 μm; E, I, K, M = 1 μm; F, G, L, P = 0.5 μm; H, N, Q = 2 μm.

Figure 3. Immunolabeling of microtubules (**A-C, G-I, M-O**) and actin filaments (**D-F, J-L, P-R**) of glandular trichomes of *Ocimum gratissimum* treated with cytoskeleton disruptor drugs, under Confocal light microscope. **A-F** Morphotype I. **G-L** Morphotype II. **M-R** Morphotype III. **A-D, G-J, M-P** Control. **B-E, H-K, N-Q** Oryzalin treatment. **C-F, I-L, O-R** Cytochalasin D treatment. Scale bars: 10 μm.

Figure 4. Immunolabeling of actin filaments (**A-C, G-I, M**-O) and microtubules (**D-F, J-L, P-R**) of glandular trichomes of *Hyptis villosa* treated with cytoskeleton disruptor drugs, under Confocal light microscope. **A-F** Morphotype I. **G-L** Morphotype II. **M-R** Morphotype III. **A-B, G-J, M-P** Control. **B-E, H-K, N-Q** Oryzalin treatment. **C-F, I-L, O-R** Cytochalasin D treatment. Scale bars: 10 μm.

Figure 5. Scanning electron micrographs of abaxial leaf surface of *Ocimum gratissimum* (**A-E**) and adaxial leaf surface of *Hyptis villosa* (**F-H**) submitted to different level of Ca^{+2}, showing the glandular trichomes. **A** 240 mgL^{-1} (control). **B, F** 160 mgL^{-1}. **C, G** 80 mgL^{-1}. **D, H** 40 mgL^{-1}. **E** 0 mgL^{-1}. Arrowhead indicates point of detachment of glandular trichomes. Scale bars: A-E = 50 μm; F-H = 20 μm.

Figure 6. Transmission electron micrographs of glandular trichomes of *Ocimum gratissimum* submitted to different level of Ca^{+2}. **A-D** morphotype I. **A** control. **B** 160

mgL^{-1}. **C** 80 mgL^{-1}. **D** 40 mgL^{-1}. **E-F** Morphotype II. **E** control. **F** 40 mgL^{-1}. **A** Detail of head cell with dense cytoplasm with plastids (Pl) and small vacuoles (Va). Cw: cell wall. **B** Head cells with walls (Cw) with infoldings and dense cytoplasm with small vacuoles (Va). Nu: nucleus. **C** Detail of degraded cytoplasm with numerous small vacuoles (Va). Nu: nucleus. **D** Head cell with walls (Cw) with loose and irregular aspects, degraded cytoplasm and plastids (Pl). **E** Head cell with walls (Cw) with regular aspects and dense cytoplasm with hyperactive dictyosomes (Di), extensive rough endoplasmic reticulum (Rer), plastids (Pl), mitochondria (Mi) and vacuoles (Va). **F** Head cell with regular cell wall (Cw), cuticle with ramification, periplasmatic space with osmiophilic impregnations (arrowhead) and degraded cytoplasm with small vacuoles (Va). Scale bars: D, F = 0.5 μm; A-C, E = 1 μm.

Figure 7. Transmission electron micrographs of glandular trichomes morphotype III of *Ocimum gratissimum* submitted to different level of Ca^{+2}. **A-B** control. **C** 160 mgL^{-1}. **D-E** 80 mgL^{-1}. **F-G** 40 mgL^{-1}. **H-I** 0 mgL^{-1}**. A** Head cells with walls (Cw) with regular aspects and labyrinthine projections (*) and cytoplasm with dictyosomes (Di), rough endoplasmic reticulum (Rer) and plastids (Pl) with osmiophilic inclusions. **B** Detail of head cell showing the walls (Cw) with labyrinthine projections (*) and extensive rough endoplasmic reticulum (Rer). **C** Head cell with walls (Cw) with labyrinthic projections (*) and abundant cytoplasm with mitochondria (Mi) and extensive rough endoplasmic reticulum (Rer). Inset showing plastids with osmiophilic inclusions. **D** Detail showing the cell wall (Cw) with labyrinthine projection (*). **E** Detail showing the cytoplasm with plastids (Pl) with osmiophilic inclusions and extensive rough endoplasmic reticulum (Rer). **F** Head cell with wide subcuticular space (Ss) and cytoplasm with mitochondrias with dilated cristae and vacuoles (Va). Cw: cell wall. **G** Deatil showing the cell wall

(Cw) with irregular aspect and plastids (Pl) with osmiophilic inclusions. **H** Head cell with wide subcuticular space (Ss), cell wall (Cw) with irregular and loose aspects, and cytoplasm with dictyosomes (Di). **I** Detail showing the cell wall (Cw) with irregular and loose appearance. Mi: mitochondria. Scale bars: A, E, F, G = 0.5 μm; B-D H, I = 0.2 μm.

Figure 8. Transmission electron micrographs of glandular trichomes of *Hyptis villosa* submitted to different level of Ca^{+2}. **A-C** morphotype I. **D-F** morphotype II. **A, D** 160 mgL^{-1}(Control). **E** 80 mgL^{-1}. **B, C, F** 40 mgL^{-1}. **A** Head cells showing dense cytoplasm with plastids (Pl) devoid of grana and small vacuoles (Va). Cw: cell wall. **B** Detail of head cell showing the nucleus (Nu), numerous electron dense plastids (Pl) with plastoglobules and vacuoles (Va). **C** Detail of head cell showing the walls (Cw) with irregular projection and cytoplasm with plastids (Pl) with plastoglobules and small vacuoles (Va). **D** Head cells showing walls (Cw) with labyrinthine projections (*) and cytoplasm with plastids (Pl) and dictyosomes (Di), in addition to a large vacuole (Va). **E** Head cells showing walls (Cw) with deep labyrinthine projections (*). Arrowhead indicates mieline-like figure. Mi: mitochondria, Va: vacuole. **F** Head cell showing walls (Cw) with labyrinthine projections (*) less developed, and cytoplasm with vesicles (Ve) and vacuole (Va). Scale bars: A-C, E = 2 μm; D = 1 μm.

Figure 9. Transmission electron micrographs of glandular trichome morphotype III of *Hyptis villosa* submitted to different level of Ca^{+2}. **A** 160 mgL^{-1}(Control). **B** 80 mgL^{-1}. **C** 40 mgL^{-1}. **A** Head cell with thin walls (Cw), and dense cytoplasm with plastids (Pl) devoid of grana, rough endoplasmic reticulum (Rer), dictyosomes (Di), vesicles (Ve) and small vacuoles (Va). Nu: nucleus. **B** Head cell with thin walls (Cw) and cytoplasm

with mitochondria (Mi) with dilated cristae, extensive rough endoplasmic reticulum and vacuoles (Va). **C** Head cell with thin wall (Cw), and cytoplasm with rough endoplasmic reticulum (Rer), plastids (Pl), small vacuoles (Va), and degraded organelles (Og). Scale bars: 1 μm.

Figure 10. Labeling of the f-actin and microtubules in three morphotypes of glandular trichomes in *Ocimum gratissimum* L. submitted to different Ca^{+2} levels. **A-E** Glandular morphotype I. **F-J** Glandular morphotype II. **K-O** Glandular morphotype III. **A, F, K** 240 mgL^{-1} (control). **B, G, L** 160 mgL^{-1}. **C, H, M** 80 mgL^{-1}. **D, I, N** 40 mgL^{-1}. **E, J, O** 0 mgL^{-1}. Scale bars: 10 μm.

Figure 11. Labeling of the f-actin and microtubules in three morphotypes of glandular trichomes in *Hyptis villosa* submitted to different Ca^{+2} levels. **A-F** Glandular morphotype I. **G-L** Glandular morphotype II. **M-R** Glandular morphotype III. **A-B, G-I, M-O** Phalloidin-rhodamine (F-actin labeling). **D-F, J-L, P-R** anti-β-tubulin-FITC (microtubule labeling). **A, D, G, J, M, P** 240 mgL^{-1} (control). **B, E, H, K, N, Q** 80 mgL^{-1}. **C, F, I,L,O,R** 40 mgL^{-1}. Scale bars: 10 μm.

Figure 12. Leaf gas-exchange in *Ocimum gratissimum* L. submitted to different Ca^{+2} levels. **A** Photosynthetic rate. **B.** Stomata conductance. **C.** Intracellular carbon concentration. **D.** Transpiration rate. **E.** Water use efficiency. **F.** Carboxylation efficiency. Means followed by different letter indicate statistical differences (Tukey test $p < 0.05$).

FIGURES

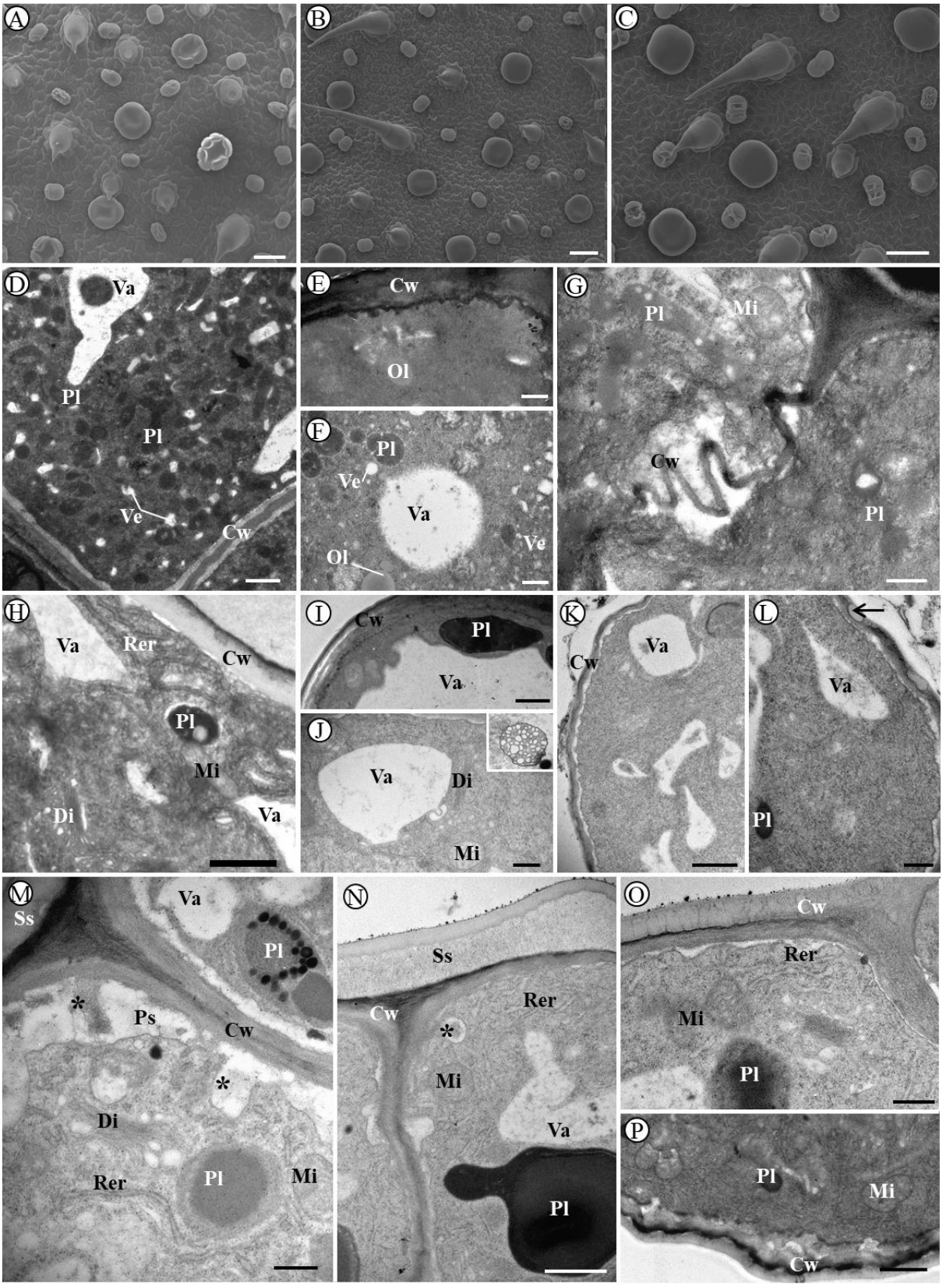

Figure 1

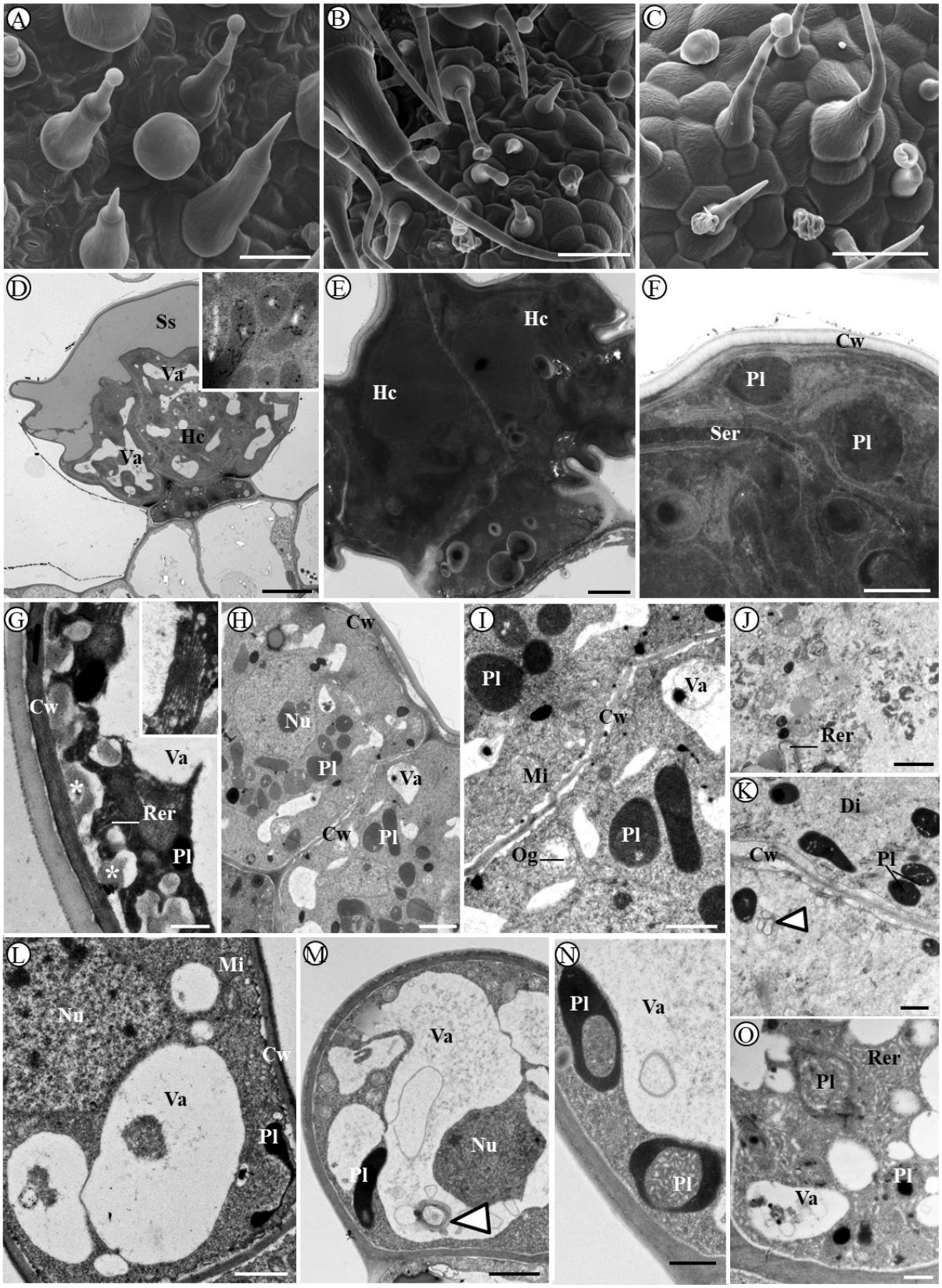
A
B
C
D
Ss
Va
Hc
Va
E
Hc
Hc
F
Cw
Pl
Ser
Pl
G
Cw
Va
Rer
Pl
H
Cw
Nu
Pl
Va
Cw
Pl
I
Pl
Va
Cw
Mi
Pl
Og
J
Rer
K
Di
Cw
Pl
L
Mi
Nu
Cw
Va
Pl
M
Va
Nu
Pl
N
Pl
Va
Pl
O
Rer
Pl
Pl
Va

Figure 2

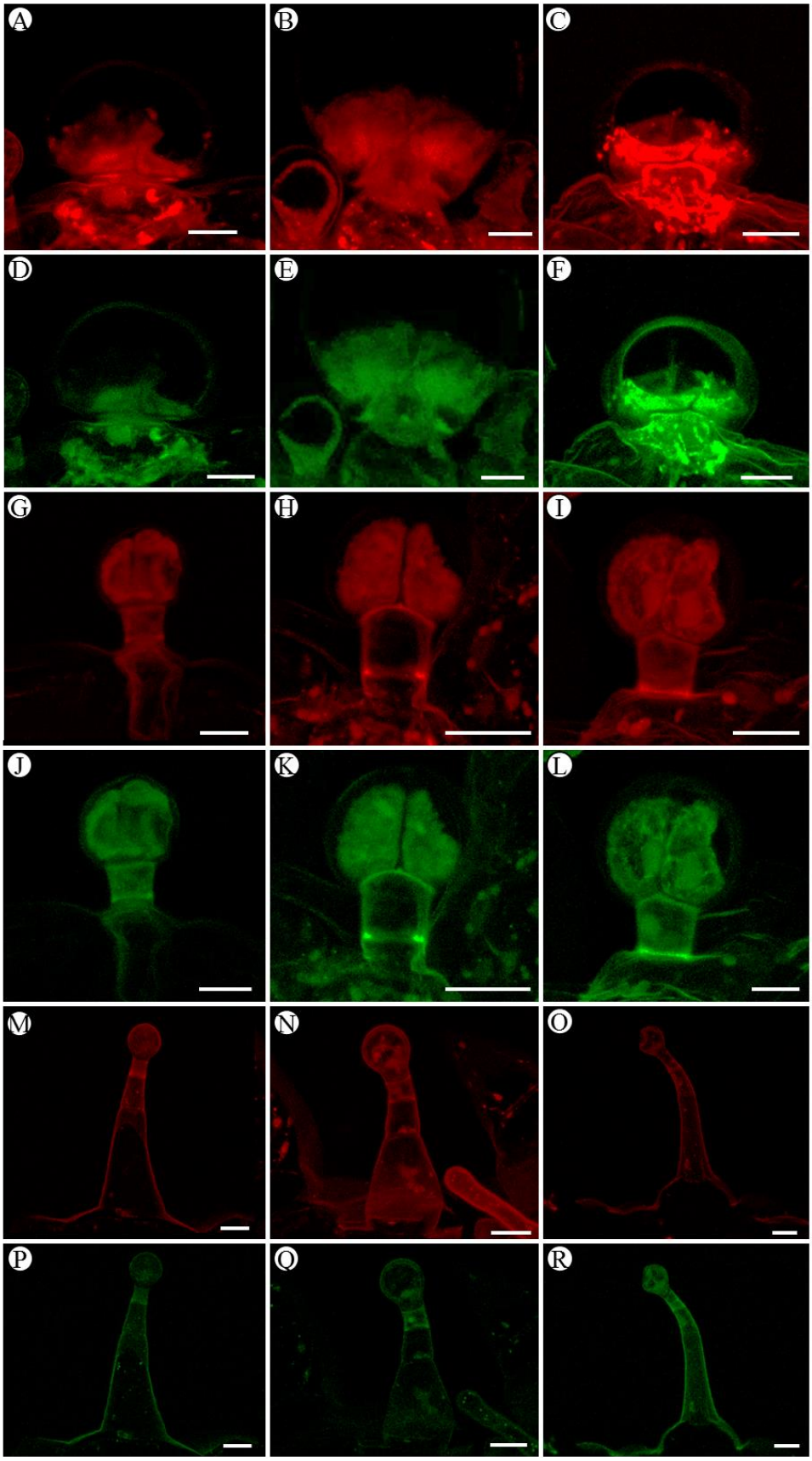

Figure 3

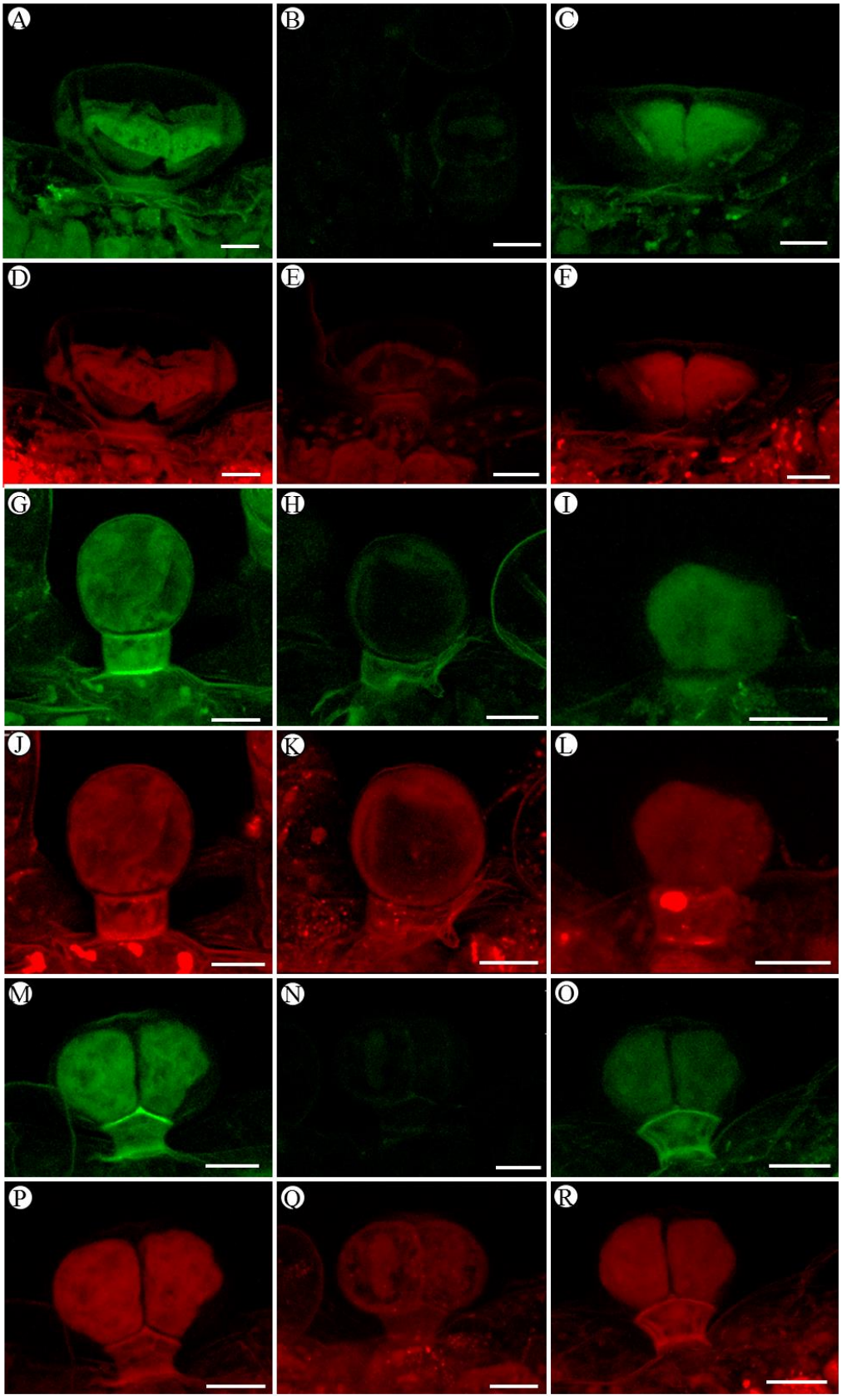

Figure 4

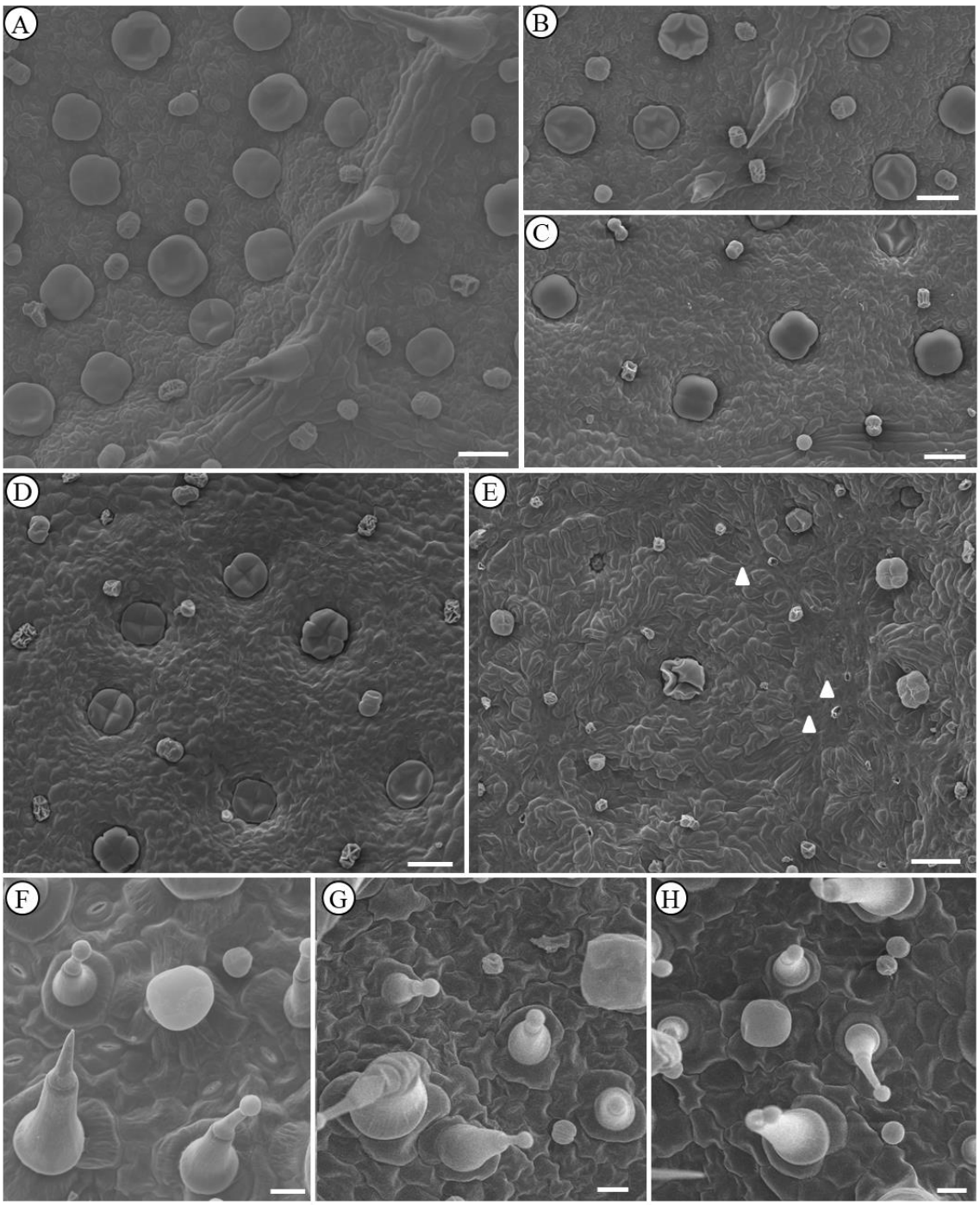

Figure 5

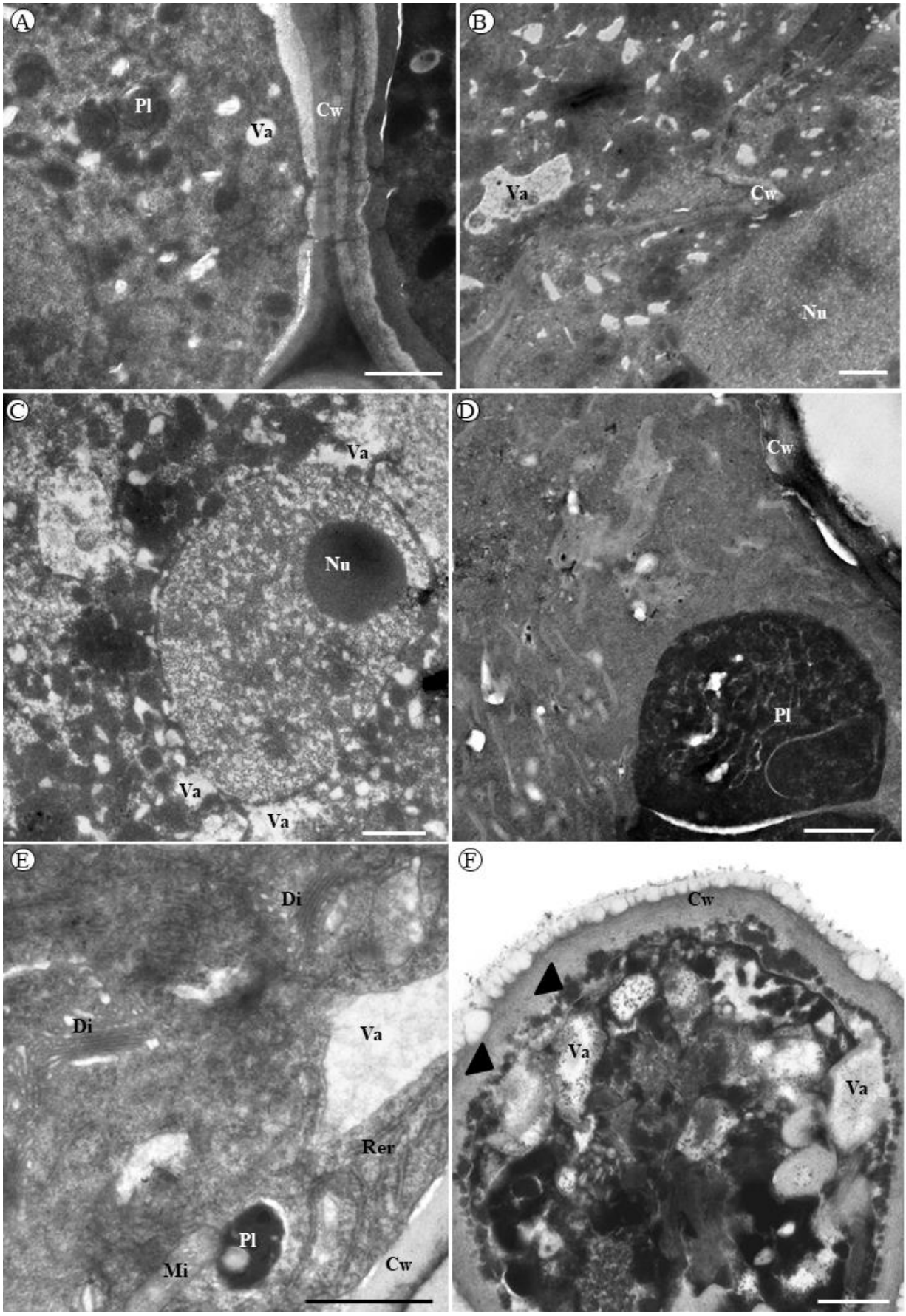
A
Pl
Va
Cw
B
Va
Cw
Nu
C
Va
Nu
Va
Va
D
Cw
Pl
E
Di
Di
Va
Rer
Pl
Mi
Cw
F
Cw
Va
Va

Figure 6

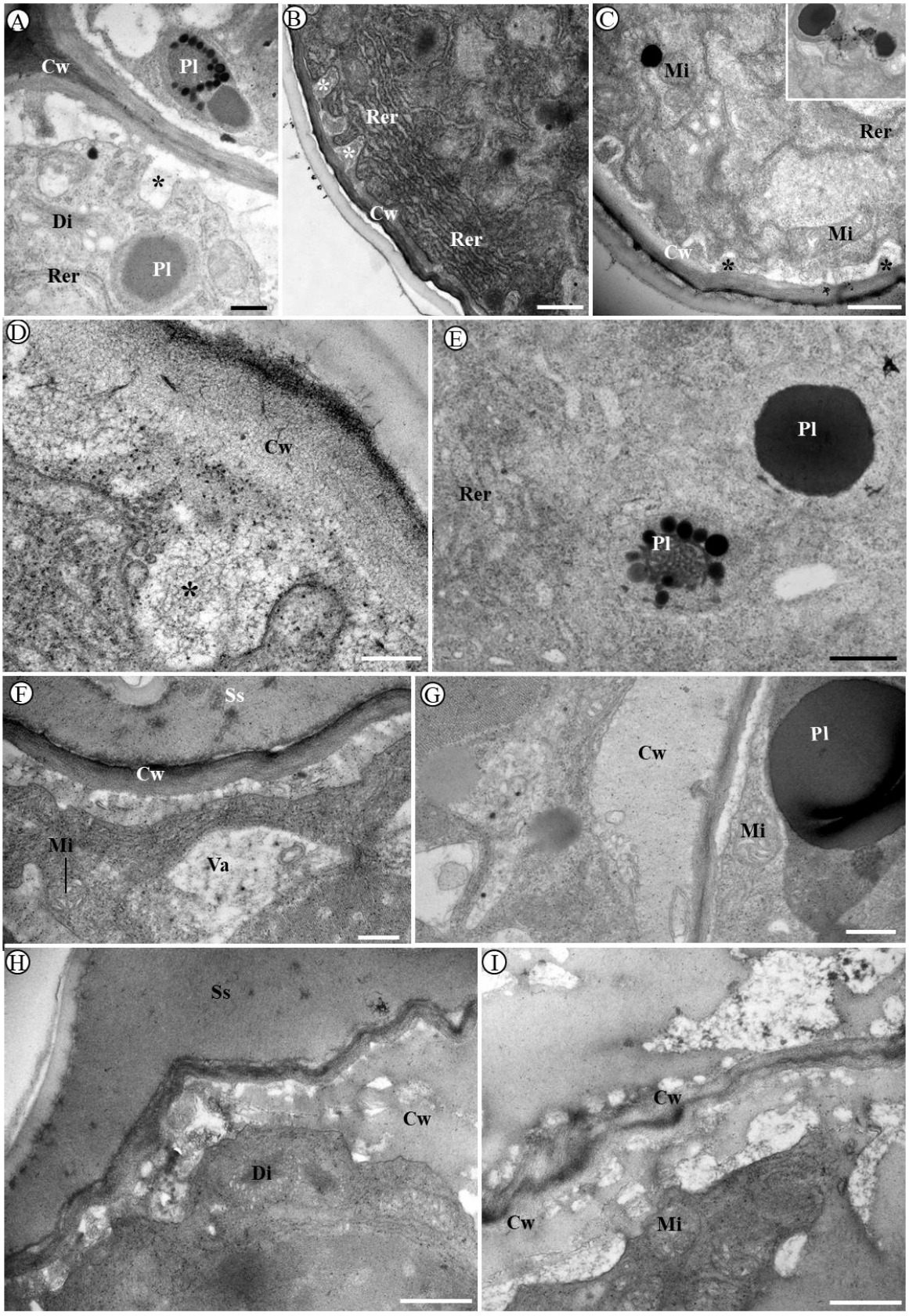
A
Cw
Pl
Di
Rer
Pl
B
Rer
Cw
Rer
C
Mi
Rer
Cw
Mi
D
Cw
E
Pl
Rer
Pl
F
Ss
Cw
Mi
Va
G
Cw
Pl
Mi
H
Ss
Cw
Di
I
Cw
Cw
Mi

Figure 7

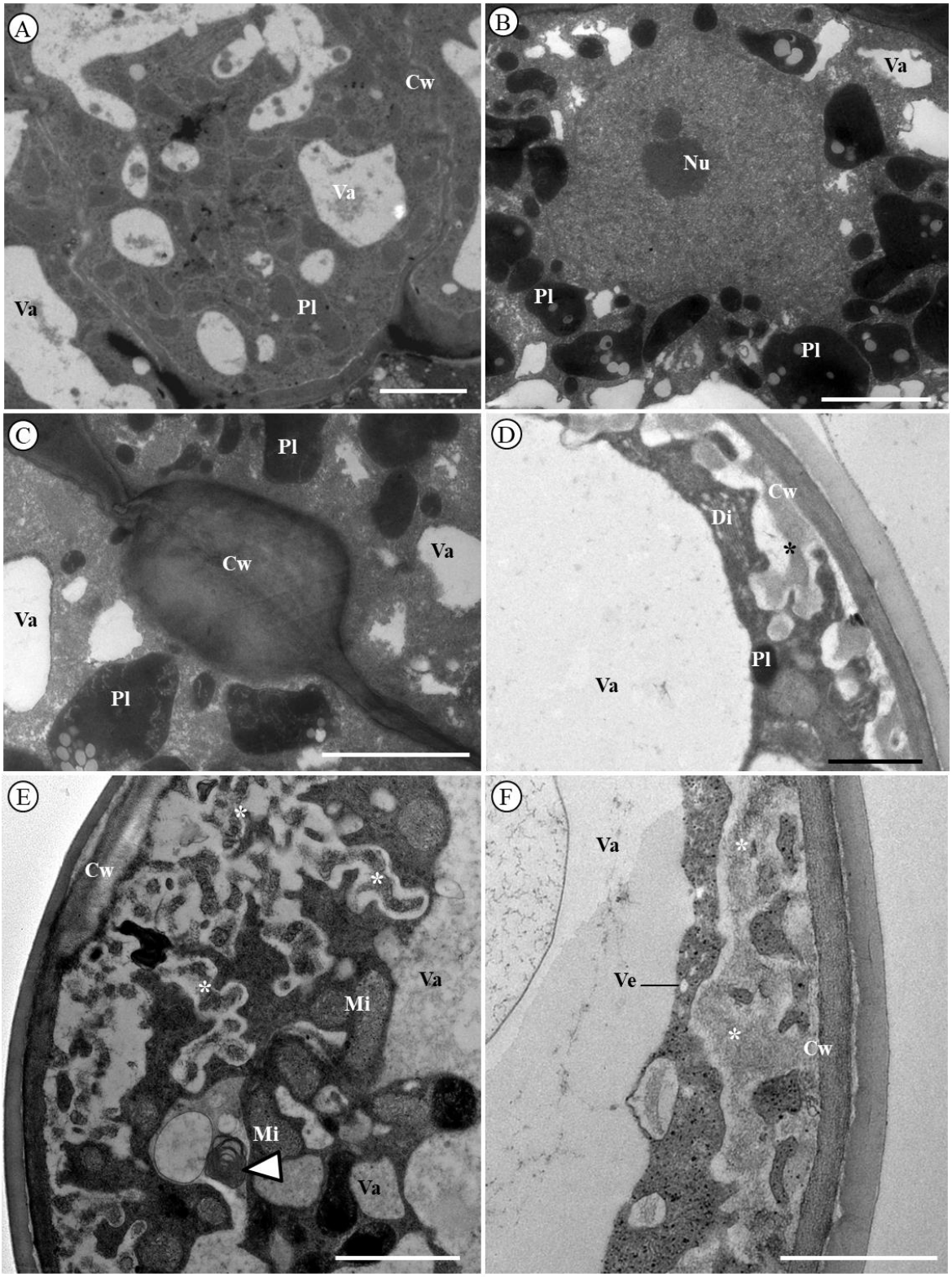
A
Cw
Va
Va
Pl
B
Va
Nu
Pl
Pl
C
Pl
Cw
Va
Va
Pl
D
Cw
Di
*
Pl
Va
E
*
Cw
*
*
Va
Mi
Mi
Va
F
Va
*
Ve
*
Cw

Figure 8

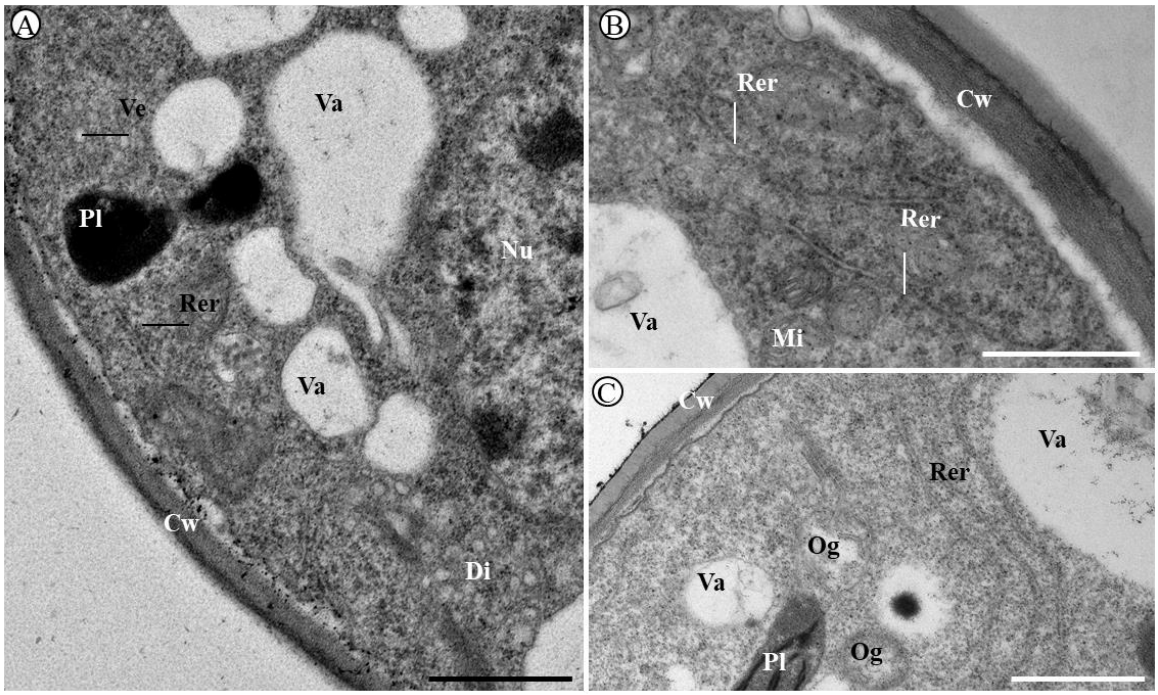

Figure 9

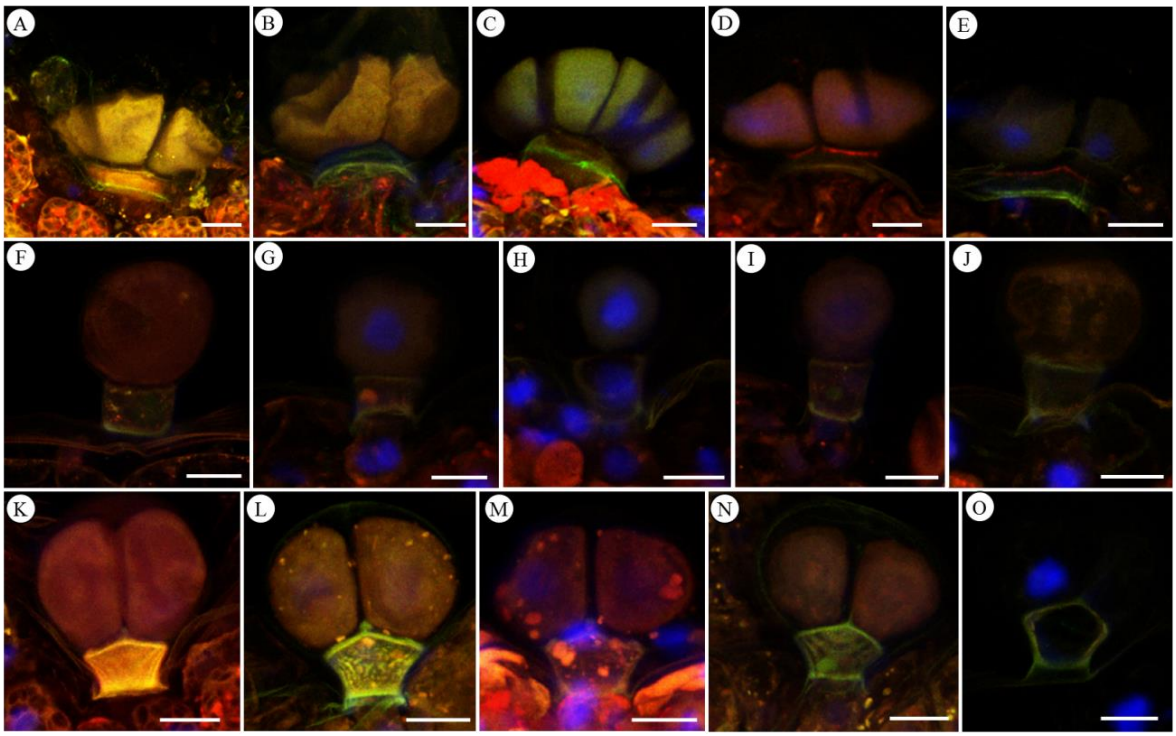

Figure 10

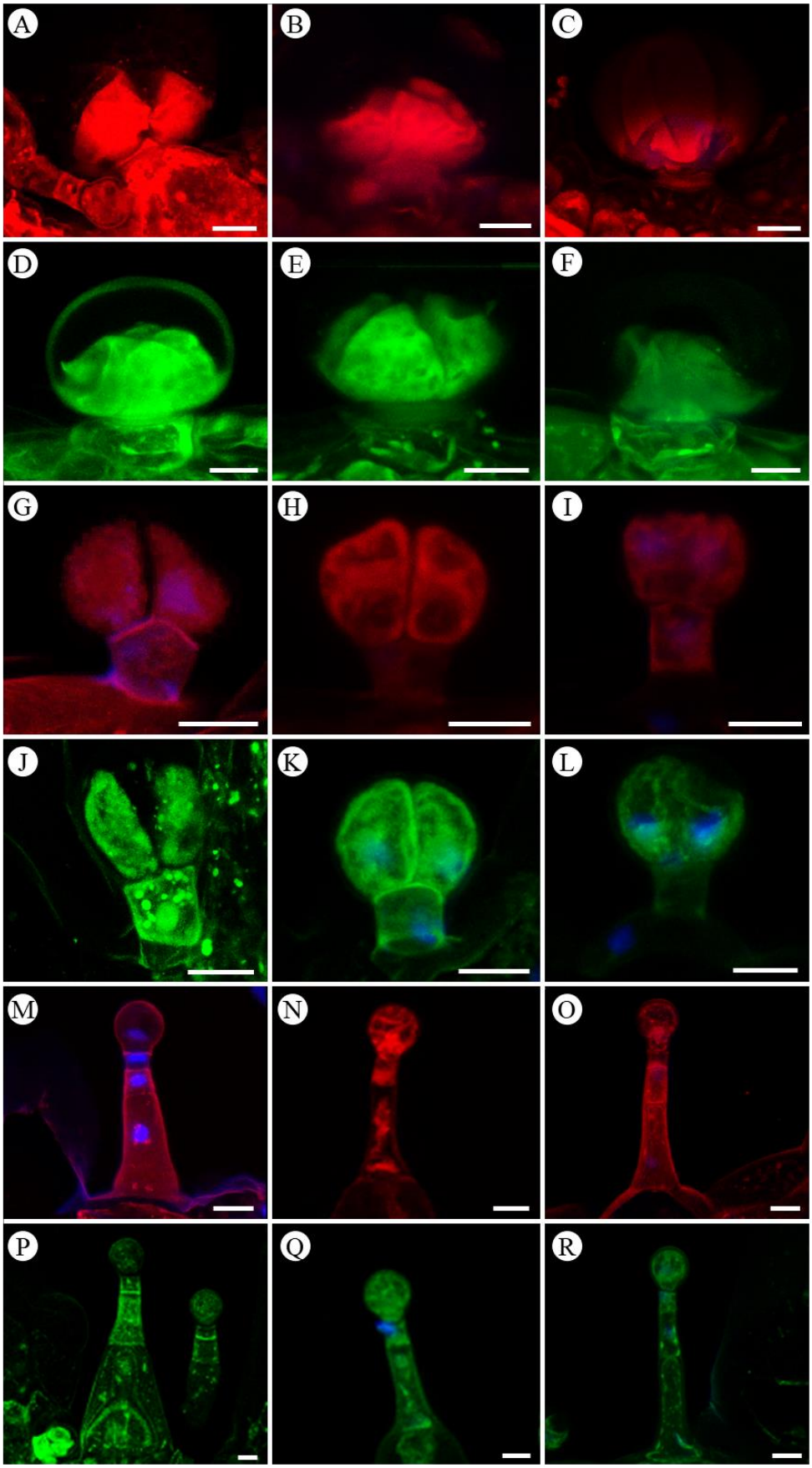

Figure 11

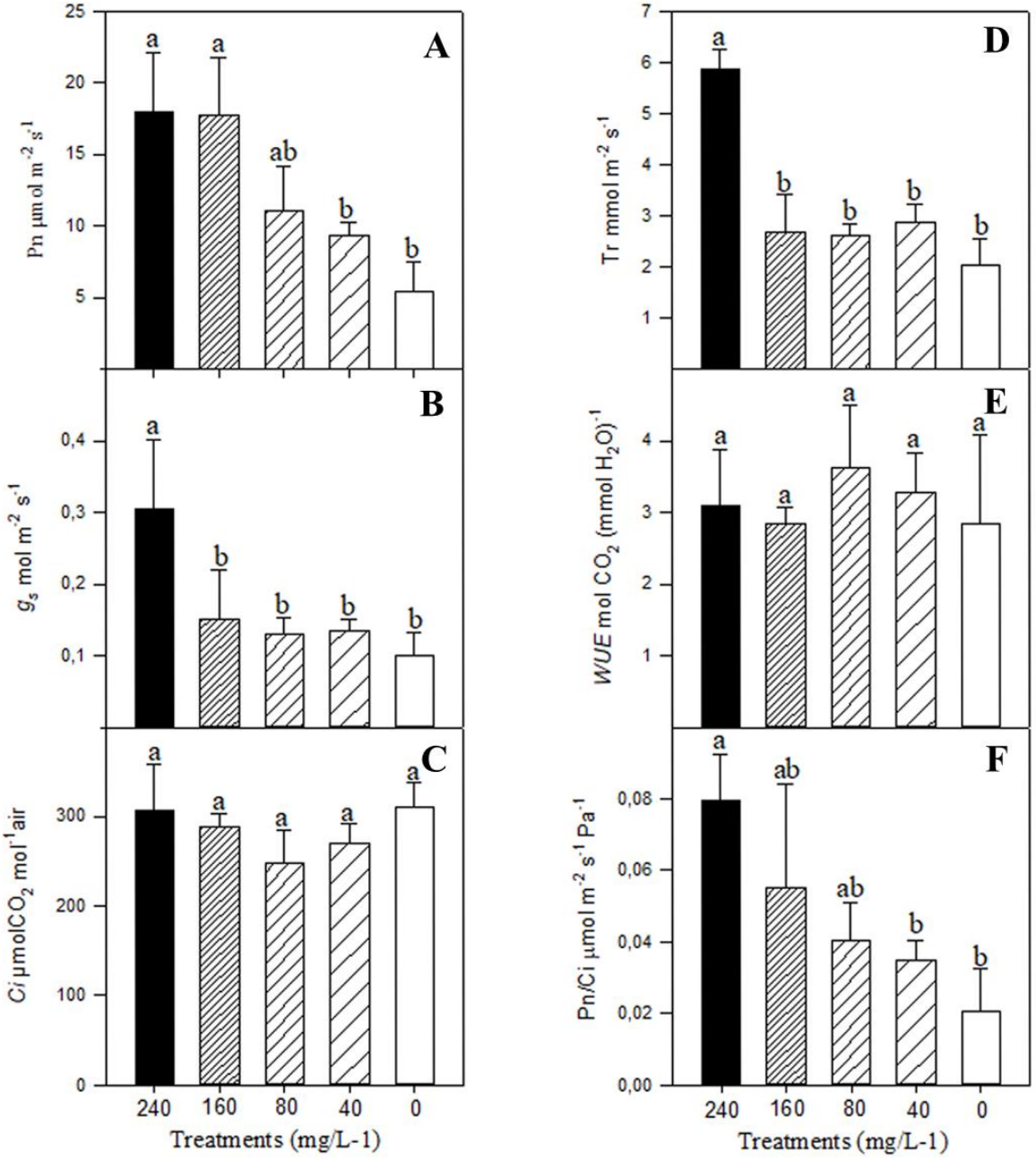
A
B
C
D
E
F
Pn µmol m-2 s-1
gs mol m-2 s-1
Ci µmolCO2 mol-1air
Tr mmol m-2 s-1
WUE mol CO2 (mmol H2O)-1
Pn/Ci µmol m-2 s-1 Pa-1
240
160
80
40
0
Treatments (mg/L-1)

Figure 12

CAPÍTULO 3

Dynamic of intracellular lipid drop transport involves actin filaments and endoplasmic reticulum in Tobacco cells

Luiz Ricardo dos Santos Tozin[1,2], Tatiane Maria Rodrigues[1], Jaideep Mathur[2]*

[1] São Paulo State University (UNESP), Institute of Biosciences of Botucatu (IBB), Department of Botany, Botucatu, SP, Brazil.

[2] University of Guelph, Department of Molecular and Cellular Biology, Laboratory of Plant Development and Interactions, Guelph, ON, Canada.

*Author for correspondence (jmathur@uoguelph.ca)

ABSTRACT

Lipid droplets (LDs) are an important energy source to living cells of prokaryotes and eukaryotes. Such inclusions are constituted by several classes of neutral lipids and are surrounded by a monolayer of phospholipid with embedded integral and peripheral proteins. Whereas investigations on the cellular machinery involved in the LDs production are easily found in the literature, LD behavior has been poorly studied in plant cells. We analyzed the intracellular movement of LDs using a model plant species. For this, we infiltrated Tobacco leaves with *Agrobacterium tumefaciens* containing different DNA sequences targeted to lipid droplets, plastids, endoplasmic reticulum, actin filaments and microtubules and analyzed leaf samples using confocal laser scanning microscopy. We observed that LD displacement is driven by the endoplasmic reticulum on the actin filaments. In addition, observations suggested a correlation

between the LDs and plastids. Our data suggests a movement mechanism of LDs different from that described for animal cells.

Keywords: actin, endoplasmic reticulum, lipid drops, microtubules, live imaging, plastids.

INTRODUCTION

The lipids are an important energy source for many organisms and their presence is almost universal among the living cells (Thiam et al. 2013). For plants, the presence of lipid drops (LDs) immersed in the cytoplasm has been described in cells of vegetative and reproductive organs of ancestral and modern plants (Huang et al. 2013).

The LDs generally have a spherical appearance and are constituted by several classes of neutral lipids surrounded by a monolayer of phospholipid with embedded integral and peripheral proteins (Murphy 2001; Martin and Parton 2006). One such class of structural proteins are the oleosins (Huang et al. 2013), and one of their functions is to regulate of the oil body repulsion (Heneen et al. 2008), avoiding the coalescence of different oil bodies.

The intracellular dynamic involved in the synthesis and transport of LDs in plant cells is still poorly known (Miquel et al. 2014). The endoplasmic reticulum (ER) and plastids are responsible for the intracellular synthesis of lipophilic compounds in plants (Fahn 1979; Wanner et al. 1981; Evert 2006; Tozin et al. 2015; Silva et al. 2016; Pyc et al. 2017); however, the level of involvement of such organelles in the intracellular transport of LDs remains relatively unknown (Wahlroos et al. 2003).

The intracellular displacement of LDs has been described to be microtubule-dependent in *Drosophila* (Welte et al. 1998) and mammals (Targett-Adams et al. 2003) cells. For plants, it is well established that the actin filaments are the major components

involved in the movement and anchorage of vesicles and organelles (Evert 2006 and references therein; Geitmann and Nebenführ 2015), and that the microtubules are involved, mainly, in cell structure maintenance and cell wall deposition (Evert 2006; Ehrhardt and Shaw 2006; Nick 2008). To the best of our knowledge, studies on the role of the cytoskeleton elements in transport dynamic of LDs in plant cells have not been carried out.

The use of live imaging techniques in plants has proven to be an excellent tool for understanding a wide diversity of intracellular processes (Schattat et al. 2011; Barton et al. 2017). Here, we analyzed the intracellular movement and behavior of LDs in Tobacco leaves transiently expressing proteins targeted to lipid droplets, plastids, the endoplasmic reticulum, actin filaments and microtubules.

MATERIAL AND METHODS

Plant material

Nicotiana benthamiana (Tobacco) seeds were germinated on sterilized Sunshine mix LA4 (Sun Gro Horticulture, USA) under a long-day light regime (16-h-light–8-h-dark). Single, double and triple transient expression experiments were carried out through *Agrobacterium tumefaciens* mediated infiltration (Table 1).

To infiltrate, four weeks old Tobacco plants were utilized. Modified *Agrobacterium* growing in YEB media were resuspended in *Agrobacterium* Infiltration Media (AIM). Subsequently, the solution with each modified *Agrobacterium* was mixed according to Table 1, and infiltrated in an expanded leaf. Leaf discs were collected and the transient expressions analyzed 48 h after the agro-infiltration. For induce stromule formation from plastids the leaf discs were treated with 40 mM sucrose solution for 3 h or exposed to light for 1 h.

Table 1. Transient expression in Tobacco used to understanding the intracellular oil drops dynamics.

Double transient expression	**Highlighted subcellular compartment**
mTalin:GFP, Oleosin1:RFP	Actin filaments green, LD red
Map4:GFP, Oleosin1:RFP	Microtubules green, LD red
ER:GFP, Oleosin1:RFP	ER lumen green, LD red
tpFNR:GFP, Oleosin1:RFP	Plastid stroma green, LD red
NCHUP:GFP, Oleosin1:RFP	Plastid membrane green, LD red
Triple transient expression	
ER:GFP, tpFNR:YFP, Oleosin1:RFP	ER lumen green, plastid stroma yellow, LD red

Confocal microscopy

To obtain the live-imaging and videos, samples were mounted in water and imaged using a Leica TCS-SP5 confocal microscopy system equipped with a 488 nm Ar laser and a 543 nm HeNe Laser. GFP fluorescence was acquired at 500–520 nm, RFP fluorescence at 570–620 nm, YFP fluorescence at 530–550 nm and chlorophyll autofluorescence at 660–750 nm. All confocal images were acquired at a resolution of 1024×512 or 1024×1024 pixels. Three-dimensional (x,y,z) stacks were collected with a step-size of 0.99 μm and successive frames in x, y, t time lapse series were obtained 1.935 s apart.

Images were processed using proprietary Leica (LSM SPII) software, ImageJ (Schneider et al., 2012) and Adobe Photoshop CS6. Quick time 7 and Videator v2 (Stone Design Corp., New Mexico) were used for assembling and annotating time-lapse movies.

RESULTS

Lipid droplets (LD) were found in both epidermal and mesophyll cells. Concerning the cytoskeletal elements, actin filaments are localized in the whole cell

(Fig. 1A-B). The LDs were always found moving along actin filaments (Video 1). However, LD motility was not observed in cells where the actin filaments were stabilized (Video 2). Microtubules were visualized in the cortical portion (Fig. 1C-D) while the LDs are more frequent in the central portion of cells, often found aggregating in the peri-nuclear region (Fig. 1E). It was concluded that microtubules and LDs are localized in different cellular portion and there is no direct association between them (Video 3).

In dual labelling experiments the ER and LDs were observed at the same time, and they are always found in close contact each other (Fig. 2A-B). The ER appears to act as a track for LDs displacement (Video 4). Furthermore, LDs were occasionally found in contact with the plastid body (Fig. 2B-D; Video 5) and stromules (Fig. 2C-D) for several minutes (Video 6). However, some LDs that do not associate with the plastids were also observed (Video 5). When stimulated by the 40 mM sucrose solution or exposure to light, the stromule formation increased and the LDs appeared to be aggregated more around the plastids (Fig. 2C-D).

DISCUSSION

Our live imaging based data shows for the first time the transport dynamics of LDs in plant cells. We demonstrated that the LDs produced by ER and plastids (Evert 2006) move along the ER on the actin filaments. Although earlier investigations in animal cells have suggested that the LD displacements to be microtubule-dependent (Welte et al. 1998; Targett-Adams et al. 2003), no relation was identified between the LDs movement and the microtubules for the plant cells. Since the LDs and microtubules are spatially separated in Tobacco cells, we suggest that the mechanism which drives

LDs in plants and animal cells is different. In addition, a possible conditional relation between the LDs and the plastids is suggested.

Our results evidenced a close association between ER and LDs. Although an attachment between the ER and LDs has been demonstrated in plant cells by Wanner et al. (1981) and Wahlroos et al. (2003), we showed this association using live imaging for the first time here. Our observations concur with Pyc et al. (2017), who state that the ER form a "lens-like structure" during the process of origin of LDs which keeps them attached with the ER membrane. So, we can consider that the ER represents the track responsible for LDs displacement. The ER organization, as well as the movement of other organelles and vesicles, are facilitated by actin filaments (Evert 2006 and references therein; Geitmann and Nebenführ 2015) in an actin polymerization and depolymerization dependent manner (Geitmann and Nebenführ 2015). This fact corroborate our observations on LDs are always moving in association with the actin filaments; in fact, when actin filaments are stabilized, the movement of LDs does not occur. So, we can affirm that LDs move on the ER through interactions with the actin filaments.

The association between LDs and plastids seems to be conditional, since some LDs were seen very close to the plastids while others were localized far away from these organelles. This differential behavior of LDs might reflect their origin and contents. The involvement of plastids in the process of oil synthesis in plant cells is well documented (Wanner et al. 1981; Turner et al. 1999; Evert 2006; Tozin et al. 2015) and LDs formed by compounds coming from the plastids probably will be close to this organelle. Turner et al. (1999) showed for peppermint that the limonene comes from leucoplast, exclusively. So, the oil drops formed by limonene might be associated with this organelle. On the other hand, it is known that the plastids are not the exclusive

organelles involved in oil synthesis. As previously discussed here, the ER is responsible for the production of a large fraction of lipidic content in plant cells (Evert 2006; Pyc et al. 2017). So, we suggest that LDs formed by compounds coming from, exclusively, the ER will not be near the plastid body and stromules. Plastids are known to produce stromules - stroma-filled tubules (Gray et al. 2001), and its relation with other organelles, such mitochondria, endoplasmic reticulum, peroxisomes and another plastids have been demonstrated (Schattat et al. 2011; Delfosse et al. 2016; Barton et al. 2017). In this context, the importance of stromules in LD biogenesis and transport in plant cells deserves some attention. As showed by previous studies, the light intensity and sucrose solution increased stromule frequency (Schattat et al. 2012; Delfosse et al. 2016; Barton et al. 2017) in Tobacco cells and promoted the aggregation of oil drops around the plastids. Both, under light and sucrose, increasing the stromule frequency have been attributed to a link between photosynthesis and this phenomenon (Delfosse et al. 2016). However, the real reason why the LDs became aggregated around the plastids requires further investigation.

This study using live imaging enabled us to see what really happens with the LD in a real time inside a plant cell. New studies using stable transgenic model are being conducted since the transient expression based observations might create an over-estimation of the LD size and numbers in a cell. However, the mechanism of LD motility described here, probably, does not change. In addition, futures studies with several other native species which form the source for OLEOSIN cDNAs should be conducted to establish a more general pattern for plant cells.

CONCLUSION

Here, the intracellular LD transport dynamics using epidermal and mesophyll cells of Tobacco leaves are described. LDs movement through the endoplasmic reticulum on the actin filaments in cells of a model plant are shown and a conditional relationship is suggested between plastids and lipid droplets. Most important, our data suggest a movement mechanism that is different from that described for animal cells.

ACKNOWLEDGEMENTS

We thank the CAPES Foundation for provide the scholarship for doctoral research as a Visiting Student (PDSE process: 88881.131495/2016-01) at University of Guelph for the first author.

REFERENCES

Barton KA; Wozny MR; Mathur N; Japipargas EA; Mathur J. 2017. Chloroplast behaviour and interactions with other organelles in *Arabidopsis thaliana* pavement cells. Journal of Cell Science 0: 1-11.

Delfosse K, Wozny MR, Jaipargas EA, Barton KA, Anderson C, Mathur J. 2016. Fluorescent Protein Aided Insights on Plastids and their Extensions: A Critical Appraisal. Frontiers in Plant Science. 6: 1253.

Evert RF. 2006. Esau's plant anatomy. 3rd. edn. New Jersey, Wiley- Interscience.

Ehrhardt DW, Shaw SL. 2006. Microtubule dynamics and organization in the plant cortical array. Annu. Rev. Plant Biol. 57: 859–875.

Fahn A. 1979. Secretory tissues in plants. London, Academic Press.

Geitmann A, Nebenführ A. 2015. Navigating the plant cell: intracellular transport logistics in the green kingdom. Molecular Biology of the Cell. 26: 3373-3378.

Heneen WK, Karlsson G, Brismar K, Gummeson PO, Marttila S, Leonova S, Carlsson AS, Bafor M, Banas A, Mattsson B, Debski H, Stymne S. 2008. Fusion of oil bodies in endosperm of oat grains. Planta 228: 589–599.

Gray JC, Sullivan JA, Hibberd JM, Hansen MR. 2001. Stromules: Mobile protrusions and interconnections between plastids. Plant Biol. 3: 223-233.

Huang NL, Huang MD, Chen TLL, Huang AHC. 2013. Oleosin of subcellular lipid droplets evolved in green algae. Plant Physiol. 161: 1862–1874.

Martin S, Parton RG. 2006. Lipid droplets: a unified view of a dynamic organelle. Nat. Rev. Mol. Cell. Biol 7: 373–378.

Miquel M, Trigui G, D'Adréa S, Kelemen Z, Baud S, Berger A, Deruyffelaere C, Trubuil A, Lepiniec L, Dubreucq B. 2014. Specialization of Oleosins in Oil Body Dynamics during Seed Development in *Arabidopsis* Seeds. Plant Physiol. 164: 1866-1878.

Murphy DJ. 2001. The biogenesis and functions of lipid bodies in animals, plants and microorganisms. Prog. Lipid Res 40: 325–438.

Nick P. 2008. Plant Microtubules, Berlin: Springer.

Pyc M, Cai Y, Greer MS, Yurchenko O, Capman KD, Dyer JM, Mullen RT. 2017. Turning Over a New Leaf in Lipid Droplet Biology. Trends in Plant Science 22(7): 596-609.

Schattat MH, Barton K, Baudisch B, Klosgen RB, Mathur J. 2011. Plastid stromule branching coincides with contiguous endoplasmic reticulum dynamics. Plant Physiol. 155: 1667-1677.

Schneider CA, Rasband WS, Eliceiri KW. 2012. NIH image to ImageJ: 25 years of image analysis. Nature Met. 9: 671-675.

Silva SCM, Tozin LRS, Rodrigues TM. 2016. Morphological and histochemical characterization of secretory sites of bioactive compounds in *Lantana camara* L. (Verbenaceae) leaves. Botany 94: 321-336.

Targett-Adams P, Chambers D, Gledhill S, Hope RG, Coy JF, Girod A, McLauchlan J. 2003. Live cell analysis and targeting of the lipid droplet-binding adipocyte differentiation-related protein. J. Biol. Chem 278: 15998–16007.

Thiam AR, Farese Jr RV, Walther TC. 2013 The biophysics and cell biology of lipid droplets. Nat. Rev.Mol.Cell. Biol. 14(12): 775–786.

Tozin LRS, Carvalho SF, Machado SR, Rodrigues TM. 2015. Glandular trichome diversity on leaves of *Lippia origanoides* Kunth and *Lippia stachyoides* Cham. (Verbenaceae): morphology, histochemistry and ultrastructure. Botany 93: 297-306.

Turner G, Gershenzon J, Nielson EE, Froehlich JE, Croteau R. 1999. Limonene Synthase, the Enzyme Responsible for Monoterpene Biosynthesis in Peppermint, Is Localized to Leucoplasts of Oil Gland Secretory Cells. Plant Physiol. 120: 879-886.

Wahlroos T, Soukka J, Denesyuk A, Wahlroos R, Korpela T, Kilby NJ. 2003. Oleosin Expression and Trafficking During Oil Body Biogenesis in Tobacco Leaf Cells. Genesis 35: 125-132.

Wanner G, Formanek H, Theimer RR. 1981. The Ontogeny of Lipid Bodies (Spherosomes) in Plant Cells. Planta 151: 109-123.

Welte MA, Gross SP, Postner M, Block SM, Wieschaus EF. 1998. Developmental regulation of vesicle transport in *Drosophila* embryos: forces and kinetics. Cell 92: 547–557.

LEGENDS OF FIGURES AND VIDEOS

Figure 1. Cytoskeletal elements and lipid drops distribution in leaf epidermal cells of Tobacco plants. **A-B** Actin filaments (arrow) (mTalin:GFP) and lipid drops (Ld) (Oleosin1:RFP) interactin. **C-E** Cells labeled for microtubules (arrowhead) (map4:GFP) and lipid drops (Ld) (Oleosin1:RFP). **C-D** Outer portion of cell showing the cortical microtubules. **E** Internal portion of cell showing the presence of lipid drops and the absence of microtubules. Scale bars: 5 µm.

Figure 2. Organelles and lipid drops in leaf epidermal cells of Tobacco plants. **A** Endoplasmic reticulum (Er) (ER:GFP) and lipid drops (Ld) (Oleosin1:RFP) association. **B** Endoplasmic reticulum (Er) (ER:GFP), lipid drops (Ld) (Oleosin1:RFP) and plastids (Pl) (tpFNR:YFP) interaction. **C** Plastids (NCHUP:GFP) showing increased stromules (St) and lipid drops (Ld) (Oleosin1:RFP) after 1 h light. **D** Lipid drops (Oleosin1:RFP) associated with the plastids body (NCHUP:GFP) after 40 mM sucrose for 3h. Scale bars: 5 µm.

Video 1. Lipid drops (Oleosin1:RFP) associated with actin filaments (mTalin:GFP).

Video 2. Lipid drops (Oleosin1:RFP) do not move itself after the actin filaments (mTalin:GFP) stabilization.

Video 3. Lipid drops (Oleosin1:RFP) moving independently on the microtubules (map4:GFP).

Video 4. Oil drops (Oleosin1:RFP) moving on the ER (ER:GFP) and close to the plastids (tpFNR:YFP).

Video 5. Lipid drops (Oleosin1:RFP) showing facultative association with plastids (tpFNR:GFP).

Video 6. Lipid drops (Oleosin1:RFP) associated with plastid (NCHUP:GFP) body and stromules.

FIGURES

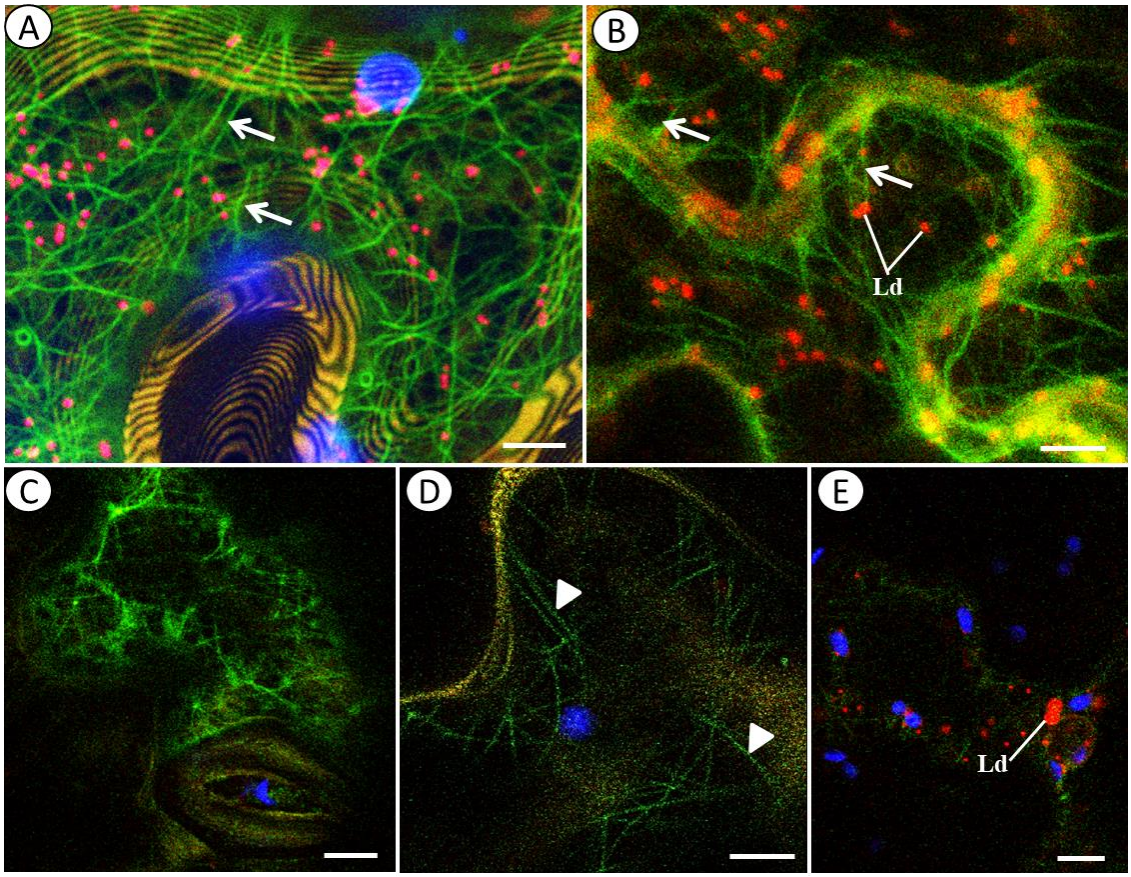

Figure 1

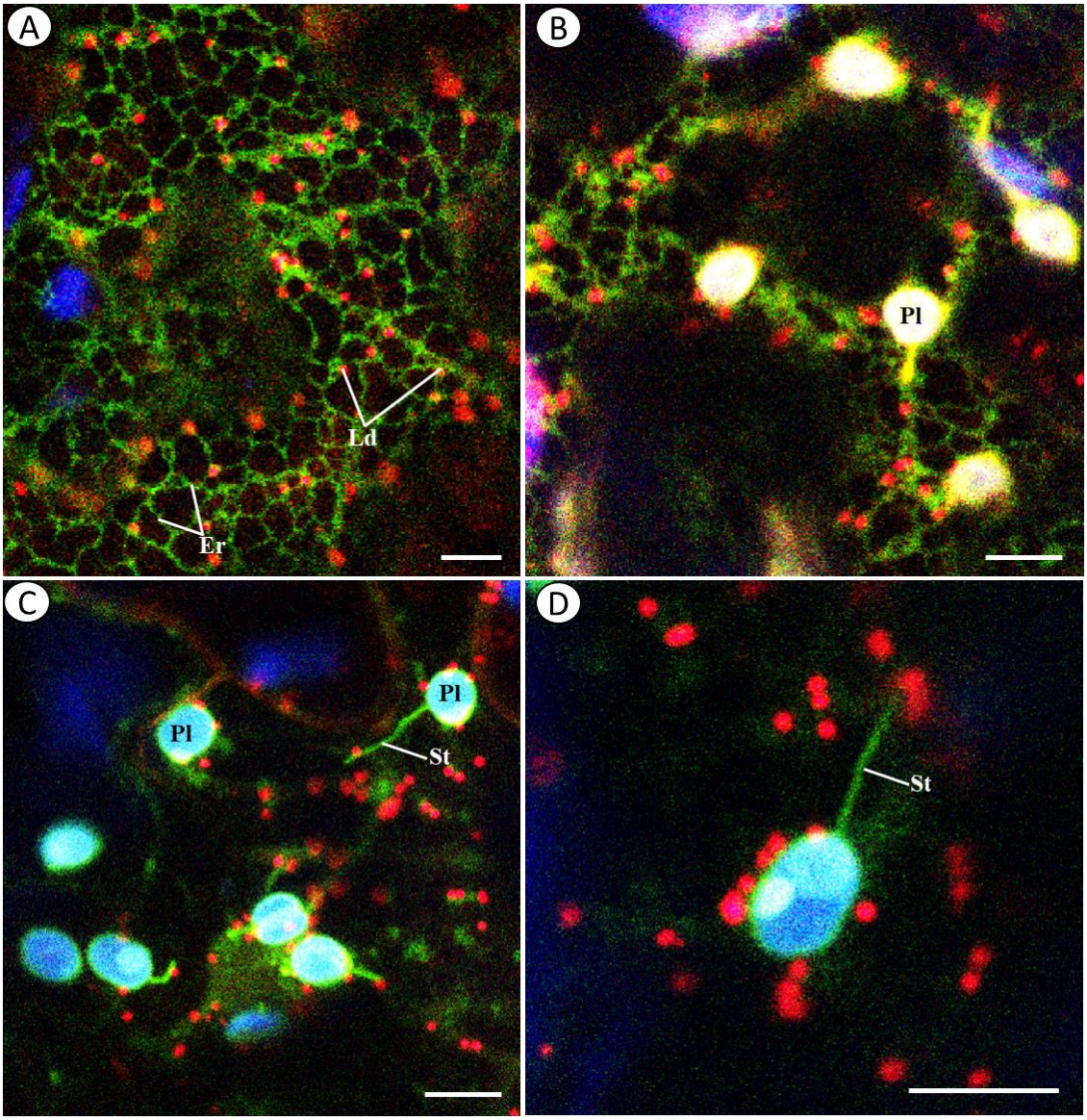

Figure 2

CAPÍTULO 4

Herbivory by leaf-cutter ants changes the glandular trichomes density and the volatile components in an aromatic plant model

Luiz Ricardo dos Santos Tozin[1]*, Marcia Ortiz Mayo Marques[2], Tatiane Maria Rodrigues[1]

[1]São Paulo State University (UNESP), Institute of Biosciences of Botucatu (IBB), Department of Botany, Botucatu, SP, Brazil.

[2]Instituto Agronômico (IAC), Laboratory of Natural Products, Campinas, SP, Brazil.

*Corresponding author (ricardo.tozin@gmail.com)

ABSTRACT

Herbivory can induce several structural and functional alterations in the plant secretory system. Glandular trichomes are the main sites of production of volatile organic compounds (VOC) with several chemical properties in Lamiaceae species. *Ocimum* species usually have three morphotypes of glandular trichomes (morphotype I is peltate and has a wide four-celled head; morphotypes II is capitate and has a unicellular head; and morphotype III is capitate with a bicellular head) which produce a great amount of terpenes, although other chemical categories of substances are also produced. Despite the abundance of trichomes producing important anti-herbivory components in their leaves, the association between *Ocimum* species and leaf-cutter ants has been commonly registered in Brazil. We investigated the effect of leaf-cutter ant attack on the density of the glandular trichomes and on the chemistry of the VOCs released from leaves of *O. gratissimum*. Plants were subjected to *Acromyrmex rugosus* attack until 90% of leaves

were removed. After 40 days from the leaf-cutter attack, both treatments were sampled. The glandular trichome density was analyzed by scanning electron microscopy. The VOCs were extracted utilizing headspace solid-phase microextraction (HS-SPME) technique and analyzed by gas-chromatography. Generally, the density of glandular trichomes increased in the adaxial leaf surface of the attacked plants. However, we bring novelties on this topic since we analyzed the density of each morphotype separately. The morphotype I decreased in the abaxial leaf surface, and increased in the adaxial leaf surface; the morphotype II increased in both leaf surfaces; and the morphotype III decreased in the abaxial leaf surface and remained constant in the adaxial leaf surface of attacked plants. In leaves of attacked plants, the (Z)-β-ocimene increased by 50%, the α-selinene by 13%, and the germacrene D by 126%, whereas the eugenol decreased by 70%. Our data point to a differential response of each glandular morphotype in *O. gratissimum* and are consistent with the idea of a compartmentalization of functions among the different glandular morphotypes in the plant defense against environmental factors.

KEYWORDS: *Acromyrmex rugosus*, Gas chromatography, Herbivore induced plant volatiles (HIPV), *Ocimum*, Terpenes.

INTRODUCTION

Glandular trichomes can be viewed as a combination of structural and chemical defenses against several abiotic and biotic factors (Werker 2000; Tozin et al. 2015a), such as herbivory. These defenses are due the fact that glandular trichomes form a protect layer around the leaves (Werker 2000), and produce substances that can be poisonous or repellent to herbivorous organisms (Dalin et al. 2008). Several plant species respond to damage caused by herbivores by producing new leaves with an

increased density of trichomes. The magnitude of the reported increase in trichome density is commonly between 25% and 100%, but in some cases it is as large as 500% – 1000% (Dalin et al. 2008). Such responses involving changes in density of trichome are expressed within days or weeks (Baur et al. 1991; Agrawal 2000; Rautio et al. 2002).

A wide range of plant species have been shown to emit new herbivore-induced plant volatiles (HIPVs) or increased amounts of constitutive HIPVs from glandular trichomes following herbivore damage (Dicke et al. 2003; Unsicker et al. 2009). Some species exhibit a rapid response to herbivory attacks, and the HIPVs can be detected in the first 45 minutes after feeding (Kigathi et al. 2009).

The effect of a herbivore attack on trichome production may vary according to the identity of the herbivore (Dalin et al. 2008), and not all herbivorous insects induce changes in trichome production (Traw and Dawson 2002). Different species of herbivores could induce different responses due to differences in substances present in their saliva (Turlings et al. 1993; Geervliet et al. 1997). Herbivory caused by leaf-cutter ants is known to cause losses in agriculture estimated in the billions of dollars (Hölldobler and Wilson 1990). The leaf-cutter ants are the most important pest insect in agriculture (Zanuncio et al. 1996) and cultivated forest of the Neotropic (Della Lucia et al. 1993). *Acromyrmex* ants are among the most damaging invertebrates in the Neotropic (Boulogne et al. 2012) and have been registered in different regions of America (Farji-Brener & Ruggiero1994). In Brazil, *Acromyrmex* ants have been commonly found in several States and their association with different plants with economic importance, including *Ocimum* species, is well known (Rando & Forti 2005).

Ocimum genus comprises aromatic species of Lamiaceae with particular importance in the medicine and culinary due to the production of essential oils (Silva et al. 2008). Such species are featured by the presence of three morphotypes of glandular

trichomes with differential morphological and functional aspects (Werker et al. 1993; Naidoo et al. 2013). The morphotype I is peltate and has a wide four-celled head; the morphotypes II is capitate and has a unicellular head; and the morphotype III is capitate and has a bicellular head (Werker et al. 1993; Naidoo et al. 2013). In addition to their morphological and subcellular peculiarities, differences in the composition of the produced secretion have been histochemically detected in each one of these glandular morphotypes (Naidoo et al, 2013).

Ocimum gratissimum present these three morphotypes of glandular trichomes in their leaves (Tozin & Rodrigues *In Prep*), and is important for the production of essential oils widely exploited by the pharmaceutical industry, like eugenol (Silva et al. 1999; Fernandes et al. 2013) and 1-8 cineol (Silva et al. 1999), among others. In addition, *O. gratissimum* is cultivated in gardens, and is used in the popular medicine to treat rheumatism, paralysis, epilepsy and mental illness, and contain biologically active substances with insecticide, nematicide, fungicide and antimicrobial proven properties (Efraim 2001).

In this paper we investigated the effect of leaf-cutter ant attacks on the density of the glandular trichomes and on the VOCs chemical composition in leaves of *O. gratissimum*. We hypothesized that the plant attack by leaf-cut ants could induce the increase in the glandular trichome density and lead to the production of different volatile compounds in an effort of an incremental protection against future attacks.

MATERIAL AND METHODS

Plant material

For cuttings, stem fragments of *Ocimum gratissimum* approximately 10 cm long were collected from six individuals growing in the medicinal garden belonging to

Sao Paulo State University (UNESP), in Botucatu municipality (22°52 S, 48°26 W), in central-west region of São Paulo State, in southeastern Brazil. The stem cuts were placed in trays containing commercial substrate (Bioplant®, Nova Ponte, Minas Gerais, Brazil) and 20 individuals were obtained. The plants were maintained under humid conditions until rooting. After 40 days, the plants saplings were transferred to 6.0 L pots filled with complete Hoagland and Arnon's (1950) n^{o}. 2 nutrient solution with 75% ionic concentration. The pots were kept in a greenhouse under mean maximum and minimum air temperatures of 26.5°C and 21.5°C, respectively, and mean relative humidity of 70%. The solutions were prepared using deionized water and were constantly aerated and renewed every week to minimize nutrient depletion or pH changes.

Vouchers were deposited in the Irina Delanova Gemtchújnicov Herbarium (BOTU), of the Department of Botany, Institute of Biosciences of Botucatu, IBB, UNESP, Botucatu, Sao Paulo, Brazil, under registration number 32798.

Experimental design

At 65 days after transplanting to the hydroponic system, the plants were placed in a greenhouse naturally infested by leaf-cutter ants. The experiment consisted of two treatments, a control (protected from ant attacks; n= 8) (Fig. 1A) and attacked plants (n=8). The pots with control plants were placed inside a container filled with water and dishwashing detergent (that surrounded the pots without enter them), to avoid the ant approach. The attacked plants were exposed to *Acromyrmex rugosus* (leaf-cutter ant) for 48 h, until 90% of leaves were removed by the herbivores (Fig. 1B). Posteriorly, the pots were arranged in a randomized design in a greenhouse, and the apical meristems were labeled to ensure that the analyzed leaves were produced at the same time. After

40 days (Fig. 1C), the fully expanded leaves that were formed after the herbivore attacks and leaves from control plants were collected to analyze the density of glandular trichomes and the volatile components chemical composition. To analyze the glandular trichomes density, we collected leaves with the same size produced at the same time.

Density of glandular trichomes

To evaluate the glandular trichomes density, eight leaves of each treatment (two leaves per plant, being one for each leaf surface analyzis) were fixed in 2.5% glutaraldehyde with 0.1 M phosphate buffer, pH 7.3, overnight at 4 °C, dehydrated in a graduated acetone series, critical-point dried, mounted on aluminum stubs, and gold-coated (Robards 1978). The material was examined with a FEI Quanta™ scanning electron microscope.

The glandular density in leaves was calculated in 1 mm^2 using the Scandium software with an image-capture system coupled to the scanning electron microscope. The density of all glandular trichomes and of each morphotype was calculated in the middle region of the leaf blade, in both abaxial and adaxial leaf surface.

Extraction and analysis of volatile organic compounds (VOCs)

The extraction and analysis of VOCs were conducted in leaf samples collected from both treatments (n=8).

The headspace solid-phase microextraction (HS-SPME) technique was used to extract the volatile compound. For capture of the volatile constituents samples with 0.45 g of leaves were placed in clear screw cap vials with 15 mL of deionized water. The vial was placed in water bath at 95 °C for 1h. The volatile phase was exposed to

CAR/PDMS fiber (Carboxen/Polydimethylsiloxane, film thickness 75 μm, Supelco, Bellefonte, PA, EUA) for 15 min.

The qualitative and quantitative (area normalization method) analysis of the volatile components were performed on a gas chromatograph coupled to a mass spectrometer (CG-MS, Shimadzu, QP- 5000), with an OV-5 fused silica capillary column (30 m x 0.25 mm x 0.25 μm, Ohio Valley Specialty Chemical, Inc.), operating at an MS ionization voltage of 70 eV, with helium as the carrier gas (1.0 mL/min.). The following chromatography conditions were used: injector at 240 °C, detector at 230 °C, split 1/20, and the temperature program: 50 °C, 2 min; 50 °C - 180 °C, 3 °C/min; 180 °C – 230 °C, 10 °C/min. The compounds were identified by comparison of the acquired mass spectra with those stored in the GC/MS database of the system (NIST 62 lib.) and retention indices (Adams 2007). The retention indices (RI) were obtained from the injection of a mixture of n-alcanes (Sigma-Aldrich, C9-C24), employing the same temperature program conditions described above for GC/MS, applying the equation of Van den Dool and Kratz (1963). For each sample the fiber was conditioned in GC-FID (Shimadzu, GC-2010/AOC-20i) with the temperature program: 50 °C - 240 °C, 7 °C/min.

Statistical Analyses

Data referring to the total density of glandular trichomes, the relative density of each glandular morphotype and the concentration of each volatile compound in the essential oil were tested by one-way ANOVA. Tukey test ($P<0.05$) was conducted to compare the different treatments.

RESULTS

Density of glandular trichomes

Both leaf surfaces of *O. gratissimum* (Fig. 2A-B) presented three morphotypes of glandular trichomes (Fig. 2C-E) occurring side by side. The glandular trichome density increased in the adaxial leaf surface in the attacked plants ($p = 0.035$; $F_{(1,14)} = 7.332$) and did not vary in the abaxial leaf surface ($p = 0.085$; $F_{(1,14)} = 4.253$) in plants attacked by ants. However, we registered a differential response of each glandular morphotype to the ant attacks. In the attacked plants, the density of the morphotype I decreased in the abaxial leaf surface and increased in the adaxial leaf surface of attacked plants ($p < 0.001$; $F_{(3,28)} = 11.429$); the density of the morphotyte II increased in both leaf surfaces ($p < 0.001$; $F_{(3,28)} = 18.732$); and, in the morphotype III, the density decreased in the abaxial leaf surface and remained constant in the adaxial leaf surface ($p = 0.011$; $F_{(3,28)} = 6.152$) (Fig. 3).

Volatile Organic Compounds (VOCs)

Twenty-nine compounds were chemically identified in control plants of *O. gratissimum* and twenty in individuals submitted to ant attacks. In both cases the compounds identified represented approximately 97% of volatile components present in the chromatogram. Overall, the major compounds identified were 1,8-cineole (25.79%), β-selinene (17.39%), eugenol (16.61%), (E)-caryophyllene (11.13%), (Z)-β-ocimene (6.38%) and α-selinene (4.55%) (Table 1). In the attacked plants the (Z)-β-ocimene increased by 50%, the α-selinene by 13%, and the germacrene D by 126%, whereas the eugenol decreased by 70% (Table 1). In addition, the attack by *A. rugosus* promoted the increase of five minority substances and the decrease of three minority substances in the leaves of *O. gratissimum* (Table 1).

In a general way, the hydrocarbon monoterpenes increased, and the oxygenated monoterpenes decreased in the VOCs of leaves from attacked *O. gratissimum* plants (Table 1).

DISCUSSION

Our data showed a differential response of each glandular morphotype in leaves of *O. gratissimum* plants attacked by *A. rugosus*; in addition, significant alterations were registered in the composition of the VOCs of attacked plants. Our work is novel in the sense that we presented the density alterations to each glandular morphotype separately. All studies present in the literature report the total density of glandular trichomes (Molina-Montenegro et al. 2006; Dalin et al. 2008), and this could not show what happens with each glandular trichomes.

The increasing of density of glandular trichome after attack of herbivores has been demonstrated in different groups of plants (Levin 1973; Dalin et al. 2008), but not in each glandular morphotype individually. The differential variation of the glandular morphotypes density could be related to the specific substances produced by each morphotype. Several studies have demonstrated that different morphotypes of glandular trichomes could produce secretion with a different chemical nature (Fahn 1979; Tozin et al. 2015a; Silva et al. 2016). In *Ocimum* species, studies have also demonstrated histochemical variations in the substances produced by each morphotype of glandular trichomes (Naidoo et al. 2013; Tozin & Rodrigues *In Prep*). Naidoo et al. (2013) have showed that for *O. obovatum*, peltate trichomes (morphotype I) are more active in the production of lipophilic substances than capitate trichomes (morphotypes II and III). At the same time, whether the essential oil composition produced by each morphotype of glandular trichome varies need to be better investigated. New research is being

conducted to identify the chemical composition of the volatile components produced by each morphotype of glandular trichomes. This research involves using of techniques of microdissection and microextration to search for an association between the density of each morphotype of glandular trichome and volatile components composition produced. In a general way, the increase of HIPV, such germacrene D and (Z)-β-ocimene, was significant in plants attacked by *A. rugosus* and can be related to the attraction of generalist natural enemies of herbivores (Turlings et al. 1998; Dudareva et al. 2003; De Boer & Dicke 2004), or can be associated with the production of substances which act as insecticide or astringent (Kiran & Devi 2007; Tozin et al. 2015b). The increasing in β-ocimene production has been demonstrated after spider mite attacks in *Lotus japonicus* (Arimura et al. 2004). The germacrene D, which increased by 126%, is known by its insecticidal activity against mosquitoes (Kiran & Devi 2007) and repellent role against ticks (Birkett et al. 2008) and aphids (Bruce et al. 2005). In addition, germacrene D plays a role as a precursor of several sesquiterpenes, such as selinenes (Bülow et al. 2000; Telascrea et al. 2007). So, the increasing of α-selinene can be associated with the increasing of germacrene D; and the role of α-selinene in plant defense must be better understood.

Eugenol is known as a toxicant, antifeedant, deterrant, irritant and repellant chemical substance (Tan & Nishida 2012). Nevertheless, some insect species are known to be attracted to eugenol for unknown reasons (Tan & Nishida 2012). Considering that the eugenol decreased by 70% in *O. gratissimum* after leaf-cutter ant attack by *A. rugosus*, we could suggest that *A. rugosus* seems to be an example of these insects. However, new experimental tests are required to confirm this hypothesis.

Whether the compounds produced by the new leaves would prevent new leaf-cutter ants attack in *O. gratissimum* remains unknown. However, Kost et al. (2011)

tested the “induced defence hypothesis” in lima bean and provided the first empirical evidence that the foraging behaviour of Leaf–cutter ants is affected by the volatile organic compounds after herbivory. In addition, Thiele et al. (2014) showed that the leaf-cutter ants could exhibit a delay to reject leaves with new VOCs profile. The leaf-cutter ants may spend five days until they detect the new VOCs produced. This happens because the new VOCs could present antifungal properties and avoid the fungal grow in the ants colonies (Thiele et al. 2014). New works should be conduct to investigate the ants’ foraging behavior in the leaves developed after herbivory in *O. gratissimum*.

CONCLUSIONS

Our work showed that the three morphotypes of glandular trichomes of *O. gratissimum* respond differently to leaf-cutter ant attacks, and the volatile organic components are changed after herbivory. Our findings lead to the idea of a compartmentalization of functions among the different glandular morphotypes in the plant defense against environmental factors. If this hypothesis is confirmed, this work can support future studies concerning plant breeding, to produce plants more resistant.

SOURCE OF FUNDINGS

The first author receives doctoral scholarship from CAPES; and the second author receives productivity scholarship in research from CNPq.

CONTRIBUTIONS BY THE AUTHORS

L.R.S.T. and T.M.R. conceived the idea; L.R.S.T. designed and conducted the experiments; all authors analyzed and discussed the results; L.R.S.T. and T.M.R. wrote the manuscript; and M.O.M.M. commented on the manuscript.

ACKNOWLEDGEMENTS

We thank the staff of the Centro de Microscopia Eletrônica (CME), IBB, UNESP, for helping in the sample preparation; the Dr. Roberto da Silva Camargo from College of Agronomic Sciences, São Paulo State University, for the ants' identification; the writing service at University of Guelph for language revision; and the "Programa de Internacionalização da UNESP – PROINTER" - PROPe/PROPG (Edital 08/2017; application number 1758) for the financial assistance with the payment of publication fee.

LITERATURE CITED

Adams RP. 2007. Identification of essential oil components by gas chromatography/mass spectroscopy, Allured Publ. Corp, Carol Stream, 804 p.

Agrawal AA. 2000. Specificity of induced resistance in wild radish: causes and consequences for two specialist and two generalist caterpillars. *Oikos* **89**:493–500.

Arimura GI, Ozawa R, Kufimiya S, Takabayashi J, Bohjmann J. 2004. Herbivore-Induced Defense Response in a Model Legume. Two-Spotted Spider Mites Induce Emission of (E)-b-Ocimene and Transcript Accumulation of (E)-b-Ocimene Synthase in *Lotus japonicas*. *Plant Physiology* **135**:1976-1983.

Baur R, Binder S, Benz G. 1991. Non glandular leaf trichomes as short-term inducible defence of the grey alder, *Alnus incana* (L.), against the chrysomelid beetle, *Agelastica alni* L. *Oecologia* **87**:219–226.

Birkett MA, Al Abassi S, Krober T, Chamberlain K, Hooper AM, Guerin PM, Pettersson J, Pickett JA, Slade R, Wadhams LJ. 2008. Antiectoparasitic activity

of the gum resin, gum haggar, from the East Africa plant, *Commiphora holtziana*. *Phytochemistry* **69**:1710–1715.

Boulogne I, Petit P, Ozier-Lafontaine H, Desfontaines L, Loranger-Merciris G. 2012. Insecticidal and antifungal chemicals produced by plants: a review. *Environ. Chem. Lett.***10:** 325-347.

Bruce TJA, Birkett MA, Blande J, Hooper AM, Martin JL, Khambay B, Prosser I, Smart LE, Wadhams LJ. 2005. Response of economically important aphids to components of *Hemizygia petiolata* essential oil. *Pest Management Science* **61**:1115–1121.

Bülow N, König WA. 2000. The role of germacrene D as a precursor in sesquiterpene biosynthesis: Investigation of acid catalyzed, photochemically and thermally induced rearrangements. *Phytochemistry* **55**:141–168.

Dalin P, Agren J, Björkman C, Huttumen P, Kärkkäinen K. 2008. Leaf Trichome Formation and Plant Resistance to Herbivory. In: Schaller A. (ed). Induced Plant Resistance to Herbivory. Springer Science+Business Media.

De Boer JG, Dicke M. 2004. The role of methyl salicylate in prey searching behavior of the predatory mite *Phytoseiulus persimilis*. *Journal of Chemical Ecology* **30**:255–271.

Della Lucia TMC, Fowler HG, Moreira DDO. 1993. Espécies de formigas cortadeiras no Brasil, p.26-30. In Della Lucia TMC (ed) As formigas cortadeiras. Viçosa, Editora Folha de Viçosa, 262p.

Dicke M, Agrawal AA, Bruin J. 2003. Plants talk, but are they deaf? *Trends in Plant Science* **8**:403–405.

Dudareva N, Martin D, Kish CM, Kolosova N, Gorenstein N, Fäldt J, Miller B, Bohlmann J. 2003. (E)-beta-Ocimene and myrcene synthase genes of floral

scent biosynthesis in snapdragon: Function and expression of three terpene synthase genes of a new terpene synthase subfamily. *Plant Cell* **15**:1227–1241.

Effraim KD, Jacks TW, Sodipo OA. 2001. Histopathological studies on the toxicity of Ocimum gratissimum leave extract on some organs of rabbit. *African. Journal Biomedical Research* **6**: 21-25.

Fahn A. 1979. Secretory tissues in plants. Academic Press, London.

Farji-Brener AG, Ruggiero A. 1994. Leaf-cutting ants (*Atta* and *Acromyrmex*) inhabiting Argentina: Patterns in species richness and geographical range sizes. *Journal of Biogeography* **21:** 391-399.

Fernandes VF, Almeida LB, Feijó EVRS, Silva DC, Oliveira RA, Mielke MS, Costa LCB. 2013. Light intensity on growth, leaf micromorphology and essential oil production of *Ocimum gratissimum. Revista Brasileira de Farmacognosia* **23(3):** 419-424.

Geervliet JBF, Posthumus MA, Vet LEM, Dicke M. 1997. Comparative analysis of headspace volatiles from different caterpillar-infested or uninfested food plants of Pieris species. *Journal of Chemical Ecology* **23**:2935–2954.

Hoagland DR, Arnon DI. 1950. The Water Culture Method for Growing Plants Without Soils. California Agriculture Experimental Station, Berkeley, CA.

Hölldobler B, Wilson EO. 1990. The Ants. Belknap Press of Harvard University Press. Cambridge. USA. 732 p.

Kigathi RN, Unsicker SB, Reichelt M, Kesseimeier J, Gershenzon J, Weisser WW. 2009. Emission of Volatile Organic Compounds After Herbivory from *Trifolium pratense* (L.) Under Laboratory and Field Conditions. *Journal of Chemical Ecology* **35**:1335-1348.

Kiran SR, Devi PS. 2007. Evaluation of mosquitocidal activity of essential oil and sesquiterpenes from leaves of *Chloroxylon swietenia* DC. *Parasitology Research* **101**:413–418.

Kost C, Tremmel M, Wirth R. 2011. Do Leaf Cutting Ants Cut Undetected? Testing the Effect of Ant-Induced Plant Defences on Foraging Decisions in Atta colombica. *PLoS One* **6:** e22340.

Levin DA. 1973. The role of trichomes in plant defence. *Quartely review of biology* **48**:3–15.

Molina-Montenegro MA, Ávila P, Hurtado R, Valdivia AI, Gianoli E. 2006. Leaf trichome density may explain herbivory patterns of *Actinote* sp. (Lepidoptera: Acraeidae) on *Liabum mandonii* (Asteraceae) in a montane humid forest (Nor Yungas, Bolivia). *Acta Oecologica* **30**:147-150.

Naidoo Y, Kasim N, Heneidak S, Nicholas A, Naidoo G. 2013. Foliar secretory trichomes of *Ocimum obovatum* (Lamiaceae): micromorphological structure and histochemistry. *Plant Syst Evol* **299**: 873-885.

Rando JSS, Forti LC. 2005. Ocorrência de formigas *Acromyrmex* Mayr, 1865, em alguns municípios do Brasil. *Acta Sci. Biol. Sci.* **27(2)**: 129-133.

Rautio P, Markkola A, Martel J, Tuomi J, H¨arm¨a E, Kuikka K, Siitonen A, Riesco IL, Roitto M. 2002. Developmental plasticity in birch leaves: defoliation causes shift from glandular to nonglandular trichomes. *Oikos* **98**:437–446

Robards AW. 1978. An introduction to techiniques for scanning electron microscopy of plant cells. in: Electron Microscopy and Cytochemistry of Plant Cells. J. L. Hall. (eds.). New York, Elsevier.

Silva MGV, Craveira AA, Matos FJA, Machado MIL, Alencar JW. 1999. Chemical variation during daytime of constituents of the essential oil of *Ocimum gratissimum* leaves. *Fitoterapia* **70**:21-34.

Silva MGV, Vieira IGP, Mendes FNP, Albuquerque IL, Santos RN, Silva FO, Morais SM. 2008. Variation of Ursolic Acid Content in Eight *Ocimum* Species from Northeastern Brazil. *Molecules* **13:** 2482-2487.

Silva SCM, Tozin LRS, Rodrigues TM. 2016. Morphological and histochemical characterization of secretory sites of bioactive compounds in *Lantana camara* L. (Verbenaceae) leaves. *Botany* **94**:321-336.

Tan KH, Nishida R. 2012. Methyl Eugenol: Its Occurrence, Distribution, and Role in Nature, Especially in Relation to Insect Behavior and Pollination. *Journal of Insect Science* **12(56)**: 1-74.

Telascrea M, Araújo CC, Marques MOM, Facanali R, Moraes PLR, Cavalheiro AJ. 2007. Essential oil leaves of *Cryptocarya mandioccana* Meisner (Lauraceae): Composition and intraspecific chemical variability. *Biochemical, Systematic and Ecology* **35**: 222−232.

Thiele T, Kost C, Roces F, Wirth R. 2014. Foraging Leaf-Cutting Ants Learn to Reject Vitis vinifera ssp. vinifera Plants that Emit Herbivore-Induced Volatiles. *J Chem Ecol.* **40:** 617-620.

Tozin LRS, Rodrigues TM. *In Prep*. Distribution and morphology of glandular trichomes in *Ocimum gratissimum* L. (Lamiaceae) emphasizing the cytoskeletal elements function in the secretory process.

Tozin LRS, Carvalho SF, Machado SR, Rodrigues TM. 2015a. Glandular trichome diversity on leaves of *Lippia origanoides* Kunth and *Lippia stachyoides* Cham.

(Verbenaceae): morphology, histochemistry and ultrastructure. *Botany* **93**: 297-306.

Tozin LRS, Marques MOM, Rodrigues TM. 2015b. Glandular trichome density and essential oil composition in leaves and inflorescences of *Lippia origanoides* Kunth (Verbenaceae) in the Brazilian Cerrado. *Anais da Academia Brasileira de Ciências* **87(2)**: 943-953.

Traw BM, Dawson TE. 2002. Reduced performance of two specialist herbivores (Lepidoptera: Pieridae, Coleoptera: Chrysomelidae) on new leaves of damaged black mustard plants. *Environmental Entomology* **31**:714–722.

Turlings TCJ, Mccall PJ, Alborn HT, Tumlinson JH. 1993. An elicitor in caterpillar oral secretions that induces corn seedlings to emit chemical signals attractive to parasitic wasps. *Journal of Chemical Ecology* **19**:411–425.

Turlings TCJ, Lengwiler UB, Bernasconi ML, Wechsler D. 1998. Timing of induced volatile emissions in maize seedlings. *Planta* **207**:146–152.

Unsicker SB, Kunert G, Gershenzon J. 2009. Protective perfumes: the role of vegetative volatiles in plant defense against herbivores. *Current Opinion in Plant Biology* **12**:479–485.

Van Den Dool H, Kratz DJ. 1963. A generalization of the retention index system including liner temperature programmed gas-liquid partition chromatography. *Journal of Chromatography* **11**:463-467.

Werker E, Putievsky E, Ravid U, Dudai N, Katzir I. 1993. Glandular hairs and essential oil in developing leaves of *Ocimum basilicum* L. (Lamiaceae). *Annals of Botany* **71**:43–50.

Werker E. 2000. Trichome Diversity and Development. Advances in Botanical Research 31.

Zanuncio JC, Cruz AP, Santos DF, Oliveira MA. 1996. Eficiência da isca Mirex-s (Sulfuramida 0,3%) no controle de *Atta cephalotes* (Hymenoptera. Formicidae) em três dosagens. *Acta Amazônica* **26**:115-120.

Table 1. Chemical composition of volatile components (%) from leaves of *Ocimum gratissimum* L. submitted to *Acromyrmex rugosus* attack and control.

Component	Control	Herbivory	P	F	RI	RI*
Hydrocarbon Monoterpenes						
α-pinene	0.52 a	0.61 a	0.356	1.086	933	939
sabinene	0.62 a	0.88 a	0.130	3.616	974	975
β-pinene	2.22 a	2.41 a	0.494	0.566	976	979
myrcene *	1.11 b	3.54 a	0.007	26.151	993	990
α-terpinene	0.06 a	0.00 a	0.374	1.000	1009	1017
ρ-cymene	0.14 a	0.00 a	0.117	3.973	1025	1024
(Z)-β-ocimene *	6.38 b	12.07 a	0.043	8.617	1041	1037
(E)-β-ocimene *	0.21 b	0.69 a	0.006	28.981	1051	1050
γ-terpinene *	0.29 a	0.00 b	0.007	26.01	1060	1059
Oxygenated Monoterpenes						
1.8-cineole	25.79 a	21.38 a	0.074	5.802	1034	1031
α-terpinol *	0.36 a	0.00 b	<0.001	165.753	1192	1188
eugenol *	16.61 a	5.1 b	0.001	60.465	1361	1359
Hydrogenated Sesquiterpenes						
α-copaene	1.29 a	1.70 a	0.152	5.125	1381	1376
β-cubebene	0.09 a	0.00 a	0.374	1.000	1395	1388
β-elemene *	0.41 b	1.26	0.034	28.136	1396	1390
(E)-caryophyllene	11.13 a	12.91	0.432	0.762	1425	1419
β-copaene	0.03 a	0.00 a	0.374	1.000	1434	1432
α-trans-bergamotene	0.78 a	1.22 a	0.268	1.654	1441	1434
α-guaiene	0.05 a	0.00 a	0.374	1.000	1443	1439
α-humulene	1.54 a	2.12 a	0.058	6.917	1458	1454
allo-aromadendrene *	0.76 a	0.00 b	<0.001	144.069	1465	1460
α-neocallitropsene	0.12 a	0.00 a	0.119	3.923	1482	1476
germacrene D *	1.86 b	4.21 a	0.044	8.467	1486	1485
β-selinene	17.39 a	18.79 a	0.276	1.592	1493	1485
α-selinene *	4.55 b	5.73 a	0.014	17.753	1501	1498
7-*epi*-α-selinene *	1.05 b	1.44 a	0.005	31.469	1522	1522
δ-cadinene *	0.38 b	0.57 a	0.015	16.770	1528	1523
Oxigenated Sesquiterpenes						
β-bourboneno	0.03 a	0.16 a	0.482	0.601	1389	1388
caryophyllene oxide	0.81 a	0.26 a	0.119	3.900	1586	1583
Hydrocarbon Monoterpenes *	3.85 b	20.20 a	0.026	14.046		
Oxygenated Monoterpenes *	42.76 a	21.38 b	0.002	47.407		
Hydrogenated Sesquiterpenes	33.17 a	49.94 a	0.073	5.820		
Oxigenated Sesquiterpenes	0.84 a	0.42 a	0.155	3.056		
Total identified	**96.57**	**97.04**				

RI= Retention index calculated; RI*= Retention index (Adams 2007); * indicates substances with statistical difference; Means followed by different letters indicate statistical differences (Tukey test $p < 0.05$).

FIGURES

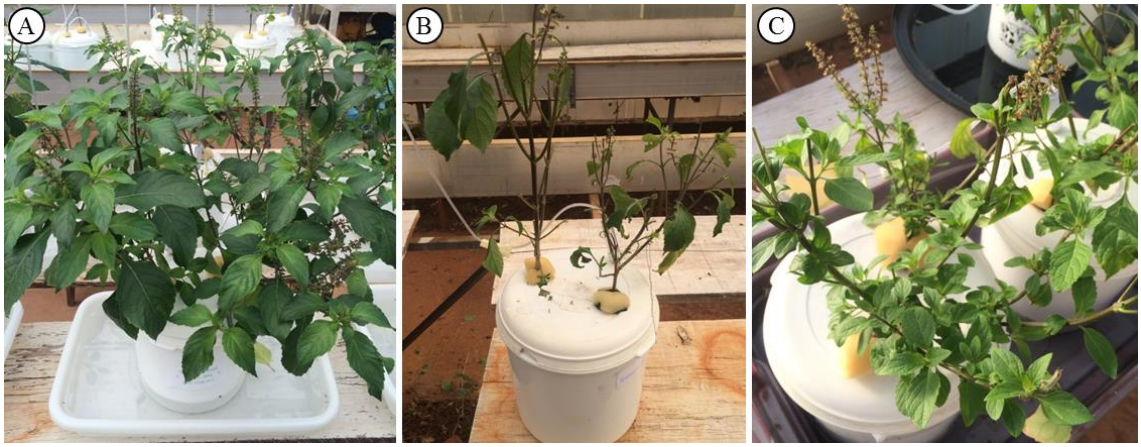

Figure 1. Experimental design of *Ocimum gratissimum* L. submitted to *Acromyrmex rugosus* attack. **A** Control plants. **B** Attacked plants by *Acromyrmex rugosus*. **C** Attacked plants after 40 days.

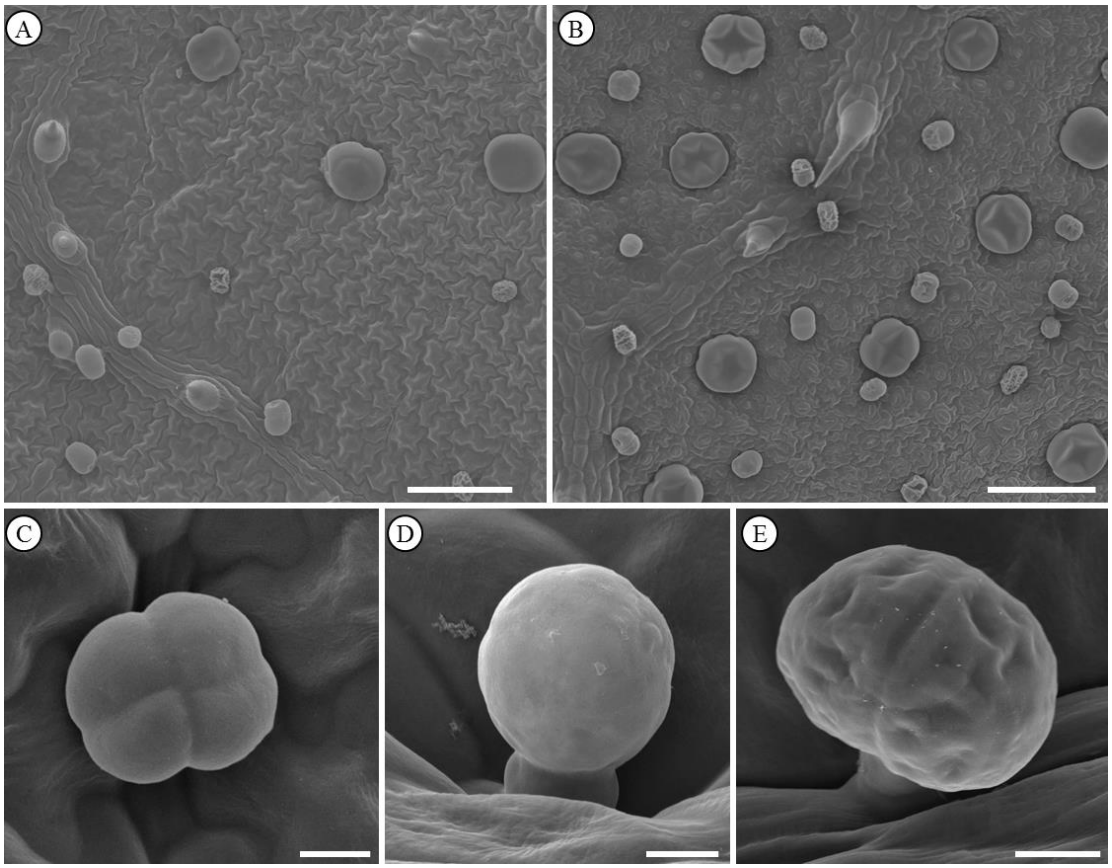

Figure 2. Scaning Electron Micrographs of adaxial (A) and abaxial (B) leaf surface of *Ocimum gratissimum*. (C-E) Glandular trichomes of *O. gratissimum.* (C) Morphotype I. (D) Morphotype II. (E) Morphotype III. Scale bars A-B = 100 µm; C-E = 10 µm.

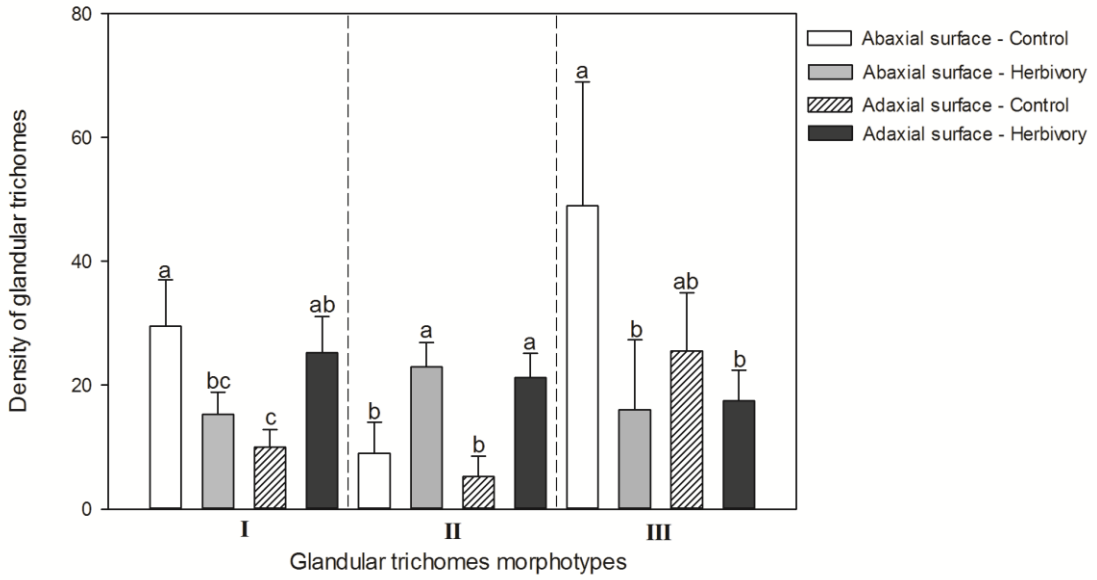

Figure 3. Density (mm²) of each morphotype of glandular trichomes in the both leaf surface of *Ocimum gratissimun* L. submitted to *Acromyrmex rugosus* attack and control. Means followed by different letters indicate statistical differences in the glandular density among treatments and leaf surfaces in each morphotype (Tukey test $p < 0.05$).

CONSIDERAÇÕES FINAIS

Esse trabalho vem preencher importantes lacunas existentes na literatura no que se refere à morfologia e funcionamento do sistema secretor de óleo em plantas, enfatizando o papel do citoesqueleto no processo secretor, além de trazer informações sobre a influência de fatores exógenos no desenvolvimento e funcionamento glandular.

Ocimum gratissimum possui três morfotipos de tricomas glandulares produtores de substâncias de natureza química diversa. A distribuição dos elementos dos filamentos de actina e dos microtúbulos nas células dos tricomas glandulares foi associada com os compostos produzidos por cada célula. Estes dados corroboram resultados obtidos por nosso grupo de pesquisa em estudo inédito realizado em tricomas glandulares e resultados conhecidos para células animais.

Ficou comprovado que o citoesqueleto exerce papel fundamental na morfologia e funcionamento dos tricomas glandulares. A utilização de drogas desestabilizadoras do citoesqueleto e de baixa disponibilidade de cálcio, numa abordagem inédita para estruturas secretoras em plantas, produziu alterações subcelulares importantes nas células glandulares de *H. villosa* e *O. gratissimum*. Cabe salientar que *O. gratissimum* mostrou-se um bom modelo para esses estudos por apresentar efetiva propagação vegetativa por meio de estacas, com 100% de enraizamento, além de moderada densidade de tricomas glandulares de três morfotipos facilmente reconhecíveis. Já *H. villosa* possui grande densidade de tricomas glandulares, o que dificulta o estudo de cada morfotipo glandular de forma individualizada; além disso, enfrentamos sérios problemas em seu enraizamento por meio de estacas, tendo obtido taxa de sucesso de apenas 6%.

Os dados apresentados no terceiro capítulo são frutos de estágio sanduíche realizado no *Laboratory of Plant Development and Interactions*, *Department of*

Molecular and Cellular Biology, *University of Guelph*, Canadá, sob orientação do Prof. Dr. Jaideep Mathur. Utilizando *Nicotiana benthamiana* como modelo, pudemos mostrar a dinâmica intracelular do transporte das gotas de óleo em células vegetais. Interessantemente, nossos dados mostraram o grande envolvimento dos filamentos de actina (ancorando porções do retículo endoplasmático) no movimento das gotas de óleo no protoplasto, contrariamente ao observado em células animais onde os microtúbulos são considerados os elementos de maior envolvimento no transporte lipídico. Assim, fica evidente que a dinâmica intracelular do transporte de óleo em células animais e vegetais pode ocorrer por diferentes mecanismos.

Embora o efeito da herbivoria na densidade de tricomas glandulares e na quantidade e composição da secreção seja conhecido, esse trabalho é inédito por considerar o efeito da herbivoria por formigas cortadeiras em cada morfotipo de tricoma glandular. Nossos resultados mostraram que cada morfotipo glandular em *O. gratissimum* responde de forma distinta ao estímulo levando a ideia de uma compartimentalização de funções no sistema de defesa das plantas. A alteração na composição química das substâncias voláteis registradas aqui por efeito da herbivoria merece atenção, principalmente pelo fato de se tratar de uma espécie amplamente utilizada como alimentícia.

As diferentes abordagens empregadas nesse estudo, várias delas inéditas para estudos com estruturas secretoras em plantas, permitiram que diferentes aspectos sobre a estrutura e funcionamento do sistema secretor de óleo em espécies vegetais fossem elucidados, gerando novas perspectivas para outras pesquisas em abordagens mais aprofundadas.